

NOTICE

**CERTAIN DATA
CONTAINED IN THIS
DOCUMENT MAY BE
DIFFICULT TO READ
IN MICROFICHE
PRODUCTS.**

USGS-OFR--89-133

DE91 001646

USGS-OFR-89-133

UNITED STATES
DEPARTMENT OF THE INTERIOR
GEOLOGICAL SURVEY

FEASIBILITY STUDY OF THE SEISMIC REFLECTION
METHOD IN AMARGOSA DESERT, NYE COUNTY, NEVADA

By

Thomas M. Brocher¹, Patrick E. Hart², and Steven F. Carle³

Open-File Report 89-133

¹USGS, 345 Middlefield Rd., M/S 977, Menlo Park, CA 94025

²USGS, 345 Middlefield Rd., M/S 999, Menlo Park, CA 94025

³USGS, 345 Middlefield Rd., M/S 989, Menlo Park, CA 94025

This report is preliminary and has not been edited for conformity with U.S. Geological Survey editorial standards and stratigraphic nomenclature. Any use of brand names is for descriptive purposes only and does not imply endorsement by the U.S. Geological Survey.

Menlo Park, California
1990

MASTER

DISTRIBUTION OF THIS DOCUMENT IS UNLIMITED

CONTENTS

	Page
Abstract.....	1
Introduction.....	2
Methods and Survey Specifications.....	3
Strategy of Acquisition Parameter Testing.....	4
Short Stack Concept.....	5
Point Receiver/Source Versus Arrays.....	5
Sources of Ambient Noise.....	7
Parameter Testing Site Selection.....	7
Noise Study "B".....	8
Noise Study "A".....	12
Line AV-1.....	15
Data Acquisition.....	15
Gravity Data Acquisition and Reduction.....	16
Comparison of Explosive and Vibroseis Shot Records.....	17
Data Processing.....	18
Data Processing of Explosive Shot Records.....	18
Data Processing of the Vibroseis Records.....	19
Analysis of Explosive Source Section for Line AV-1.....	20
Comparison of Line AV-1 to other Seismic Data sets.....	21
Comparison of the Vibroseis Stacked Section for Line AV-1 with Existing Refraction Model	22
Detachment Faults.....	24
Comparison of the Explosive and Vibroseis Sections for Line AV-1.....	24
Comparison with Nearby Deep Reflection Profiling Studies.....	26
Comparison of the Line AV-1 Lower Crustal Bright Spot to Other Bright Spots.....	27
Comparison of Gravity Models to Line AV-1.....	28
Summary and Conclusions.....	30
Acknowledgments.....	31
References.....	32

TABLES

	Page
Table 1: Acquisition Parameters for Line AV-1.....	35
Table 2: Locations of Cultural Noise Along Line AV-1.....	36
Table 3: Explosive Shot Parameters for Line AV-1.....	36
Table 4: Uphole Times and Velocities for Explosive Shots Along Line AV-1.....	37
Table 5: Comparison of Measured Windspeeds During Acquisition of Explosive and Vibroseis Shot Records.....	37
Table 6: Principal Facts for Gravity Data on Amargosa Valley Line AV-1.....	38
Table 7: Principal Facts for Gravity Data on Noise Study "B" Line.....	39
Table 8: Processing Sequence for the 0-5s Vibroseis Line AV-1 Brute Stack.....	40

APPENDIXES

	Page
APPENDIX 1: Windspeed Records.....	41
APPENDIX 2: Observer's Field Notes.....	49
APPENDIX 3: Processing Scheme for Line AV-1.....	80

ILLUSTRATIONS

Figure 1. Maps show locations of noise Studies "A" and "B" and Line AV-1 within Amargosa Desert relative to Beatty, Lathrop Wells, and Yucca Mountain. (a) General overview map of the entire study area. (b) Detailed map of Noise Study "B". (c) Detailed map of Noise Study "A" and Line AV-1.

Figure 2. Uncorrelated Vibroseis record showing the region of overlap of the reflected arrivals and the ground roll arrivals.

Figure 3. Theoretical response curves to ground roll propagating at 0.61 km/s for 50-m-long receiver arrays. Curve (a) is for a 24-element linear geophone group array; curve (b) is for the 24-element weighted geophone group array, illustrated in Figure 5.

Figure 4. Theoretical response curves to ground roll propagating at 0.61 km/s for Vibroseis source arrays. Curve (a) shows the response of a 24-element, 50-m-long linear source pattern; curve (b) shows the response of a 30-element, 70-m-long weighted source pattern.

Figure 5. Theoretical response curves to ground roll propagating at 0.61 km/s for combined 50-m-long receiver arrays and distributed Vibroseis source arrays.

Figure 6. Receiver and source array patterns tested during the feasibility study. (a) Areal design of the 50-m-long weighted receiver array, showing geophone locations as solid dots. (b) Schematic diagram showing the move-up (or vibrator pad location) pattern for the 50-m-long (165 ft.) Vibroseis array. Vibrator pad locations are shown as solid dots, and for clarity are vertically offset for each set of sweeps. For this pattern, the vibrator pads were separated by 13.1 m (43.1 ft) and were moved forward 2.13 m (7 ft) every other sweep. The number of sweeps at each vibration point are indicated by the weights on the bottom of the figure. (c) Schematic diagram showing the move-up pattern for the 70-m-long (231 ft) Vibroseis array. The vibrator pads were separated by 14.6 m (47.9 ft) and were moved forward 2.4 m (8 ft) after every sweep. Note that for this pattern the central 44-m of the array is weighted twice as much as the outer portion of the vibrator pattern.

Figure 7. Noise Study "B" record from Station 245, obtained using point (potted) receiver arrays, the 33-m-long Vibroseis source array, and an 8-40 Hz upsweep. For this and all similar plots, the short vertical ticks along the top of the record are spaced at 250 m intervals. The record is 6 km wide.

Figure 8. Noise Study "B" record from Station 245, obtained using a linear 50-m-long receiver array, the 33-m-long Vibroseis source array, and an 8-40 Hz upsweep.

Figure 9. Vibroseis records from Station 157 on the Noise Study "B" comparing (a) 6, (b) 12, and (c) 24 s long upsweeps. Twelve 8-40 Hz upsweeps were used for each test.

Figure 10. Noise Study "B" record from Station 245, obtained using point receiver arrays, the 50-m-long Vibroseis source array, and an 8-40 Hz upsweep.

Figure 11. Noise Study "B" record from Station 245, obtained using point receiver arrays, the 70-m-long Vibroseis source array, and an 8-40 Hz upsweep.

Figure 12. Noise Study "B" record from Station 245, obtained using a linear 50-m-long receiver array, the 70-m-long Vibroseis array, and an 8-40 Hz upsweep.

Figure 13. Comparison of (a) a linear 12-48 Hz upsweep, (b) a linear 14-56 Hz upsweep, and (c) a nonlinear 18-72 Hz upsweep at Station 197 on Noise Study "B". Note the hyperbolic noise trains on Figure 13a resulting from low-flying jet engines.

Figure 14. Broadside VPs at (a) 3, (b) 6, and (c) 9 km offset from the Noise Study "B" receiver array. A 12-48 Hz upsweep was used at each of these broadside locations.

Figure 15. Noise Study "B" records from Station 197 for two different windspeed conditions. For part (a) the windspeed was about 2 mph, for part (b) the windspeed ranged from 5 to 8 mph.

Figure 16. Noise Study "A" record from Station 1265, for a point receiver array, the 33-m-long Vibroseis array, and an 8-40 Hz sweep. Note that the total width of the record is 4 km and that the spacing of the vertical ticks at the top of the record is 250 m.

Figure 17. Noise Study "A" records from Station 1265, for 50-m-long receiver arrays (linear and weighted), the 33-m-long Vibroseis array, and an 8-40 Hz upsweep.

Figure 18. Noise Study "A" records from Station 1265, for point receiver arrays, the 33-m, 50-m, and 70-m-long Vibroseis arrays, and an 8-40 Hz upsweep.

Figure 19. Noise study "A" records from Station 1105, comparing linear upsweeps of (a) 12-48 Hz, (b) 14-56 Hz, and (c) 16-64 Hz.

Figure 20. Noise Study "A" records from Station 1105, comparing a (a) 10-44 Hz upsweep and (b) a 8-40 Hz upsweep.

Figure 21. Noise Study "A" record from Station 1105, showing a nonlinear 10-62 Hz upsweep.

Figure 22. Noise Study "A" records from Station 1105, for two different windspeed conditions. For part (a) the windspeed was 6-8 mph, for part (b) the windspeed was 12-14 mph.

Figure 23. Refraction model for the crustal structure along Line AV-1 from Mooney and Schapper (1988).

Figure 24. Comparison of explosive and Vibroseis Source records from Stations 1069 (a and b), 1429 (c and d) and 1789 (e and f). Both types of records are plotted in relative-amplitude format.

Figure 25. Comparison of explosive and Vibroseis source 3-second records from Stations (a) 1429 and (b) 1789. Both types of records have been automatic-gain controlled.

Figure 26. Unmigrated single-fold explosive source section for Line AV-1, plotted in relative-amplitude format.

Figure 27. Plot of average amplitude versus travel time for 40 traces from the explosive record for the shot at Station 1549.

Figure 28. Unmigrated 0-5s stack of Vibroseis Line AV-1, plotted in relative amplitude format.

Figure 29. Migrated (post-stack) 0-5s Vibroseis section for Line AV-1, plotted in relative-amplitude format. The processing steps taken to produce this 0-5 s twtt section are provided in Appendix 3.

Figure 30. Unmigrated 0-15s Vibroseis section for Line AV-1, plotted in relative-amplitude format. Processing steps taken to produce this section are provided in Appendix 3.

Figure 31. Map showing locations of COCORP, CALCRUST, and PASSCAL reflection profiles relative to Line AV-1. The basin and Range Province is shaded.

Figure 32. Gravity model based on geometry of the refraction model (Mooney and Schapper, 1988).

Figure 33. Gravity model modified from Figure 32 by changing the shape of the basin fill and basement interface.

ABSTRACT

This report presents a detailed description of a field trial comparing explosive and Vibroseis (Trademark of Conoco, Inc.) methods for acquiring deep crustal seismic reflection profiles in Nye County, Nevada. The field work was performed during January, 1988, in anticipation of a regional deep crustal reflection survey to be conducted as part of broad geological investigation of a proposed high-level nuclear waste facility in southwestern Nevada. Field trials were conducted at two sites within the Amargosa Desert, located in the Basin and Range province just to the east of Death Valley, California. Extensive testing of the Vibroseis method was performed to establish optimal acquisition parameters for the Vibroseis source. On completion of this exhaustive suite of trials, a 60-fold Vibroseis profile along a 27-km-long line was acquired using a 12-km-long symmetric split spread. Single 91-kg (200 lb.) explosive charges were fired in 76 m (250 ft.) deep shot holes along the Vibroseis profile to generate a coincident single-fold explosive source reflection profile. Within the upper crust (upper 5 s two-way travel time) the explosive and Vibroseis common-shot records are nearly equivalent. The 60-fold Vibroseis section for the upper 5 s is of high-quality and clearly shows structures related to extension inferred from coincident seismic refraction and gravity profiles. Below 5 s, however, the final sections for the coincident explosive and Vibroseis sources clearly document that the single-fold explosive source section provides a higher-quality image of the lower crust (5-10 s) due to the higher seismic energy levels produced by the explosive sources, the virtual absence of the air wave arrival, and the reduction of the ground roll arrival on the explosive data. The explosive source profile reveals subhorizontal, discontinuous reflections between 5 to 10 s. Based on older, and limited seismic refraction data, the crust was believed to be about 35 km thick. On the reflection profiles presented here, the base of the crust is defined only by the absence of high-amplitude reflected arrivals below 9 to 10 s.

INTRODUCTION

The U. S. Geological Survey (USGS) working under an Interagency agreement with the Department of Energy is engaged in a broad geoscience program to assess and identify potential repositories for high level nuclear waste at Yucca Mountain, Nye County, Nevada. The USGS program, referred to as the Yucca Mountain Project, or YMP, consists of integrated geologic, hydrologic and geophysical studies which range in nature from site specific to regional. This report is an evaluation of different acquisition methods for future regional seismic reflection studies to be conducted in the vicinity of Yucca Mountain, located in the southwestern corner of the Nevada Test Site (NTS).

In January 1988, field studies were conducted to investigate the feasibility of using the common-depth point (CDP) seismic reflection method to map subsurface geological horizons within the Amargosa Desert, Nye County, Nevada. These studies were performed under the supervision of USGS scientists by an industry contractor (Petty-Ray Geophysical Division of Geosource, Inc.). Little previous reflection profiling has been performed in the Amargosa Desert near Yucca Mountain; the goal of the field study was to investigate which seismic reflection method(s) should be used for mapping shallow to lower-crustal horizons. Therefore, a wide-variety of field acquisition parameters were tested, including point versus linear receiver group arrays; Vibroseis (service and trademark of Conoco, Inc.) versus explosive sources; Vibroseis array patterns; and Vibroseis sweep length and frequency range.

Previous high-resolution seismic reflection studies at Yucca Mountain (McGovern et al., 1983) failed to record shallow reflections from within the welded tuff in the immediate vicinity of Yucca Mountain itself. Other reflection studies near Yucca Mountain have been more successful. Only 45 km to the northeast of Yucca Mountain, reflection profiling within the Nevada Test Site at Yucca Flat using land airguns has routinely provided useful images of the basin fill and the sediment-basement interface and has been used to image an inferred detachment surface at 1.7 s two-way travel time (twtt) (McCarthur and Burkhart, 1986). Seismic reflection studies conducted to the south and west of Yucca Mountain in Death Valley and southern Amargosa Desert by COCORP, reveal reflections throughout the crust down to its base (deVoogd et al., 1986; Serpa et al., 1988).

On the basis of the success of seismic reflection studies elsewhere, a number of deeper and more regional reflection targets have been identified from geological and other geophysical studies of the Yucca Mountain area, ranging from the unsaturated zone at the top of the crust to the structure of the base of the crust (Carr, 1988). In the southern Great Basin they include: the upper and lower carbonate aquifers within the Paleozoic stratigraphic section (Winograd and Thordarson, 1975); the mylonitic, detachment-

bounded, upper surface of strongly metamorphosed Precambrian rocks exposed in the northern Amargosa Desert; the Tertiary-Paleozoic contact in the Yucca Mountain region; the mid-crustal, ductile-brittle transition zone, found at about 5 s depth in Death Valley (DeVoogd et al., 1986), and the base of the crust, found at about 10 s in Death Valley (DeVoogd et al., 1986). The seismic reflection methods selected for testing in the Amargosa Desert were thus constrained by the requirement to provide information for these and other targets throughout the entire thickness of the crust.

This report documents in chronologic order the results of the feasibility testing, and provides the rationale for the selection of the parameters employed for a 27-km-long 6-fold Vibroseis reflection line (Line-AV-1). Thus, we first present results of the test conducted near Beatty (Noise Study "B"), followed by the results from the testing conducted south of Lathrop Wells (Noise Study "A"). We then compare the 27-km-long Vibroseis and explosive source seismic reflection profiles for LINE AV-1. The locations of these noise studies and Line AV-1 relative to Yucca Mountain are shown in Figures 1 a-c. The reflection section for Line AV-1 is then compared to coincident refraction and gravity data, allowing an evaluation of its reliability and increased resolution.

METHODS AND SURVEY SPECIFICATIONS

The deep crustal objectives eliminated from consideration certain source types insufficient in strength to provide reflections from mid- and lower-crustal levels. After a thorough review of the existing literature, it was decided to test both large Vibroseis arrays (more than 72,700 kg (160,000 lbs.) peak force) and large (23-182 kg (50-400 lbs.)) chemical explosive sources, because both source types have provided useful data elsewhere under similar conditions. A large number (480) of closely (25m) separated receiver channels were used for the study for the following reasons: (1) the close receiver separation would help define short, discontinuous reflections and (2) the large number of receiver channels would simultaneously allow a greater source-receiver separation, which can be advantageous for imaging lower crustal reflections. The Vibroseis instrumentation provided by Petty-Ray Geophysical included four Failing Y2000 Vibroseis trucks, each having a peak force of 20,232 kg (44,511 lbs.), ground force control, and phase loop locking (Table 1). Recording instrumentation included an MDS-16 recording system with full-word recording and fiber-optic cables with takeouts every 67 m (220 feet) and 720 groups of 24 10-Hz geophones (Table 1). Fiber-optic cables were used to minimize noise introduced by electrical signals of man-made and natural origin. Flag locations were chained and then surveyed using electronic distance measuring equipment. Measured horizontal closure errors for the surveying are less than

one part in 2000, and vertical closure errors are less than 0.23 m (0.75 ft.) for the Noise Study "B" line and less than 0.09 m (0.298 ft.) for Line AV-1. An independent contractor (Bertram Drilling) performed the shot hole drilling and loaded the seismogel charges. To minimize unnecessary seismic noise, all shot hole drilling and loading was completed before records were acquired along Line AV-1.

For the feasibility study, it was considered critical that a field computer be available to perform advanced processing of the shot records to aid in the final selection of acquisition parameters. The truck-mounted field processing system provided by Petty-Ray Geophysical Division included a Perkin-Elmer 3210 CPU with a Floating Point Systems Array Processor, a Fujitsu Ltd. 470 mByte disk drive, three Storage Technology Corp. tape drives; and two Perkin-Elmer terminals. This system was used to demultiplex and to correlate the field records, to plot the field records on a dot-matrix printer, and to write SEG-Y formatted copies of the correlated field records. In addition, this system was used to apply various Automatic Gain Control windows and bandpass filters to the data in order to determine how various post-acquisition data processing algorithms effected the shot records. This testing allowed us to determine which filtering was required during the data acquisition and which could be performed after data acquisition.

STRATEGY OF ACQUISITION PARAMETER TESTING

The standard seismic exploration practice of testing a wide-variety of acquisition methods and parameters is particularly relevant in the Amargosa Desert since little deep crustal reflection work had been performed there. Considering the lack of success in obtaining shallow seismic reflections from the vicinity of Yucca Mountain (McGovern et al., 1983), it was considered vital that sufficient time (6 days) be given for testing a variety of acquisition methods. While a seismic reflection noise study is a fairly standard procedure, consisting of a determination of the ground roll velocity and predominant frequency followed by a testing of source and receiver arrays designed to reduce the amplitude of these arrivals, we in addition, desired to compare and contrast a number of different acquisition techniques. We also wanted to be sure that inferred results were general and not based on only a few records which might be heavily biased by a localized anomaly in surficial geology. Some differences from standard noise studies were also required to obtain reflections from the top of the crust down to the Moho. Thus, in planning this testing a number of guidelines were followed, and the ensuing examination of these guidelines may help provide insight into the manner in which acquisition parameters were tested.

Short Stack Concept

Given the previously unsuccessful seismic reflection results from Yucca Mountain itself we lacked confidence that reflections would be directly observable on individual plots of common-shot records. We believed, however, that reflections might be more easily observed on low-fold stacks. Thus we sought to generate low-fold stacks along the noise study lines which might better reveal reflections. We planned to accomplish this by deploying at least two long receiver cables having different receiver group arrays and by vibrating every 8th station along the 240-channel receiver cables. By repeating this procedure for different source parameters, being careful to alter only one source parameter at a time, we attempted to rapidly generate a large number of different stacked sections which are directly comparable, and which would allow the selection of optimal acquisition parameters. Because seismic sections represent the final product of reflection profiling it might be argued that low-fold sections provide a better basis for comparing reflection parameters than individual common-shot records. Furthermore, this field technique enables several different individual comparisons, over the length of the receiver cable used for the testing, to provide a firmer statistical basis for the selection of acquisition parameters.

Low-fold seismic sections may provide a better basis than individual shot records for determining whether the reflection method will prove useful in Nye County, Nevada. However, at the noise study site near Beatty, Nevada, no full-fold reflection line was to be acquired after the noise study was completed. Thus, much of the first day of testing for Noise Study "B" was devoted to the attempt to generate at least two different 15-fold stacks. One stack was a test of geophones grouped into a point receiver, the other stack was a test of a 50-m-long linear receiver group array. Time restrictions unfortunately prohibited us from completing either 15-fold section, but a 5-6 fold section can be obtained from the 11-12 different Vibrator Points acquired during Noise Study "B".

Point Receiver/Source Versus Arrays

Point receiver/source arrays are preferred in principle over areal arrays because point arrays lack directionality and therefore do not therefore discriminate against desired dipping reflected energy. The steep dips observed in exposed rocks near the study sites indicates that it is desirable to record all dips if possible. If permissible it is preferable to filter unwanted dipping energy only in the computer post-acquisition, where different filtering strategies are easily implemented. There are other reasons for preferring point receiver and source arrays. Logistically, point arrays are simpler to deploy and it is easier to verify that point arrays have been correctly deployed than it is for linear arrays.

While Vibroseis sources can offer significant logistical advantages over explosive sources, they do have disadvantages. Chief among them is the fact that Vibroseis sources operate at the earth's surface, and therefore are capable of generating large-amplitude surface waves. A really distributed arrays are used primarily to attenuate the amplitude of unwanted horizontally propagating source-generated energy. The need to do so in the field rather than by subsequent processing may be best justified by the realization that for a Vibroseis source the recorded data are uncorrelated in time. Thus, noise generated by the Vibroseis array persists for the entire length of the sweep, and changes frequency as the Vibroseis sweep changes frequency. As shown in Figure 2, source generated noise propagating as ground roll persists for the entire length of the sweep, masking reflected arrivals. Therefore, to preserve the dynamic range of the later arriving crustal reflections it is necessary, assuming an upsweep is used, to reduce the amplitudes of the higher frequency ground roll. It cannot be overemphasized that dynamic range can only be preserved during the acquisition of the data; dynamic range cannot be restored by post-acquisition processing. Thus, whenever there is large-amplitude ground roll it is necessary in practice to use areally distributed arrays to preserve the dynamic range of the recorded data.

The dramatic reductions in the amplitudes of ground roll energy using distributed source and receiver group arrays are illustrated in Figures 3 through 5. For all these figures the ground roll is assumed to have a velocity of 0.61 km/s. Figure 3a and 3b compare theoretical calculations of the reduction of the ground roll energy as a function of frequency for linear 50-m-long geophone group arrays having 24 geophones. A horizontal line at 0 dB indicates the response of a single geophone (point receiver), whereas a 50-m-long group array having geophones spaced at 2.2 m intervals reduces the ground roll amplitudes as shown in Figure 3a. The response of a 24-element weighted 50-m-long group array, whose plan-view pattern is shown in Figure 6a, is illustrated in Figure 3b.

Similar frequency-dependent reductions in ground roll amplitude result from the use of linear source arrays. Figure 4a compares the response of a 50-m-long source array (Figure 6b) to that of a single vibrator which produces a 0 dB response. A 70-m-long source array shown in Figure 6c is even more effective in reducing the ground roll energy (Figure 4b).

Finally, Figures 5a through 5c compare the theoretical reduction of ground roll amplitude resulting from a variety of combinations of linear and weighted receiver group and source arrays. For frequencies between 15 and 50 Hz, the combination of a 70-m-long source pattern and a 50-m-long weighted receiver group pattern produces the greatest theoretical attenuation of the ground roll energy (Figure 5c). For this combination of arrays the

theoretical reduction in ground roll amplitude exceeds 40 dB, or a factor of 100, preserving an additional 40 dB of signal level at these frequencies in the uncorrelated recorded data.

To test these theoretical reductions in ground roll amplitudes, a wide variety of receiver group and source array patterns and combination of patterns were tried during both noise studies. All of the combinations shown in Figures 3 through 5 were tested on the ground.

Sources of Ambient Noise

The last major goal of the testing was to identify all important sources of ambient noise so that effective countermeasures for these noise sources can be designed for this and future studies. One of the primary anticipated noise sources was wind. For this reason detailed measurements of windspeeds were made throughout the investigation and are tabulated in Appendix 1. These measurements were made using a Climatronics windspeed meter whose output was displayed on a digital voltmeter.

Cultural noise was not expected to be a significant problem during the noise test, in part due to the criteria used to select the noise test sites (see below). Sources of cultural noise along the Line AV-1 (Figure 1c) are summarized in Table 2, these included powerlines, nearby residences, traffic, and buried cables. An unpredictable but significant source of noise resulted from low-flying pairs of military jet aircraft on maneuvers from a nearby Air Force base. During Noise Study "B" mineral exploration drilling rigs were active about 2.5-3 km from the nearest end of the receiver array, but these rigs did not appear to significantly increase noise levels.

Parameter Testing Site Selection

Prior to the January, 1988, testing of data acquisition parameters in the Amargosa Desert, several possible roads along which the test work could be performed were visited. Ease of access, logistic feasibility, proximity of cultural noise, and length and straightness of the road were examined for each possible line location. Additional considerations for site selection included proximity to or coincidence with proposed corridors for future seismic reflection studies and/or existing seismic refraction surveys discussed by Mooney and Schapper (1988).

Two locations for the feasibility test were selected based on these considerations in the northwestern and eastern ends of Amargosa Desert. The first test line (Noise Study "B" for Beatty) was located within the northwestern corner of the Amargosa Desert approximately 9 km southwest of Beatty, Nevada, on a linear gravel access road oriented slightly oblique to State Highway 374 (Figure

1c). The second test line (Noise Study "A" for Amargosa) was located near the eastern end of the desert approximately 7.9 km south of Lathrop Wells on an E-W oriented gravel access road along Line AV-1 (Figure 6). This second test line reoccupied a portion of the 1985 seismic refraction line described by Sutton (1985), for which results are presented by Mooney and Schapper (1988). Together these test locations straddle Yucca Mountain to the west and south and provide a useful measure of the variability of near-surface conditions necessary for the design of regional seismic reflection profiles to be conducted within Amargosa Desert. Both sites were located almost exclusively on land managed by the Bureau of Land Management.

Upon completion of six days of testing of acquisition parameters at the two test sites, a 27-km-long Vibroseis reflection profile (Line AV-1) was collected along the site of the second noise test south of Lathrop Wells (Figure 1c). Eight explosive shots at 3 km intervals were also obtained along this profile, forming a single-fold stack comparable to the 27-km-long sixty-fold stack obtained using the large Vibroseis array.

NOISE STUDY "B"

Noise Study "B" was conducted along a nearly flat, straight access road located just north of State Highway 374 in the northwestern corner of the Amargosa Desert (Figure 1b). A total of 58 seismic records were acquired during the three-day study (Appendix 2).

One of the most important tests performed during the study was the comparison of point versus linear geophone group array patterns. Accordingly, two parallel receiver cables, each consisting of 240 channels over a length of 6 km, were deployed side by side. One cable consisted of point geophone arrays obtained by deploying 12 geophones in a group only a few meters wide. (This type of geophone array is sometimes referred to as a potted or clumped array.) The second cable employed 24-element 50-m-long linear geophone group arrays. For both cables the geophone groups were spaced at 25 m intervals and the geophones were not buried. During Noise Study "B" the size of the memory within the MDS-16 recording unit permitted the recording of only one cable at a time, so it was necessary to repeat each Vibroseis point to obtain records for each geophone array pattern (Appendix 2). The available memory also restricted maximum record lengths to 39 seconds using a 4 msec sampling rate for the 480 total channels. All listen times used during Noise Study "B" were 15 seconds.

The first suite of records obtained during Noise Study "B" was designed to examine the characteristics of the source-generated noise. Point receivers and clumped sources were used to obtain full wavefield records (sampled in increments of the group spacing) of the source-generated noise produced by the Vibroseis array. A point (stacked) source array was simulated using the four Vibroseis trucks deployed end-to-end in-line in a 33-m-long array centered on the Vibrator Point (VP). An upsweep of 8 to 40 Hz over a sweep length of 24 seconds was used because of previous success using this sweep for deep crustal reflection profiling in other areas. Records produced using these parameters document that the air wave, generated by the Vibroseis array, and traveling at 330 m/s, is unusually large in amplitude (Figure 7). The large-amplitude of the air wave is thought to result from the large size of the Vibroseis array, the absence of dense vegetation along the test line, the relatively flat topography, and the existence of a firm desert pavement along the test line. In any case, the air wave significantly degraded a narrow cone of reflection energy returning throughout the thickness of the crust (Figure 7).

This initial testing also detected large-amplitude ground roll having two distinct velocities. The faster ground roll arrivals have a group velocity of 0.99 km/s and a predominant frequency of close to 12 Hz. The slower ground roll arrivals have a group velocity of 0.61 km/s and a predominant frequency close to 10 Hz. Refracted first-arrivals observed on these records have velocities between 1.7 and 6.1 km/s.

The simultaneous recording of geophone group array patterns having two different lengths allowed the length of the geophone group array to be evaluated first. Direct comparison of several records which differ only in type of geophone group array used demonstrated that the linear array substantially reduced the amplitude of both the ground roll and air wave arrivals (Figures 7 and 8). This reduction in ground roll and air wave amplitudes by the linear geophone array noticeably improved the appearance of the field records without degrading the amplitudes of the refracted first-arrivals. This comparison, performed for sources in several locations along the length of the 6-km-long cables, indicated that geophone group arrays designed to reduce the amplitude of the air wave and ground roll arrivals provided substantial improvement in the signal-to-noise-ratios of mid-to lower-crustal reflections over those obtained using the point geophone group array.

An important field parameter to be investigated was the length of the Vibroseis sweep. This parameter was among the first tested (Records 1-6, Appendix 2). Simply put, the shorter the Vibroseis sweep, the less seismic energy is input into the earth. Shorter sweeps, however, speed up the rate of production over longer sweeps, and do not insonify as large a volume of the crust, thereby reducing the amount of three-dimensional backscattering from out of the plane of the reflection profile. Sweep lengths of 6, 12 and

24 seconds were compared because they represent 6 dB increases in Vibroseis energy. Figure 9 compares these records and documents that only the 24-second long sweep provided sufficient signal strength to image lower crustal reflections.

At this point in Noise Study "B", a short stack was begun to compare the point and 50-m-long geophone group array patterns (Appendix 2). Records 7 through 22 represent over 1 km of the test line with a VP every 200 m (8 stations). At the end of Record 22 it became apparent that the rate of production was insufficient to finish the short stack while properly testing other parameters, and as a result the short stack was terminated. This decision was made in part because the observations of reflections on the common-shot gathers showed that the short stacks would not be required to compare acquisition parameters. Nonetheless, these 16 records provide direct comparison of point versus linear geophone group array patterns in 8 different locations, and provide firm support for the necessity of the linear geophone group arrays. These records were augmented by four others allowing a 6-fold stack to be generated for the Noise Study "B" line.

Records 23 through 46 represent tests of various source array lengths. Three different Vibroseis array patterns were compared at several locations. These linear and weighted patterns were designed to reduce the observed ground roll and air wave amplitudes. In addition to the stacked Vibroseis array pattern, 50- and 70-m-long (165-231 ft.) Vibroseis array patterns were tested (Figures 5b and 5c). As expected from Figures 4a and 4b, a progressive improvement in noise reduction was noted as the Vibroseis source array was lengthened (Figures 7, 10 and 11).

This series of tests also allowed various combinations of source and geophone array patterns to be evaluated. The combination of a 50-m-long geophone group array and a 70-m-long Vibroseis source array reduced the amplitudes of the ground roll and air wave by over 30 dB, producing dramatic improvements in the lateral continuity of reflections from throughout the crust (Figure 12). The comparisons, obtained in several locations along the 6-km-long receiver cables from Record 23 to 45 (Appendix 2), indicate that Vibroseis methods in the Amargosa Desert require both distributed source and receiver group arrays in order to suppress large-amplitude ground roll and air wave arrivals in uncorrelated time.

Upon selection of optimal source and receiver array lengths, as well as the sweep length, the Vibroseis sweep frequency content was then varied. The main objective in obtaining Records 46 to 54 was to determine whether a high-frequency sweep would further suppress the ground roll while maintaining useful reflection strengths from the mid- to lower crust (5-10 s). Linear upsweeps of 12-48 Hz and 14-56 Hz were tested as was a nonlinear 18-72 Hz upsweep weighted on the low-frequency end (Figure 13). (Note on

Figure 13a large-amplitude hyperbolic events produced by low-flying jet planes.) The result of these tests were mixed. Ground roll energy was reduced using all the higher-frequency sweeps, but the nonlinear 18-72 Hz sweep generated excessive air wave energy. Having already selected the linear geophone group array these tests were recorded exclusively using the linear geophone group array pattern.

The last parameter tested during Noise Study "B" was the useful maximum source-receiver offset for the Vibroseis source. Although off-end (walkaway) testing on the SW end of the line was restricted by our lack of access to the Death Valley National Monument (located just west of Station 101), an off-end VP at a range of 3 km to the NE to the receiver array was acquired (Figure 1b). This VP provided data for source-receiver ranges between 6 and 9 km. To further test the efficiency of Vibroseis signal propagation, a series of 3 broadside VPs were obtained at perpendicular ranges of 3, 6, and 9 km southeast of the array (Figures 1b and 14). These broadside records (55 through 58) demonstrate that the Vibroseis array can provide useful signals to ranges of 9 km, even when located near the center of the Amargosa Desert.

Wind and weather conditions during Noise Study "B" were ideal (Appendix 1). Windspeeds were generally less than 5 mph except for a 3-hour period in the middle of the second day of the study (January 9th). Thus, no attempt was made to specifically examine the effect of windspeed on the quality of lower crustal reflections during the noise study. An indirect evaluation, however, is possible by comparing Records 22 and 30, which were both acquired at Station 197 using the linear geophone array pattern and an 8-40 Hz upsweep. Record 22 was acquired using the stacked (33-m-long) Vibroseis array pattern when the windspeed was 2 mph, whereas Record 30 was acquired using the 70-m-long Vibroseis array pattern when the windspeed was 5-8 mph (Figure 15). Considerably more high-frequency noise is present on Record 30 (Figure 15b) when windspeeds were higher. This higher noise level is not explainable by the longer Vibroseis source pattern used for Record 30, because other records demonstrate that this source pattern reduced higher-frequency noise levels. Later in the study it was noted that at windspeeds of 4-8 mph the wind caused the vegetation to shake, probably coupling wind-generated noise into the ground. The comparison of Records 22 and 30 in Figure 15 confirm that at windspeeds as low as 5-8 mph the lower crustal reflections generated by large Vibroseis sources are degraded by high-frequency wind-generated noise.

NOISE STUDY "A"

Noise Study "A" was conducted along a flat, straight portion of Line AV-1 due south of Lathrop Wells (Figure 1). A total of 66 seismic records were obtained during the four-day long noise study (Appendix 2).

Based upon the success of the linear 50-m-long geophone group array pattern in suppressing the ground roll and air wave energy during Noise Study "B", during Noise Study "A" it was decided to also test the 24-element weighted geophone group array pattern of Figure 6a. Thus, for the Noise Study "A", three parallel receiver cables, each consisting of 160 channels over a length of 4 km, were deployed side by side. These cables were deployed between Stations 1105 and 1265 of Line AV-1 with a 25 m group interval (Figure 1c). As for Noise Study "B", one cable consisted of 12 geophones deployed in a group only a few meters wide and a second employed the 24-element 50-m-long linear geophone group array pattern. The third cable employed a 24-element 50-m-long weighted geophone group array pattern. For the weighted geophone group array, two sets of 12 geophones were overlapped for seven geophone locations, forming a pattern centered on the station flag (Figure 6a). As for Noise Study "B", no geophones were buried during Noise Study "A".

Unlike Noise Study "B", for Noise Study "A" the mass memory within the MDS-16 recording unit was upgraded so that signals from all three cables (a total of 480 channels) could be recorded simultaneously (Appendix 2). Record lengths, however, were still restricted by the available mass memory to 39 seconds using a 4 msec sampling rate.

As for Noise Study "B" the first step of the testing was to obtain records of the source-generated noise. These records were obtained using the stacked (33-m-long) Vibroseis array pattern recorded by the point (clumped) receiver pattern using an 8-40 Hz upsweep. Greater variation in the characteristics of the ground roll energy was observed along Line AV-1 than at the Noise Study "B" site, probably due to a more significant variation in the depth to basement along the line. In one location the ground roll was relatively large in amplitude, and had a group velocity of about 1 km/s with a predominant frequency of 10 Hz. In another location the group velocity of the ground roll was about 0.6 km/s with a predominant frequency of about 10 Hz, and was relatively low in amplitude. While the air wave remained a significant noise contaminant, the ground roll along Line AV-1 was generally weaker in amplitude and lower in velocity than at the Noise Study "B" site (Figure 16). First-arriving refracted waves observed during Noise Study "A" had velocities between 2 and 4 km/s.

The simultaneous recording of 3 different geophone group array patterns made it possible to evaluate the length of the geophone group array first. Direct comparison of records obtained at several VPs document that both 50-m-long geophone group array patterns tested provide significantly greater attenuation of the ground roll and air wave energy than the point geophone pattern. The differences between records obtained for the linear and weighted 50-m-long geophone group array patterns are more subtle (Figure 17). Modest improvements detected in the records obtained using the weighted geophone group arrays, however, made them preferable to the 50-m-long linear geophone arrays.

Vibroseis array pattern length was the next parameter to be tested during Noise Study "A" (Records 1-9, Appendix 2). Five different Vibroseis source patterns were tested. As at Noise Study "B", progressive improvement in noise reduction was noted as the source array pattern length was increased from 33 to 70 meters (Figure 18). Additional pattern lengths of 44 m (143 ft.) and 60 m (195 ft.) were also tested on several records. These last two Vibroseis pattern lengths did not yield improved records. Thus, a Vibroseis pattern length of 70 m was selected for Line AV-1.

Having determined the lengths of both the geophone group array and Vibroseis pattern lengths, a variety of higher- frequency sweeps were tested during Records 10 through 24 (Appendix 2). As before, the purpose of these tests was to determine whether a higher-frequency sweep could minimize the ground roll and air wave amplitudes and maximize the energy of lower crustal reflections. 24-second long linear upsweeps of 12-48, 14-56, and 16-64 Hz were compared at several VPs (Figure 19). These upsweeps produced substantially higher source-generated noise levels, primarily in the air wave, than found for the 8-40 Hz sweep. Windspeeds, however, during this testing were higher than previously observed (Appendices 1 and 2), so there is a strong possibility that the observed higher ambient noise levels partially resulted from wind-generated noise.

While the tests of the higher-frequency upsweeps did not produce wholly satisfactory results, these upsweeps did offer advantages over the 8-40 Hz upsweep. Chief among these advantages is that the ground roll was severely attenuated by the higher-frequency upsweeps. During Records 31-35 (Appendix 2) we tested a 10-44 Hz sweep which was intermediate between the 8-40 Hz sweeps and the higher-frequency sweeps previously tested. It was hoped that the 10-44 Hz sweep might help to attenuate the ground roll energy and provide somewhat greater temporal resolution but would not be as sensitive to the air wave and wind noise as higher-frequency sweeps. Field testing (Figure 20) indicated that the shot records contained less ground roll energy for the 10-44 Hz upsweep than for the 8-40 Hz upsweep. Because the 10-44 Hz upsweep did not appear to be significantly more sensitive to the air wave or to wind-generated noise than the 8-40 Hz upsweep, the 10-44 Hz

upsweep was tentatively selected for Line AV-1, pending the result of testing a variety of nonlinear upsweeps.

The useful maximum source-receiver offset was the next parameter to be tested in order to establish a shooting geometry. These offsets were determined using walkaway testing during Records 40-50 and 56-62 (Appendix 2). The Vibroseis source array was moved 4 km off both the west and east ends of the cables for Noise Study "A", providing data for source-receiver offsets of between 4 and 8 km. These tests documented that under favorable wind conditions both reflected and refracted arrivals generated by the Vibroseis array could be observed at least as far as 8 km. Under less favorable wind conditions, however, the arrivals beyond ranges of 6 km were difficult to recognize. It was therefore decided to use a symmetric split spread of \pm 6 km centered on the Vibroseis array with no gap to the first active trace (Figure 6c).

Finally a few nonlinear sweeps of various lengths and input frequencies were tested, all of which emphasized the low-end of the spectrum. While a 10-62 Hz nonlinear 19-second-sweep yielded reasonable signal levels within the mid- to lower-crust (5-10 s), the field records were extremely band-limited (Figure 21). Because field processing revealed that post-acquisition bandpass filtering of the 10-44 Hz linear upsweeps resulted in records having a nearly identical appearance to those generated by these non-linear sweeps, it was decided not to apply such a severe frequency filter during data acquisition. Instead, it was decided to rely on post-acquisition bandpass filtering to improve the lateral continuity of lower crustal reflections, if necessary. We thus selected the 24-s-long 10 to 44 Hz linear upsweep for Line AV-1.

Wind and weather conditions during Noise Study "A" were much less favorable than during Noise Study "B" (Appendix 2). Windspeeds were particularly high during the second day of the study on January 11th, with windspeeds steady up to 22 mph accompanied by strong gusts. For these reasons the effect of windspeed on the signal-to-noise ratios of lower crustal reflections was specifically tested on Records 38-39 by duplicating VPs acquired during windier conditions. Records 19 and 38 were both acquired using the 50-m-long weighted geophone array and the 70-m-long Vibroseis array, using a 14-56 Hz upsweep at Station 1105 (Figure 22). The windspeed during the acquisition of Record 19 was 12-14 mph, whereas the windspeed during the collection of Record 38 was only 6 to 8 mph. Comparison of the two records indicates that the higher windspeed has noticeably degraded the quality of the lower crustal reflections below 5 s (Figure 22). Data above 5 s appear to be less sensitive to the windspeed.

LINE AV-1

Immediately after the cation of the testing for Noise Study "A", and upon selection the final acquisition parameters to be employed for the Vibroseis survey, work was begun on the acquisition of reflection data along Line AV-1. As Line AV-1 was acquired, explosive sources were periodically fired to obtain a coincident but low-fold explosive source reflection profile. In this section we present a detailed description of the acquisition of both these datasets and compare the results. Line AV-1 reoccupied 27.2 km of the refraction line named Amargosa described and interpreted by Mooney and Schapper (1988); on their Figure 7 Line AV-1 is located between km 13 and 39.725.

Data Acquisition

Line AV-1 was run from west to east for a total distance of 27.2 km. The line started at Station 889, located approximately 2.1 km west of State Highway 373, and ended at Station 1975, located about 1.6 km west of State Highway 160 (Figure 1c). The optimal field parameters described in previous sections were used to acquire these data and are summarized in Table 1.

At the beginning of Line AV-1 the Vibroseis source array was walked into the 480-channel receiver spread from Station 889 until the source array reached the center of the spread at Station 1129 (Appendix 2). To build fold quickly, every other station (50 m) was vibrated for the first 60 VPs. Beginning at Station 1009 every fourth station (100 m) was vibrated, and the spread was begun to be rolled along, after Station 1129 was vibrated. As the spread was rolled along, a symmetric split-spread was used, with 6 km of active receiver array on each side of the Vibroseis array and no gap to the first active geophone (Table 1).

As the receiver spread was rolled along the line, eight explosive shots were fired into the array. The shot holes were backfilled with drilling cuttings and/or sand and gravel. No blow-out or permanent surface deformation from any of the shots was observed indicating that the explosive energy from the shots was well-coupled into the ground. These shots were recorded for 20 seconds at a 4 msec sample rate on between 530 and 596 active channels. A variety of explosive shot sizes, shot depths, and patterns were tested (Table 3). Every 240 stations (6 km) a 91-kg (200 lb.) charge was detonated at 76 m (250 ft.) depth; this shooting geometry produced a single-fold section to compare directly to the 60-fold Vibroseis stacked section (Table 2). Shots at Stations 1065-1069 were drilled into sandy unconsolidated sediments whereas the shot at Station 1189 was drilled into Paleozoic basement (M.C. Carr, personal communication, 1988). Tables 3 and 4 provide a list of the size and location as well as other pertinent information concerning these shots.

Three explosive shots were fired between Stations 1065 and 1069 in order to determine optimal charge sizes (Table 3). Qualitative comparison of these records obtained under nearly identical conditions (Table 5) indicates that shots between 45-kg (100 lb) and 91-kg (200-lb) are optimal for imaging the lower crust in the Amargosa Desert. Significant improvement in reflection continuity and signal-to-noise ratio was noted as the shot size was increased from 23-kg (50 lb) to 45-kg (100 lb). Records obtained using 45-kg and 91-kg were more comparable. While not directly comparable to shots recorded at these stations, a 182-kg (400 lb) shot fired at Station 1189 (Table 3) provided no significant apparent enhancement of the lower crustal reflections over 41-kg shots.

No systematic trial of explosive shot depth was attempted due to our understanding that the primary control of shot efficiency was whether the charge was located within or close to water table. At Station 1429, however, we tested an array of 4 holes, centered in-line over a distance of 50 m, each 38 m (125 ft.) deep and each filled with 23-kg (50 lbs) of explosive. The record of lower crustal reflections obtained using this explosive pattern was significantly lower in quality to the single 23-kg sized explosion recorded at Station 1065. At least a portion of this degradation was produced by the significantly stronger airwave generated by the shallower shot holes. In addition, observers on the scene believed that the 4-hole shot pattern was not as well coupled into the ground as the deeper shots.

Line AV-1 was finished in a manner similar to that used to begin it. After Station 1740 was vibrated, the receiver spread was no longer rolled-along, but instead the source array walked through the now fixed receiver spread until it reached the end of the line at Station 1975 (Appendix 2). Unlike at the beginning of the line, however, during this walk-through the channels were active only from Station 1975 out to a distance of 240 channels west of the Vibroseis array. Thus the number of active channels monotonically dropped from 480 to 240 as the Vibroseis array approached Station 1975. Beginning at Station 1855 the Vibrator Point interval was halved to every other station (50 m) to maintain the 60-fold stack out to Station 1915. Data acquisition was generally halted when windspeeds exceeded 12 to 16 mph, corresponding to a 24 dB increase in noise levels due to the wind for most of the receiver array.

Gravity Data Acquisition and Reduction

Sixty-eight gravity measurements were made along Line AV-1 (Table 6); 13 gravity measurements were made along the Noise Study "B" line (table 7). The observed gravity values were referenced to the International Gravity Standardization Net 1971 (IGSN71) gravity datum (Morelli, 1974). All measurements were made relative to base station BPO at the old Beatty Post Office, Beatty, Nevada

described by Harris et al. (1988). The measurements were made with LaCoste and Romberg gravity meter G-17 at 16 receiver group (400-m or 1/4 mile) intervals along the lines. An uncertainty in the gravity measurement of 0.05 mGal is expected due to meter calibration and drift. As mentioned above, receiver group locations were surveyed by Petty-Ray Geophysical using electronic distance measurement devices. Given the horizontal and vertical closures of 1 part in 2000 and 0.23m, respectively, the maximum uncertainty due to location is 0.05 mGal. Thus, by considering the uncertainties due to the gravity measurement and location, the observed gravity values are expected to be accurate to within 0.10 mGal.

The observed gravity values were reduced to Bouguer anomaly values by methods described by Harris et al. (1988, p. 2-4). A density of 2.67 g/cm³ was assumed for the Bouguer and terrain corrections. The terrain corrections for within a distance of 68 m from the station were estimated in the field. Between 68 m to 590 m from the station, the terrain corrections were estimated from 1:24,000 or 1:62,500 scale topographic maps using the Hayford-Bowie system (Hayford and Bowie, 1912). Between 590 m to 166.7 km from the station, the terrain corrections were computed using a digital elevation model and a computer procedure by Plouff (1966, 1977). The accuracy of a terrain correction computed by this three-step procedure is generally assumed to be within 5% of the total terrain correction. Because the largest terrain corrections were about 1.0 mGal, uncertainties of less than 0.05 mGal are expected in the total terrain correction. Therefore, by considering the uncertainties of the observed gravity and the terrain correction, the Bouguer anomaly values are expected to be accurate to within 0.15 mGal. Bouguer anomaly values were reduced to isostatic gravity values by methods described by Simpson et al. (1983). The isostatic correction assumed an Airy-Heiskanen model (Heiskanen and Vening-Meinesz, 1958) with a density of 2.67 g/cm³ for the topographic load, a crustal thickness of 25 km at sea-level, and a lower-crust upper-mantle density contrast of 0.4 g/cm³.

Comparison of Explosive and Vibroseis Shot Records

The Vibroseis survey of Line AV-1 was planned so that the explosive shot hole locations also corresponded to Vibroseis positions. Windspeeds measured at the record time for both explosive and Vibroseis source profiling at the same location are compared in Table 5. This comparison indicates that windspeeds at Stations 1069, 1429, and 1789 were nearly identical for both sources. The records resulting from the two source types for these three stations are compared in Figure 24.

This comparison of coincident common-shot records suggests the superiority of the explosive over Vibroseis sources for profiling the mid- to lower crust in the Amargosa Desert. Even the smallest explosive shot (23 kg) produced lower crustal reflections with higher signal-to-noise ratios than did the Vibroseis array source. Whereas the air wave generated by the Vibroseis array normally obliterated reflection signals directly beneath it, the air wave is generally barely noticeable on the explosive shot records, hence reflections are observable from directly beneath the shot point. Only the explosive shot pattern at Station 1429, employing 4 shallow holes each only 38.1 m (125 ft.) deep, generated large amplitude air wave signals.

Comparison of the uppermost three seconds of coincident explosive and Vibroseis shot records indicates that the explosive and Vibroseis sources provide nearly equivalent records (Figure 25). At Station 1789 (Figure 25b) the explosive source record is superior to the Vibroseis record whereas at Station 1429 (Figure 25a) the Vibroseis record is superior to that of the explosive source record. We believe, however, that the shallower drill holes at Station 1429 (Table 3) may have contributed to higher-amplitude ground roll than observed on the other explosive shot records and may have degraded the uppermost three seconds of the record.

DATA PROCESSING

In the following sections we briefly describe the processing schemes used to obtain reflection sections for Line AV-1 from both the explosive and Vibroseis source data sets. Although it is fair to characterize the final processing schemes used to produce both of these sections as standard, a number of other schemes not used in the final sequence were tested to determine their effect on the final stacks. We note that due to the contrast in the fold of the explosive and Vibroseis data the processing schemes followed for each have important differences. Nonetheless, we have attempted to maintain the same processing schemes for both sections as much as possible, with the most important of these similarities being the use of relative-amplitude processing as opposed to processing using automatic gain control.

Data processing of Explosive Shots

The explosive shot records obtained along Line AV-1 were processed, using DISCO version 7.2 software, into a single-fold seismic reflection section (Figure 26). A demultiplexed SEG-Y format digital magnetic tape containing all the data recorded from the eight explosive shots was made in the field using the truck-mounted field computer. Subsequent processing included: 1) manual editing of shots and traces, 2) merging of the edited data set to insure a continuous single-fold section, 3) application of a

temporal bandpass filter (10-40-Hz), 4) determination and application of an empirical time varying gain to remove the effect of geometrical spreading and attenuation, and 5) application of a whole trace balance. Common-midpoint coverage along the section is continuous between field stations 979 and 1882 (Figure 1c), corresponding to CDP locations 180 to 1985 on the Vibroseis line (discussed below). Corrections for normal-moveout were not applied to the single-fold gathers.

Data Processing of the Vibroseis Records

The Vibroseis shot records obtained along Line AV-1 were processed by Geosource Inc. to produce 0-5 and 0-15 s twtt seismic reflection sections. The processing sequences used by Geosource Inc. are documented in Appendix 3. One of the initial processing steps included the division of the Vibroseis data into a shallow (0-5 s) and a deep (0-15 s) data set. Each data set was processed independently. The 4 msec data included in the processing for the shallow section consisted of traces within 6 km from the Vibroseis source array, resulting in a nominal 60-fold section. The deep section is also nominally 60-fold but was resampled to an 8 msec sample rate.

The routine processing sequence used to produce the initial brute stack of the 0-5 s Vibroseis section is listed in Table 8. Subsequent processing of this section is described in Appendix 3 and included the application of surface-consistent deconvolution, post-stack time-varying band-pass filter, and post-stack migration using 90% of the stacking velocity. The post-stack algorithm used to perform the migration is based on the 15° finite-difference approximation described by Claerbout (1976). The migration velocity was selected from a suite of migrations performed at 10% increments in stacking velocity from 70 to 110%. These tests were performed on the western one-third of Line AV-1. Fan (velocity) filters were tested prior to stack but did not significantly enhance the resulting section and therefore were not included in the final processing. The resulting section is displayed in Figures 28 and 29. Improved stacking velocities yielded the greatest enhancement in the appearance of the stacked section from that produced at the brute stack level of processing.

A similar processing sequence was followed in the generation of preliminary stacked sections for the 0-15 s Vibroseis data for Line AV-1 (Appendix 3). For the most part, parameters selected for the 0-5 s Vibroseis section were also employed for the 0-15 s Vibroseis section. While additional velocity analysis for the 5-15 s portion of the section was required, few other steps needed to be incorporated into the processing scheme used for this section. The significant differences in the preliminary processing of the 0-15 s section included: surface consistent deconvolution was not applied, a 1.5 s long prestack automatic-gain control (AGC)

was applied, a fan filter was applied prior to stack, and the preliminary stack was not migrated.

Based upon a direct comparison of Vibroseis stacks obtained with and without the use of velocity fan-filtering, we do not believe that the reflectivity observed in the lower crust (5-10 s) on the Vibroseis section for Line AV-1 is an artifact of the fan-filtering. Nonetheless, fan-filtering can produce artificial reflection events, as Hamilton (1988) has argued for certain reflection events on Death Valley COCORP data. Because fan-filtering did not dramatically improve the quality of the section, and because fan-filtering may produce spurious events, we decided to eliminate all fan-filtering from the final processing sequence. None of the final seismic reflection sections shown in this report have been fan filtered.

As the initial goal of the processing was to determine the geometry of reflections, all the initial processing incorporated automatic-gain control (AGC) of various window lengths. After selection of processing parameters based on the AGC'd data, another suite of stacks was obtained which attempted to maintain the relative-amplitude content of the section. We note that while reflection continuity at depths of 5-10 s was superior on the Vibroseis section which had been AGC'd than on the relative-amplitude section, there was little or no relative amplitude information on the AGC'd section. The non-AGC'd sections provide important information on the relative strength of reflecting horizons. For this reason, final comparisons of the seismic sections of Line AV-1 obtained from the Vibroseis and explosive sources were made using these relative-amplitude stacks. The 0-15 s Vibroseis section for Line AV-1 is shown in Figure 30; the final processing scheme used to generate this section is provided in Appendix 3.

ANALYSIS OF EXPLOSIVE SOURCE SECTION FOR LINE AV-1

Large-amplitude, discontinuous, and subhorizontal reflection events are observed between 5 and 10 s two-way travel time (twtt) along the explosive source section for Line AV-1 (Figure 26). These events are thought to represent reflections from the mid- to lower-crust on the basis of several lines of evidence. First, as these reflections are present on records obtained using both explosive and Vibroseis sources, they can not be an artifact of either the Vibroseis correlation method or of the explosive source method. Second, the mid- to lower-crustal reflections are clearly not intra-crustal multiple reflections. Third, the lateral continuity of the reflective zone indicates that the reflective zone is observed for more than a single shot-receiver array configuration arguing against the arrivals originating as an artifact of the recording instrumentation.

The reflection amplitudes within the reflective zone between 5 and 10 s are neither spatially nor temporally uniform (Figure 26). In places a strong reflection doublet is observed, with subparallel reflections separated by 0.7 s. Elsewhere either a single reflection or a complex set of reflections is observed. An unusually strong reflection occurs at 8.4 s near CDP 1200 (Station 1492), where amplitude versus travel time plots indicate that the reflection is at least 8 dB above the general amplitude decay curve (Figure 27). This reflection event will be discussed later in relation to similar results observed elsewhere in the Basin and Range Province.

While the reflections within the reflective zone in the lower crust are generally subhorizontal, there is an important exception beneath Station 1549. In this location a reflection rises to the east from an initial depth of 8.4 s to a depth of 7.4 s near Station 1613 (for a total rise of approximately 3 km), over a distance of only 1.6 km. Although a major portion of this apparent dip may result from velocity-pull-up, part may reflect true dip in the mid-crust.

Above and below the reflective interval between 5 and 10 s, there is a lesser number of lower-amplitude, discontinuous, and subhorizontal reflection events. While the events above 7 s suggest that the middle crust is weakly reflective, the low-amplitude events below 10 s are probably best interpreted as resulting from intracrustal multiple reflections and possibly from side-scattered energy.

The base of the crust is not defined by a single nearly continuous Moho reflection, but rather is poorly defined by the absence of large-amplitude reflection events below 9 to 10 s. Assuming an average crustal velocity of 6.0 km/s, this travel time would indicate a crustal thickness of 27 to 30 km. Limited and unreversed refraction data suggest a crustal thickness of approximately 35 km, and the crustal model inferred for these data suggest a total two-way travel time through the crust of 12 s (Hoffman and Mooney, 1984). The resolution of this apparent disagreement of the seismic methods must await the planned acquisition of longer reversed refraction data within the Amargosa Desert.

COMPARISON OF LINE AV-1 TO OTHER DATA SETS

Apart from the subjective interpretation of the profiles themselves, a more objective means of assessing the quality of the reflection profiles acquired along Line AV-1 is to compare them to other data sets acquired either nearby or elsewhere within the Basin and Range. Firstly, the reflection profiles can be contrasted with structural models inferred from coincident seismic refraction and gravity profiles to determine whether the structures

inferred from the reflection profiles are reasonable. Secondly, the coincident explosive and Vibroseis source profiles for Line AV-1 image the identical structure, thus their comparison ought to lead to strong conclusions concerning both the two methods used and the resulting images. Thirdly, the reflection profiles can be compared to those obtained using identical methods elsewhere in the Basin and Range Province to determine whether the structures they image are comparable. One of the more interesting similarities between Line AV-1 and the Death Valley COCORP reflection profiles is the existence of a lower crustal bright spot within the Amargosa Desert. In the remainder of this section we present these comparisons.

Comparison of the Vibroseis Stacked Section for Line Av-1 with Existing Refraction Model

The final processed versions of the Vibroseis profiles for Line AV-1 present a classic image of Basin and Range Province structure. The post-stack migrations of the 0-5 s Vibroseis section for Line AV-1 reveals two broad asymmetric sedimentary basins bounded by three basement horst blocks (Figure 29). In a qualitative sense the locations of the horsts and grabens as well as the depth of the grabens as inferred from the reflection section compare favorably with the structure in Figure 23 determined from the coincident refraction profiling (Mooney and Schapper, 1988). This comparison was quantified by calculating normal-incidence synthetic seismograms from the refraction model for the crustal structure shown in Figure 23 using two-dimensional ray theory. The synthetic seismograms were generated by the AIMS/Release 3.0 Level 3.3 software package, owned and leased by Geoquest International of Houston, Texas. This synthetic comparison enabled us to quantitatively compare observed reflection travel times for Line AV-1 with those predicted by the refraction model. In the remainder of this section we present a more detailed discussion of the Basin and Range structures imaged by the Vibroseis and refraction profiles.

Refraction mapping of acoustic basement, where acoustic basement is defined arbitrarily here as having compressional wave velocities of 4.2 km/s and greater, indicates that it has over 1 km of vertical relief along Line AV-1 (Figure 23) (Mooney and Schapper, 1988). Low relief (less than a few hundred meters high) basement horsts are inferred from the refraction data between Stations 1149 and 1189, 1669 and 1709, and 1900 and 1949. The horsts are separated by basins more than several hundred meters thick. In general, the thickness of basin fill inferred from the refraction profiling increases to the west along Line AV-1.

Starting on the western end of Line AV-1, the Vibroseis profiles clearly show a subhorizontal reflection sequence between Stations 889 and 970 extending to a depth of 1.5 s (Figure 29). The reflective sequence dips toward the east and appears to define the eastern boundary of a sedimentary basin extending further to the west in the Amargosa Desert. As shown in Figure 23, low-velocities defining a sedimentary basin are well-imaged by the coincident refraction study (Mooney and Schapper, 1988).

Over a distance of about 8 km (between Stations 970 and 1310) the prominent reflections defining the base of the extensional basins are shallow and are cut by series of reflections defining extensional faults. The reflections from the tops of these blocks, which are each about 1 km wide, appear to dip towards the east whereas the reflections defining the block-bounding faults appear to dip more steeply to the west. Shot hole drilling indicates that Paleozoic sedimentary rocks, locally defining the base of the Tertiary sedimentary fill, lie only 24 m (80 ft.) beneath Station 1189. (Note that this Station also served as the location for Shotpoint 22 for the refraction study reported by Mooney and Schapper 1988). The refraction profiles are also consistent with a broad, shallow horst block in this location, although the reflection profiles provide significantly higher resolution on the structure of this horst block feature.

To the east of this broad, shallow block, the reflection sequence defines a half-graben dipping to the east. This graben is located between Stations 1310 and 1650 and is 8.5 km wide. The reflections near the base of the graben, which dip gently to the east, may correlate to outcrops in the vicinity of Station 1280. The prominent reflections defining the base of this graben are offset in several places. Near the eastern end of the graben the reflective section is nearly 1 s deep, in close agreement with that predicted by the seismic refraction study (Mooney and Schapper, 1988). While the refraction model also indicates that the basin is asymmetric, the reflection profiling provide significant refinements of the geometry of the basin and of the sedimentary fill within it.

The eastern boundary of this half-graben corresponds to a very narrow (1.25 km) wide basement horst block located between Stations 1650 and 1700. The location of this horst block correlates with that of a north-south oriented spur of Paleozoic sedimentary rocks running southward from the Specter Range. While the location of this basement horst block correlates with that of a shallow, high-velocity block inferred from the refraction study, the width of the block inferred from the refraction data is significantly larger than is shown by the reflection data.

This narrow horst block is the western boundary of another thicker sequence of reflections which define a half-graben. Stations between 1700 and 1925 are underlain by a 1.2 s thick sequence of reflections which dips to the west. This sequence of reflections thins to the east, and the event defining the base of the sedimentary reflections indicates that Stations 1925 to 1975 are underlain by shallow basement rocks. While low-velocity material is inferred from the refraction profile for this location, the inferred basin is not asymmetric (Figure 23) and is thus not wholly consistent with the reflection profiles. Reflections from beneath this basin are also present, and these will be discussed in the following section.

Detachment Faults

Subhorizontal and continuous reflections from the upper crust (above 5 s) are observable on records obtained using both explosive and Vibroseis sources. One of the more prominent of these events is located on the eastern half of reflection Line AV-1 at a depth of 3 s. Other less prominent and laterally continuous events are present, one such event lies beneath the middle basin in the center of the line at a depth of 1.5 s. All of these reflection events have reasonable stacking velocities and appear to be valid in-plane reflection events. One possible explanation for these events is that they represent subhorizontal detachment of decollement surfaces whose existence has been proposed by a number of workers (eg. Hamilton, 1988). Some of these detachment surfaces may represent reactivated Mesozoic thrust faults. Other geologic explanations for these reflections are more speculative, and would include frozen upper level magma intrusions (such as sills). Given the inferred importance of detachment surfaces in the Basin and Range, we prefer the interpretation that (at least some of) these reflection events represent detachment surfaces.

Comparison of the Explosive and Vibroseis Sections for Line AV-1

As we previously noted, it is the comparison of the stacked reflection sections themselves which provide the fairest comparison of the Vibroseis and explosive source methods for mapping the lower crust. This comparison should be most favorable to the Vibroseis method which is predicated on the requirements for a high-CDP-fold to enhance signal quality. Images of the lower crust (5-10 s) along Line AV-1 obtained using explosive and Vibroseis sources can be compared in Figures 26 and 30. While both sections have been processed in an attempt to preserve the relative amplitudes between traces along the sections, the explosive source profile is single-fold compared to the 60-fold Vibroseis profile. Even with the 60-times higher fold the reflections from the lower crust imaged on the stack of the Vibroseis data have lower signal-to-noise ratios and less spatial continuity than do those imaged by the explosive sources.

These general observations can be illustrated by a few specific examples. Consider three segments of the two profiles between CDPs 1050-1250, 1400-1600, and 1825-2025. Each of these segments is exactly 2.5 km long. In each of these segments the explosive source profile clearly reveals a zone of high-amplitude reflections between 7.5 and 8.5 s depth. In the first segment of the explosive source profile at least two strong reflections are observed in this depth range. In contrast, the Vibroseis source profile shows only faint, discontinuous reflections from the same depth ranges. This relationship is also true for the second segment. On the last of these segments the amplitudes of the reflections on the Vibroseis profile are more comparable to those observed on the explosive source profile, but the reflections on the Vibroseis profile are not as laterally continuous. Comparison of these segments, however, documents that higher-quality reflection data from the lower crust was obtained using explosive sources in sedimentary basins.

Considering that future reflection studies near Yucca Mountain may be regional in scope, it is interesting to compare portions of the reflection profiles for which the lower crust is overlain by basement horst blocks. A limited portion of the explosive source reflection profile (CDPs 770 to 900) was acquired using a shot in a horst block. Comparison of the profiles between CDPs 770 and 900 indicates that the explosive sources also provided higher-quality lower crustal data for shots in basement horst blocks.

We believe that several observations account for the relative superiority of the lower crustal section made using the explosive sources. First, the complexity of the near-surface (upper 1-2 s) geology in the Basin and Range introduces large time perturbations (statics) into the reflections from the lower crust which are difficult to accurately recover and remove. Thus, in such structure, CDP stacking of 60 traces may not provide the expected theoretical advantages. Second, vibrator-ground resonance problems and the large-amplitude air wave on the Vibroseis data generally made traces near the source array useless for the stack of the lower crust. Third, the quality of lower crustal reflections produced by the Vibroseis array was more sensitive to the wind speed than those of the dynamite records, and significantly degraded whenever the windspeed exceeded 8-10 mph, which occurred frequently during the study (Appendix 1). The explosive sources, being more energetic than the individual Vibroseis sweep efforts, were less sensitive to wind conditions. Thus, this comparison supports the hypothesis that in complex terrain, where traditional assumptions used in the CDP method are commonly violated, impulsive sources provide a more useful means of imaging the lower crust than a larger number of weaker sources.

Comparison with Nearby Deep Reflection Profiling Studies

The Consortium for Continental Reflection Profiling (COCORP), the California Consortium for Crustal Studies (CALCRUST), and the Program for Array Seismic Studies of the Continental Lithosphere (PASSCAL) have acquired a series of regional deep crustal profiles which nearly encircle the NTS (Figure 31). COCORP has performed an E-W transect across northern Nevada at a latitude of 40°N (Allmendinger et al., 1987), a more southerly E-W transect which includes a segment in the Mojave Desert, California (Cheadle et al., 1986), a segment in the southern half of Death Valley, California (deVoogd et al., 1986; Serpa et al., 1988), and a segment in Western Arizona across the transition zone to the Colorado Plateau. A small gap in the southern COCORP transect at the longitude of the NTS is partially filled by CALCRUST profiling near the Whipple Mountains in SE California (Heney et al., 1987), and by Line AV-1, reported here. Both the COCORP and CALCRUST surveys relied on Vibroseis sources. The central part of the COCORP 40° transect has been resurveyed by PASSCAL using a variety of seismic methods (1986 PASSCAL Basin and Range Lithospheric Seismic Experiment Working Group, 1988).

The reflection data acquired along these transects strongly resemble those from Line AV-1 in the sense that they generally provide evidence for a reflective lower crust. While the depth to the top of the reflective lower crust varies, these regional transects provide evidence for large-amplitude, discontinuous, subhorizontal reflection events from depths between 4 and 10 s twtt.

No such uniformity results from the images of the reflection Moho obtained along the two transects. The Death Valley COCORP survey imaged the reflection Moho as a distinct event only a few cycles long centered at 10 s (Serpa et al., 1988). The reflection Moho was imaged on the northern end of Mojave COCORP survey as a horizontal reflection sequence up to 1 s thick to a depth of 10 s (Cheadle et al., 1986). Along the 40°N Nevada COCORP transect the reflection Moho is a sharp, large amplitude event (Klemperer et al., 1986). A remarkable feature of the reflection Moho on the 40°N transect is the apparent splitting of the Moho into 2 distinct reflections as much as 1.2 s apart (Klemperer et al., 1986). In contrast, the reflection Moho is ill-defined along the CALCRUST Whipple Mountain Survey (Heney et al., 1987) and along the piggyback reflection survey in Western Arizona (E. Goodwin, pers. comm., 1988). The absence of a clear Mono reflection in Western Arizona is similar to that found for Line AV-1.

Comparison of the Line Av-1 Lower Crustal Bright Spot to other Bright Spots

An unusually high-amplitude reflection within the lower crust was observed on the explosive source profile for Line AV-1 at a depth of 8.4 s on a laterally restricted segment of the line centered on CDP 1200. On a common-shot gather the amplitude of this bright spot reflection is approximately 8 dB above the background of the average amplitude versus travel time decay (Figure 27). In many respects, but particularly because of its high-amplitude above the background, this reflection is similar to lower crustal bright spots imaged by COCORP in Death Valley, California, and near Socorro, New Mexico, in the Rio Grande rift (deVoogd et al., 1986). Both of these bright spots have been interpreted as reflections from thin, discontinuous molten magma chambers, based largely on the apparently high reflection coefficient of the Socorro bright spot (Brown et al., 1979; Brocher, 1981) and other geophysical evidence (Sanford et al., 1977).

In Death Valley and in the Rio Grande rift the bright spot is observed at a depth of 6 s, at or near the top of the reflective lower crust, whereas in the Amargosa Desert the bright spot is found nearly 2.4 s deeper, within the middle of the reflective lower crust. The significance of this observed difference is poorly understood at this time.

While it is possible to explain the high amplitude of the Amargosa Desert bright spot as a reflection from a magma chamber, there are other explanations which may account for this high amplitude. The most likely of these explanations is that the bright spot represents a composite or interference reflection from a large number of thin and highly-laminated solid horizons. Solid-solid boundaries are capable of producing high-amplitude reflections if there is a sufficient number of them separated vertically by distances expected to produce reflections at about 20 Hz. This explanation for the Death Valley bright spot was proposed by Hamilton (1988), who suggested that the lamination resulted from the Miocene crustal extension. Lateral variations in the thicknesses and compositions of these lamination may explain the laterally restricted characteristics of the bright spot reflection. Alternatively, the lateral restriction of the bright spot may result from focusing of the upcoming wavefront from the lower crust due to irregular topography within the subsurface. Until each of these and other possibilities is examined and eliminated, we do not at this time prefer the interpretation of the Amargosa Desert bright spot as representing the reflection from a magma chamber.

Comparison of Gravity Models to Line AV-1

A two-dimensional gravity model along Line AV-1 was obtained using a modeling program described by Saltus and Blakely (1983). As described above, Line AV-1 is coincident with a 65-km-long refraction model (Mooney and Schapper, 1988) between the ranges of 13 to 40 km. The geometry and P-wave velocities of the refraction model were used to define the geometry and densities of the gravity model. Edge effects of the gravity model were removed by extending the model beyond the ends of Line AV-1 to the ranges of 0 and 65 km on the refraction model. Prior to forward modeling, a 35 mGal constant and -0.25 mGal/km gradient was subtracted from the isostatic anomaly values to remove a regional trend, which presumably reflects a source deeper than that defined by the refraction data.

Initially, the geometry of the gravity model was constrained to have the geometry of the refraction model with modifications to account for topography (Figure 32). The densities of the units were estimated from the P-wave velocities using the P-wave velocity-density conversion curve of Nafe and Drake (Grant and West, 1965, p. 200). Because this conversion curve was based on core samples of marine sedimentary rocks, the basin fill unit and the basement unit immediately underlying the basement fill were adjusted to more probable densities. The density contrast at the basin fill-basement interface has the largest effect on the amplitude of the gravity anomaly, therefore, better estimates of these densities were made by fitting the amplitudes of the observed and calculated gravity anomalies. Figure 32 represents the best fit that could be obtained between the observed and calculated gravity anomalies by a gravity model constrained to have the geometry of the refraction model of Mooney and Schapper (1988).

In Figure 32, the misfit between the observed and calculated gravity is mainly due to the shape of the basin fill-basement interface. In Figure 33, the misfit is very small, and the geometry of the gravity model differs from the refraction model only in the shape of the basin fill-basement interface. Thus, in Figure 33, the gravity model relied on the geometrical constraints of the refraction model where density contrasts are small (within the basin fill and within the basement) and was allowed geometrical changes only where the density constraints are large (at the basin fill-basement interface). This procedure minimized the changes to the geometry of the refraction model necessary to fit the gravity data, which was desired due to the non-uniqueness of gravity interpretation.

The gravity model indicates four narrow basement highs between 15 and 21 km (Figure 33). These basement highs correlate with four similar highs in the seismic reflection data (Figure 28 or 29). Because the gravity highs (1-2 mGal) associated with the basement highs are several times larger than the accuracy of the gravity

anomaly values (0.15 mGal), they are probably not related to errors in gravity measurement and reduction. However, these gravity highs may be related to unmapped variations in density within the basin fill. The gravity model also indicates a basement peak at 33 km. Because of the shortness of the wavelength of the gravity anomaly, and in better agreement with the reflection data (Figure 29), this basement high is modeled in Figure 33 as being narrower and steeper-sided than the corresponding basement high in the refraction model (Figure 32).

Between 38 and 39 km the refraction model indicates basement near the surface (Figure 32). West of 38 km in the refraction model, the basin fill-basement contact dips at about 18° W into a "V" shaped basin. In agreement with reflection profile, the gravity model in Figure 33 suggests that the basement is near the surface at 39.2 km and that the basin fill-basement contact dips more steeply at about 30° W into a flat-bottomed basin. The extension of this dipping contact to depth is nearly coincident with a contact defined by the refraction model between the 2.75 g/cm³, the 2.60 g/cm³, and the 2.67 g/cm³ units. This dipping feature may represent a normal fault bounding the basin and extending to several km in depth.

This interpretation demonstrates the usefulness and importance of integrated gravity and seismic interpretations. For example, gravity detected the four basement peaks that were not interpreted in the refraction model, but were later detected in the reflection data. The refraction model shows contacts with small density contrasts that normally cannot be interpreted by gravity alone. At the basin fill-basement interface, where there are clear P-wave velocity and density contrasts, it is evident that refraction and gravity can yield different interpretations. Combined geophysical interpretations can define complementary models, and permit more confident and detailed geological interpretations.

SUMMARY AND CONCLUSIONS

Extensive field testing of methods for deep crustal seismic reflection profiling was performed in two different locations within the Amargosa Desert, Nye County, Nevada, in January, 1988. Upon completion of the detailed testing of Vibroseis acquisition parameters, a 27-km-long 60 fold Vibroseis reflection profile was acquired along east-west trending Line AV-1 south of Lathrop Wells. During the acquisition of this profile 8 explosive shot holes were fired to obtain a single-fold explosive profile to compare to the Vibroseis profile. Both Vibroseis and explosive sources provided high-quality reflections in the depth range between 0-5 s.

The first 5 s of the 60-fold Vibroseis profile along Line AV-1 reveals typical extensional structures similar to those imaged elsewhere in the Basin and Range Province. To be more specific, the reflection profiles define broad asymmetric half-grabens bounded by extensively faulted horst blocks. Comparison of the migrated reflection profile with coincident seismic refraction and gravity anomaly profiles demonstrates the importance of the acquired reflection data. Although variations in the depth to the base of inferred Tertiary sediments can be correlated between models derived from each data set, the seismic reflection profiles provide much greater structural detail than either the gravity or seismic refraction data. Beneath the base of the inferred Tertiary sedimentary section, steeply dipping reflections appear to define normal or reverse faults within the Paleozoic basement which are in turn underlain by subhorizontal reflections which may represent detachment surfaces.

Both large explosive and Vibroseis sources provided useful reflection energy to depths of 8 to 9 s twtt. The 45 to 91-kg (100-200 lb.) explosive sources in single shot holes, however, provided significantly higher-quality images of the crust below 5 s. This explosive source profile reveals an image of the lower crust which appears to be characteristic of the Basin and Range Province. There are pronounced along-profile variations in the seismic character of the lower crust. The top of the lower reflective crust varies between 5 and 6 s and the reflective sequence varies in thickness between 2 and 4 s. The Moho is defined only by the absence of large-amplitude reflections below 9 to 10 s.

Based solely on the criterion of the quality of the deep crustal seismic profiles, the optimal method for future reflection surveys in the vicinity of Yucca Mountain would employ explosive sources for low-fold profiling. If the use of explosive sources proves impractical in some locations, however, the Vibroseis (or possibly the land air gun) method provides high-quality reflection data to a depth of 5 s. Augmentation of the Vibroseis sources with explosive sources at an interval sufficient to produce a single-fold stack should provide a practical and cost-effective

means of imaging both the upper and lower crust simultaneously.

ACKNOWLEDGMENTS

Eric Geist assisted the field reconnaissance of possible line locations, assembled and tested the windspeed meter hardware, and with Jon Childs, assisted in the field work. Warren Lyle of Petty-Ray Geophysical Division of Geosource, Inc. helped to design and evaluate the field parameter testing and generated Figures 2 through 4. Field data were collected by Crew 6806 of Petty-Ray. Data processing of the Vibroseis data for Line AV-1 was performed by Mike Vervalin of Petty-Ray. Shot hole drilling and loading was performed by Ken Heidl and Cary Jackson of Bertram Drilling, Inc. Windspeed records at Indian Springs Air Force Base and Yucca Mountain were provided by Sam McCown of the National Oceanic and Atmospheric Administration (NOAA) and Hugh Church of Sandia National Laboratory, respectively. Funding for this investigation was provided by the Department of Energy (DOE). We thank Eric Geist and Mike Moses for critical reviews of previous versions of the report.

References

Allmendinger, R. W., T. A. Hauge, E. C. Hauser, C. J. Potter, S. L. Klemperer, K. D. Nelson, P. Knuepfer, and J. Oliver, Overview of the COCORP 40°N Transect, Western United States: The fabric of an organic belt, *Geol. Soc. Amer. Bull.*, 98, 308-319, 1987.

Brocher, T. M., Geometry and physical properties of the Socorro, New Mexico, magma bodies, *J. Geophys. Res.*, 86, 9420-9432, 1981.

Brown, L. D., P. A. Krumhanse, L. E. Chapin, A. R. Sanford, F. A. Cook, S. Kaufman, J. E. Oliver, and F. S. Schilt, COCORP seismic reflection studies of the Rio Grande Rift, in Riecker, R. E., Ed., Rio Grande rift: tectonics and magnetism, Washington, D. C., American Geophysical Union, p. 169-185, 1979.

Carr, M. D., Geologic setting of Yucca Mountain, U. S. Geological Survey Open-File Report, in review.

Cheadle, M. J., B. L. Czuchra, T. Byrne, C. J. Ando, J. E. Oliver, L. D. Brown, S. Kaufman, P. E. Malin, and R. A. Phinney, The deep crustal structure of the Mojave Desert, California, from COCORP seismic reflection data, *Tectonics*, 5, 293-320, 1986.

Claerbout, J. F., Fundamentals of geophysical data processing, New York, McGraw-Hill, 274 p., 1976.

deVoogd, B., L. Serpa, L. Brown, E. Hauser, S. Kaufman, J. Oliver, B. W. Troxel, J. Willemin, and L. A. Wright, Death Valley bright spot: A midcrustal magma body in the southern Great Basin, California?, *Geology*, 14, 64-67, 1986.

Grant, F. S., and G. F. West, Interpretation theory in applied geophysics, McGraw-Hill Book Company, 200 p., 1965.

Hamilton, W., Detachment faulting in the Death Valley region, California and Nevada, U. S. Geol Surv., Bulletin 1790, in press, 1988.

Harris, R. N., Healy, D. L., Ponce, D. A., and Oliver, H. W., Principal facts for about 15,000 gravity stations in the Nevada Test Site and vicinity: U.S. Geological Survey Open-File Report 88-XXX, 43 p., 1988.

Hauser, E. C., J. Gephart, T. Latham, J. Oliver, S. Kaufman, L. Brown, and I. Lucchitta, COCORP Arizona transect: Strong crustal reflections and offset Moho beneath the transition zone, *Geology*, 15, 1103-1106, 1987.

Hayford, J. R., and Bowie, W., The effect of topography and isostatic compensation upon the intensity of gravity: U.S. Coast and Geodetic Survey Special Publication No. 10, p. 132, 1912.

Healy, D. L., R. R. Wahl, and H. W. Oliver, Death Valley Sheet, Bouguer Gravity Map of Nevada, Nevada Bureau of Mines and Geology, Map 69, scale 1:250,000, 1980.

Heiskanen, W. A., and Vening Meinesz, F. A., The earth and its gravity field, McGraw-Hill Book Company, Inc., New York, 470 p., 1958.

Heney, T. E., D. A. Okaya, E. G. Frost, and T. V. McEvilley, CALCRUST (1985) seismic reflection survey, Whipple Mountains detachment terrane, California: An overview, *Geophys. J. R. astr. Soc.*, 89, 111-118, 1987.

Hoffman, L. R., and W. D. Mooney, A seismic study of Yucca Mountain and vicinity, Southern Nevada; Data report and preliminary results, U. S. Geological Survey, Open-File Report 83-588, 50 pp., 1984.

Klemperer, S. L., A relation between continental heat-flow and the seismic reflectivity of the lower crust, *J. Geophys.*, 61, 1-11, 1987.

McCarthur, R. D., and N. D. Burkhart, Geological and geophysical investigations of Mid-Valley, Lawrence Livermore National Laboratory UCID 20740, 92 pages, 1986.

McGovern, T. F., L. W. Pankratz, and H. D. Ackerman, An evaluation of seismic reflection studies in the Yucca Mountain area, Nevada Test Site, U. S. Geological Survey, Open-File Report 83-912, 58 p., 1983.

Mooney, W. D., and S. G. Schapper, Seismic refraction profiles, in Report on the Status of regional geophysics: NNWSI program, U. S. Geological Survey, Open-File Report , in press.

Mooney, W. D., and T. M. Brocher, Coincident seismic reflection/refraction studies of the continental lithosphere: A global review, *Rev. Geophysics*, 25, 723-742, 1987.

The 1986 PASSCAL Basin and Range Lithospheric Seismic Experiment Working Group, The 1986 PASSCAL Basin and Range Lithospheric Seismic Experiment, *EOS, Trans. Amer. Geophys. Un.*, v. 69, n. 20, p. 593, 596-598, 1988.

Morelli, C., The International Gravity Standardization Net, 1971, International Association of Geodesy Special Publication No. 4, 194 p., 1974.

Plcuff, D., Digital terrain correction based on geographic coordinates [abs.]: *Geophysics*, v. 31, no. 6, p. 1208, 1966.

_____, Preliminary documentation for a FORTRAN program to compute gravity terrain corrections based on topography on a geographic grid: U.S. Geological Survey Open File Report 77-535, 45 p., 1977.

Saltus, R. W., and Blakely, R. J., HYPERMAG-an interactive, two dimensional gravity and magnetic modeling program: U.S. Geological Survey Open-File Report 83-241, 28 p., 1983.

Sanford, A. R., R. P. Mott Jr., P. J. Shuleski, E. J. Rinehart, F. J. Caravella, R. M. Ward, and T. C. Wallace, Geophysical evidence for a magma body in the crust in the vicinity of Socorro, New Mexico. *The Earth's Crust: It's Nature and Physical Properties*, Ed. by J. G. Heacock, p. 385-404, American Geophysical Union, Washington, D. C., 1977.

Serpa, L., B. de Voogd, L. Wright, J. Willemin, J. Oliver, E. Hauser, and B. Troxel, Structure of the central Death Valley pull-apart basin from COCORP profiles in the southern Great Basin, *Geological Society of America Bulletin*, v. 100, 1437-1450, 1988.

Simpson, R. W., Jachens, R. C., and Blakely, R. J., AIRYROOT: a FORTRAN program for calculating the gravitational attraction of an Airy isostatic root out to 166.7 km: U.S. Geological Survey Open-File Report No. 83-883, 66 p., 1983.

Sutton, V. D., Data report for the 1985 seismic-refraction experiment at Yucca Mountain and vicinity, Southwestern Nevada, U. S. Geological Survey Open-File Report 85-591, Menlo Park, 1985.

Winograd, I. J., and W. Thordarson, Hydrogeologic and hydrochemical framework, South-Central Great Basin, Nevada-California, with special reference to the Nevada Test Site, U. S. Geological Survey Professional Paper 712-C, 126 pp., 1975.

Table 1: Acquisition Parameters for Line AV-1

Recording Instrumentation:	MDS-16 with fiber optic cables and full-word recording
Source Array:	Four Failing Y2000 Vibroseis trucks, each providing a peak force of 44511 lbs. with force control and phase loop locking
Source pattern:	Four vibrators in a 12-element pattern, with a pad spacing of 47.9 feet and an 8 foot move-up between sweeps for a total pattern length of 231 feet.
Vibrator Control Electronics:	Geosource SHV-310C
Sweep frequency:	10 to 44 Hz upsweep with a 0.25 s taper
Sweep length:	24 seconds
Listen time:	15 seconds
Record length:	39 seconds
Field Filters:	Low cut 9 Hz/36 dB octave; high cut (Anti-alias) 62.5 Hz; Notch out
No. sweeps per VP:	12
VP interval:	100 m
Receiver pattern:	24 geophones, deployed in two strings of 12 geophones overlapped by 7 geophones, with overlap centered on the pin flag.
Receiver pattern length:	50 m
Receiver group spacing:	25 m
Geophone type:	Geosource, 10 Hz
No. active channels:	480
Receiver array configuration:	Symmetric split spread, ± 6 km with no center gap
CDP fold:	60
Recording format:	SEG-D at 6250 BPI

Table 2 : Locations of Cultural Noise along Line AV-1

<u>station</u>	<u>Noise Source*</u>
971	State Highway 373
973	Buried cable and overhead singlepole 4 wire line
1013	Single pole power-line
1025	Houses approximately 1/4 mile north of line
1049	Double-pole power line
1918	Buried Cable

*Note that without exception all cables, lines and roads are orthogonal to Line AV-1.

Table 3: Explosive Shot Parameters for Line AV-1

Seismic Record No.	Shot Station No.	Date in 1988	Approx. Local Time	Shot Size (lbs.)	No. of Caps	Shot depth (ft.)	Active Station No.'s	Wind-Speed (mph)
47	1065	1/15	1057	50	2	250	889-1484	7-9
48	1067	1/15	1114	100	2	250	889-1484	6-8
49	1069	1/15	1122	200	3	250	889-1484	4-5
50	1189*	1/15	1140	2x200	5	250	889-1484	4-5
136	1309	1/19	1340	200	5	250	1050-1587	1-2
137	1429	1/19	1410	4x50	8	125	1050-1587	6-9
197	1549	1/21	1121	200	8	250	1286-1819	3-5
251	1790	1/23	1020	200	4	250	1390-1975	1-3

*This shot was located within 10 m of Shotpoint 22 reported by Mooney and Schapper (1988).

Table 4 : Uphole Times and Velocities for Explosive Shots Along Line AV-1

Shot Station No.	Uphole Time (s)	Depth to First Cap (feet)	Depth to Top of Uphole Charge (ft)	Velocities* ft/s	Velocities* m/s
1065	0.070	230	228	3257	993
1067	0.057	210	206	3614	1102
1069	0.050	164	162	3240	988
1189	0.025	164	162	6480	2314
1309	0.030	164?	162	5400	1646
1429	0.025	105?	103	4120	1256
1549		164?	162		
1790		164?	162		

*Based on depth to top of the charge.

?Indicates uncertainty due to absence of detailed notes in driller's log.

Table 5: Comparison of Measured Windspeeds During Acquisition of Explosive and Vibroseis Shot Records

Shot Station No.	Windspeed during Explosive Shot (mph)	Windspeed during Vibroseis Record (mph)
1065	7-9	-
1069	4-5	5-6
1189	4-5	8-11
1309	1-2	9-12
1429	6-9	4-5
1549	3-5	-
1789	1-3	2-5

TABLE 6.—Principal Facts for gravity data on line AV1.

STATION NAME	LAT deg min	LON deg min	ELEV ft	OG mGal	AC	FAA mGal	SBA mGal	ITC mGal	TC mGal	CBA 2.67	ISO 2.67
AV1-0889	36 34.39	116 28.10	2452.9	979601.99	P313	-35.08	-118.74	0.00	D	0.07	-119.57
AV1-0908	36 34.38	116 25.78	2457.2	979602.06	P313	-34.60	-118.41	0.00	D	0.07	-119.24
AV1-0924	36 34.37	116 25.51	2458.2	979602.97	P313	-33.58	-117.42	0.00	D	0.07	-118.25
AV1-0940	36 34.36	116 25.24	2460.4	979604.50	P313	-31.83	-115.75	0.00	D	0.07	-116.57
AV1-0956	36 34.35	116 24.98	2463.6	979606.22	P313	-29.79	-113.82	0.00	D	0.08	-114.04
AV1-0972	36 34.34	116 24.71	2466.2	979608.07	P313	-27.68	-111.80	0.00	D	0.08	-112.62
AV1-0988	36 34.33	116 24.44	2465.1	979609.90	P313	-25.94	-110.02	0.00	D	0.08	-110.84
AV1-1004	36 34.33	116 24.17	2467.4	979611.83	P313	-23.79	-107.95	0.00	D	0.08	-108.77
AV1-1020	36 34.32	116 23.90	2471.1	979614.58	P313	-20.69	-104.97	0.01	D	0.10	-105.77
AV1-1036	36 34.31	116 23.64	2463.8	979614.88	P313	-21.00	-105.09	0.00	D	0.10	-105.89
AV1-1052	36 34.30	116 23.37	2464.9	979614.01	P313	-21.81	-105.88	0.00	D	0.11	-106.67
AV1-1068	36 34.30	116 23.10	2464.9	979614.37	P313	-21.46	-105.52	0.00	D	0.12	-106.30
AV1-1084	36 34.29	116 22.83	2465.7	979615.21	P313	-20.52	-104.62	0.00	D	0.13	-105.39
AV1-1100	36 34.28	116 22.56	2464.8	979616.12	P313	-20.68	-104.74	0.00	D	0.14	-105.51
AV1-1116	36 34.28	116 22.29	2472.3	979614.21	P313	-20.88	-105.20	0.00	D	0.14	-105.97
AV1-1132	36 34.27	116 22.03	2482.2	979615.16	P313	-18.99	-103.65	0.00	D	0.14	-104.41
AV1-1148	36 34.26	116 21.76	2493.1	979616.22	P313	-16.88	-101.92	0.01	D	0.16	-102.67
AV1-1164	36 34.25	116 21.49	2501.9	979614.46	P313	-17.82	-103.15	0.01	D	0.16	-103.90
AV1-1180	36 34.25	116 21.22	2515.2	979614.76	P313	-16.28	-102.05	0.00	D	0.16	-102.80
AV1-1196	36 34.24	116 20.95	2533.8	979613.46	P313	-15.81	-102.23	0.00	D	0.16	-102.99
AV1-1212	36 34.24	116 20.69	2547.0	979610.82	P313	-17.19	-104.06	0.00	D	0.16	-104.83
AV1-1228	36 34.23	116 20.42	2554.3	979609.57	P313	-17.74	-104.86	0.00	D	0.16	-105.63
AV1-1244	36 34.22	116 20.15	2563.6	979609.18	P313	-17.24	-104.68	0.00	D	0.16	-105.45
AV1-1260	36 34.22	116 19.88	2568.7	979609.08	P313	-16.86	-104.47	0.00	D	0.15	-105.25
AV1-1276	36 34.21	116 19.61	2574.8	979608.52	P313	-16.83	-104.65	0.00	D	0.15	-105.43
AV1-1292	36 34.21	116 19.34	2602.7	979606.85	P313	-16.88	-105.65	0.02	D	0.16	-106.43
AV1-1308	36 34.21	116 19.08	2643.1	979602.85	P313	-16.08	-106.23	0.02	D	0.16	-107.02
AV1-1324	36 34.19	116 18.81	2649.2	979601.74	P313	-16.59	-106.95	0.02	D	0.17	-107.73
AV1-1340	36 34.16	116 18.54	2614.6	979602.88	P313	-18.06	-107.84	0.02	D	0.17	-108.61
AV1-1356	36 34.14	116 18.28	2604.6	979602.25	P313	-20.20	-109.03	0.01	D	0.17	-109.80
AV1-1372	36 34.15	116 18.01	2598.1	979601.53	P313	-21.55	-110.16	0.02	D	0.19	-110.91
AV1-1388	36 34.16	116 17.75	2592.5	979600.88	P313	-22.74	-111.16	0.01	D	0.19	-111.91
AV1-1404	36 34.11	116 17.48	2584.3	979600.04	P313	-23.68	-111.82	0.00	D	0.19	-112.57
AV1-1420	36 34.07	116 17.22	2576.3	979600.31	P313	-24.70	-112.57	0.00	D	0.20	-113.30
AV1-1436	36 34.02	116 16.96	2571.1	979599.95	P313	-25.48	-113.17	0.01	D	0.22	-113.88
AV1-1454	36 33.94	116 16.68	2551.6	979600.64	P313	-26.50	-113.53	0.02	D	0.25	-114.21
AV1-1470	36 33.84	116 16.44	2544.3	979600.72	P313	-26.97	-113.75	0.01	D	0.25	-114.42
AV1-1486	36 33.76	116 16.19	2527.6	979601.37	P313	-27.77	-113.98	0.01	D	0.27	-114.63
AV1-1500	36 33.68	116 15.98	2517.5	979601.70	P313	-28.28	-114.14	0.00	D	0.27	-114.79
AV1-1516	36 33.60	116 15.73	2514.2	979601.79	P313	-28.38	-114.14	0.01	D	0.29	-114.76
AV1-1532	36 33.51	116 15.48	2494.0	979603.08	P313	-28.86	-113.93	0.01	D	0.31	-114.52
AV1-1548	36 33.43	116 15.23	2486.0	979603.60	P313	-28.89	-113.68	0.00	D	0.32	-114.26
AV1-1564	36 33.35	116 14.99	2472.9	979604.76	P313	-28.94	-113.28	0.00	D	0.33	-113.86
AV1-1580	36 33.26	116 14.74	2460.1	979605.98	P313	-28.79	-112.70	0.00	D	0.35	-113.25
AV1-1596	36 33.18	116 14.49	2448.3	979606.90	P313	-28.80	-112.37	0.01	D	0.39	-112.87
AV1-1612	36 33.10	116 14.24	2437.9	979607.67	P313	-28.95	-112.10	0.01	D	0.42	-112.58
AV1-1628	36 33.01	116 14.00	2434.6	979607.97	P313	-28.84	-111.88	0.00	D	0.43	-112.34
AV1-1644	36 32.93	116 13.75	2431.3	979609.14	P313	-27.86	-110.79	0.00	D	0.45	-111.23
AV1-1668	36 32.86	116 13.53	2426.4	979612.27	P313	-25.00	-107.85	0.01	D	0.49	-108.25
AV1-1674	36 32.79	116 13.28	2433.7	979615.62	P313	-20.95	-103.96	0.04	D	0.52	-104.33
AV1-1690	36 32.77	116 13.02	2442.7	979613.61	P313	-22.09	-105.41	0.02	D	0.51	-105.79
AV1-1706	36 32.70	116 12.77	2448.0	979610.09	P313	-25.01	-108.51	0.00	D	0.49	-108.91
AV1-1722	36 32.58	116 12.55	2449.4	979608.04	P313	-26.75	-110.29	0.00	D	0.49	-110.70
AV1-1738	36 32.58	116 12.28	2455.3	979606.37	P313	-27.87	-111.61	0.00	D	0.50	-112.01
AV1-1754	36 32.60	116 12.02	2465.4	979605.21	P313	-28.11	-112.20	0.00	D	0.52	-112.58
AV1-1770	36 32.63	116 11.75	2479.8	979604.15	P313	-27.86	-112.44	0.00	D	0.53	-112.82
AV1-1786	36 32.66	116 11.48	2492.7	979603.53	P313	-27.31	-112.33	0.00	D	0.55	-112.68
AV1-1802	36 32.69	116 11.22	2506.6	979603.09	P313	-26.49	-111.98	0.00	D	0.56	-112.33
AV1-1818	36 32.70	116 10.96	2517.6	979602.92	P313	-25.64	-111.61	0.01	D	0.59	-111.83
AV1-1834	36 32.65	116 10.71	2527.4	979602.99	P313	-24.57	-110.77	0.00	D	0.59	-111.10
AV1-1850	36 32.71	116 10.46	2542.6	979602.73	P313	-23.49	-110.21	0.01	D	0.63	-110.50
AV1-1866	36 32.78	116 10.21	2557.1	979602.72	P313	-22.24	-109.45	0.01	D	0.65	-109.73
AV1-1882	36 32.84	116 9.94	2570.1	979602.02	P313	-21.20	-108.86	0.01	D	0.69	-109.10
AV1-1898	36 32.91	116 9.69	2589.5	979602.19	P313	-19.90	-108.23	0.01	D	0.72	-108.44
AV1-1914	36 32.98	116 9.44	2609.0	979602.70	P313	-17.66	-106.65	0.01	D	0.74	-106.85
AV1-1929	36 33.02	116 9.19	2625.6	979603.50	P313	-15.37	-104.92	0.00	D	0.76	-105.10
AV1-1946	36 33.06	116 8.91	2651.7	979605.08	P313	-11.38	-101.83	0.01	D	0.77	-102.01
AV1-1962	36 33.14	116 8.67	2669.4	979604.41	P313	-10.51	-101.55	0.01	D	0.80	-101.71
											20.14

TABLE 7.—*Principal Facts for gravity data on Beatty Noise Study line.*

STATION NAME	LAT deg min	LON deg min	ELEV ft	OG mGal	AC	FAA mGal	SBA mGal	ITC mGal	TC mGal	CBA 2.87	ISO 2.67
BNS-0101	36 50.31	116 52.77	3568.3	979560.00	P313	4.81	-116.90	0.01	1.01	-117.06	11.76
BNS-0148	36 50.81	116 52.28	3542.0	979562.62	P313	4.24	-116.57	0.02	0.95	-116.79	12.81
BNS-0164	36 50.98	116 52.12	3530.3	979564.39	P313	4.66	-115.75	0.01	0.93	-115.99	13.87
BNS-0180	36 51.15	116 51.95	3518.2	979566.14	P313	5.03	-114.97	0.00	0.91	-115.22	14.90
BNS-0191	36 51.27	116 51.84	3511.6	979566.89	P313	4.99	-114.78	0.01	0.92	-115.03	15.28
BNS-0224	36 51.62	116 51.50	3502.1	979568.53	P313	5.22	-114.22	0.00	0.90	-114.48	16.36
BNS-0238	36 51.77	116 51.35	3497.2	979569.09	P313	5.11	-114.17	0.01	0.92	-114.41	16.66
BNS-0254	36 51.94	116 51.18	3497.3	979570.35	P313	6.13	-113.15	0.02	0.93	-113.38	17.95
BNS-0269	36 52.10	116 51.03	3498.9	979572.34	P313	7.85	-111.42	0.04	0.97	-111.61	18.97
BNS-0285	36 52.27	116 50.86	3488.6	979573.18	P313	7.66	-111.33	0.02	0.98	-111.50	20.33
BNS-0301	36 52.44	116 50.70	3481.4	979573.41	P313	6.97	-111.77	0.04	1.04	-111.89	20.20
BNS-0324	36 52.69	116 50.46	3484.4	979573.30	P313	6.78	-112.06	0.03	1.09	-112.13	20.34
BNS-0340	36 52.86	116 50.29	3498.7	979572.24	P313	6.82	-112.51	0.05	1.16	-112.51	20.22

DESCRIPTION OF ABBREVIATIONS USED IN TABLES 6 AND 7

OG	observed gravity
AC	accuracy code, see Harris et al. (1988, p. 42)
FAA	free-air anomaly
ITC	terrain correction for Hayford-Bowie zones A thru D, see Hayford and Bowie (1912)
TC	total terrain correction
CBA	complete Bouguer anomaly
ISO	isostatic anomaly

Table 8: Processing Sequence for the 60-fold
Vibroseis Line AV-1 Brute Stack

Demultiplex

Correlation with sweep (performed by field computer)

Temporal Bandpass Filter (10-44 Hz)

Automatic Gain control (1500 msec long window)

Fan Filter (1000-6000 ft/s reject window)

CDP Sort (60-fold)

Datum Statics (to a floating datum)

Velocity Analysis (every 200 CDPS-2.5 km
with velocities between 1500-7000 m/s)

Normal Moveout

Mute (constant for entire line)

Stack

Temporal Bandpass Filter (10-44 Hz)

Fixed window trace balance (500 msec long)

APPENDIX 1: Windspread Records
BEATTY NOISE STUDY "B"
Station 197

<u>Local Time</u>		<u>Wind-Speed (mph)</u>
750	1/7/88	2-5
1030		1-2
1135		3-5
1215		3-4
1310		3-5
1510		3-4
1625		2-3
1719		2
	1/8/88	
853		3-4
945		3-4
1030		3-6
1100		6-7
1140		5-8
1306		3-6
1345		2-4
1450		2
1600		2-2.5
1645		1-1.5
1845		3
	1/9/88	
0800		1.3-1.5
0906		1-2
0955		1-2
1002		2-4

AMARGOSA NOISE STUDY "A"
Station 1089

<u>Local Time</u>	<u>Direction</u>	<u>Windspeed (mph)</u>
1615	1/10/88	1.8
1705		1.6-2.0
1800		1.8-2.1
1852		1.6-1.8

1/11/88

0837		3-4
0939		1-2
1032		4-5
1130		6-8
1135	S	10-15
~24 dB of noise intrusion at this time		
1216		12-14
1230		10-12 Gusts to 20 mph
1235		15-18 Gusts to 20 mph
1305		6-8
1335		10-12
1345		6-8
1405		16-18
1420	N	18-22
1444		15-21 Gusty
1518		15-20 Gusty
1545		18-20
1620		10-16
1700		8-12
1745		3-4
1816		3-4
1914		3-4

1/12/88

0900	N-NE	5-7
0930	NW	3-5
0957	WNW	6-8

At this time the noise intrusion is 24dB

<u>Local Time</u>	<u>Direction</u>	<u>Windspeed (mph)</u>
1023		5-8
1044	NNW	5-8
1102		3-6
1123		3-4
1138	ENE	2-5
1205		2-3
1223		5-6
1246	E	1-2
	with occasional gusts	
1303		3-4
1322		2-5
1346		2

*Note: Prior to 1354L 1/12/88 all seismic record times on the OB sheets are 10 minutes earlier than the local times recorded for windspeeds.

1405	E	1-1.2
1430	S	3-4
1454	SW	4-5
1519	S	3-4
1545	W	2-3
1554	WSW	3
1621	WSW	2-2.5
1640	-	0.0
1658	W	1-1.4
1720	ENE	1.8-2.0
1753	W	2
1830		2.3-2.5
1923	N	1.6-2.5
1955		4-5

Station 1042

1/14/88

0943		1.5-2
1031	E-ENE	0.9-1.4
1142	E	3-4
1238	SWS	3.2-4
1311	S	3.8-4.4
1344	S	2.7-4.2
1407	S	4.6
1448	S	4-5
1528	S	2.0-3.0
1556	SSE	2.4-4.1
1625	SE	1.2-1.6
1653	ESE	2.6-3.4

Local Time Direction Windspeed (mph)

1/15/88

0955	W	2.8-3.6
1026	SW	2.6-5
1036		12dB noise intrusion
1050	W	6-8
1103	W	7-9
1114	WNW	6-8
1125	W-WNW	4-5
1149	W-WNW	4-5
1154	WNW	4-steady
1245	W	3-steady
1327	W	2-4
1407	NW	2
1452	NW	1.2-1.4
1535	E	2-3
1622	NW	2.2-2.5
1700	NW	2-steady

1/16/88

1100	5-6
1200	5-6
1300	8-10 gusts to 15
1330	12-16

Noise intrusion was 18 dB, 24 dB on
some of the western channels

1400	8-14
1500	11-13
1530	10-12
1600	8-11
1630	6-8

Station 1382

1/18/88

0950	WNW	13-14
1005	WNW	8-10
1019	WNW	8-16 Gusty
1115	NW	6-14
1145	W	8-16

1/19/88

0940	NNW	3-4
At 0947 AM the noise intrusion was 12dB peaking to 18 dB		
0947		0
0958	NNE	1.6-4.6
1013	ENE	4.0-6.0
Gusty to 10 mph		
1028	NE	3.6-6.5
Gusty to 9 mph		
1058	NE	3.8-7.8

<u>Local Time</u>	<u>Direction</u>	<u>Windspeed (mph)</u>
1128	W	1.6-4.0
Gusts to 6 mph		
1157	NE	4.0-7.0
Gusts to 8.4 mph		
1231	N	3.0-6.8
1257	N	2.4-4.8
1320	SW	1-2
1408	NE	6-9
1428	NNE	6.0-10.8
1447	NE	8-12 Gusty
1510	NNE	9-12 Gusty
1528	NE	6.6-12 Gusty
1558	NE	6.8-11
Gusts to 13.6 mph		
1627	NNE	5.8-10.6
1655	N	5-8.5
1725	N	4-7

1/20/88

1052	NNW	3.6-6
1121	NW	3-3.5
1222	NW	4-5.5
1240	N-NNW	6-8
1313	NW	2.6-3.5
1343	NW	1.8-4.5
1412	NW	1.2-2.4
1440	N-NNE	3.2-4.6
1510	NW	3.8-5
1540	NNW	3.2-5.4
1610	N-NNE	2.6-3.4
1640	N	2.7-4
1710	NW	2.4-3
1733	NW	5-6
1757	NW	2.4-4.4

1/21/88

0952	SSE	2.4-5.8
12dB peaking to 18dB noise	intrusion at approx. 1000L	
1036	NNE	1.4-4.8
1058	E	3.6-8.2
1120	S	3.0-5.0
1143	NNW	6.2-9.0
Gusts up to 15.6 mph		
1202	NE	5.4-8.2
Gusts up to 12.4 mph		
1227	NNE	4.4-13.4
Gusts up to 20 mph		

<u>Local Time</u>	<u>Direction</u>	<u>Windspeed (mph)</u>
1/22/88		
1009	NNE	6.8-10.2
1039	N-NNE	2-8 with gusts
1114	N-NE	4-7 with gusts
Wind Direction and speed variable		
1143	NNE	4.0-6.6, gusts to 10
1212	NNE	8.6-12.0 gusts to 18
1216L 18dB noise intrusion on western half, 24 dB noise intrusion on eastern half		
1232	NNE	6.0-12.0 gusts to 15
1251	NNE	8.2-13.0 gusts to 14.4
1310	N	6.2-13.2
1333	NE	6.1-12.1 gusts to 14
1348	NE	4.4-8, gusts to 12
1410	NNE	8.2-12 gusts to 16
1410L 24dB noise intrusion on western half, 30 dB noise intrusion on eastern half.		
1433	NE	6.2-10 gusts to 13
1443	NNW	4.2-8.1
1509	NNW	4.0-8.0
1531	NNE	5.2-8.6 gusts to 11
1551	NNW	3.8-8.6 gusts to 11
1605	N	6.0-10.8
1627	NW	3.8-10.8
1646	N	5.0-10.6
1707	NNW	5.0-11.0
1726	NW	4.8-8.5
1748	NE	3.6-6.4

1/23/88

1044	S	1.2-2.6
1155	W	1
1229	W	1.8-4.2
1302	NW	1.8-4.6
1331	NW	0.5-2.6
1352	NNE	3.6-7.0
1410	NNE	4.4-8.4
1426	NNE	4.8-10.2
1439	NNE	6.0-11.0 Gusts to 14
Noise intrusion is 12-18 dB along line		
1456	NNE	6.8-11.0 Gusts to 14
1508	NE	8.0-12.0 Gusts to 15
1527	NE	7.0-12.0 Gusts to 15
Noise intrusion is 18 dB, peaking to 24dB		
1546	NE	5.8-11.0 Gusts to 14
1603	NE	6.0-12.2
1620	NE	5.0-9.8
1640	NNE	5.8-13.0
1701	N	3.6-7.4
1721	W	1.8-7.0
1734	NW	1.2-4.0

<u>Local Time</u>	<u>Direction</u>	<u>Windspeed (mph)</u>
1751	NE	4.4-7.0 Gusts to 11
1813	NE	6.2-11 Gusts to 13
1826	NE	5.8-11 Gusts to 15
1847	NE	5.4-12.2
1900	NE	2.8-5.6

1/24/88

1016	NNE	5.4-12.2
18dB noise intrusion with peaks to 24 dB		
1037	NNE	3.8-9.4
1057	NNE	5.4-11.8
1117	N	5.0-12.0
Noise intrusion of 24 dB for over 50% of the channels		
1137	N	4.8-12.2
1159	NNE	6.8-13.0 Gusts to 18
1216	N	6.4-14.4
1256	NNE	5.0-10.6

Production started with 24dB noise intrusion on less than 25% of the channels

1316	NE	5.4-11.0
1335	NE	6.4-12.0
1345	NNE	8.0-15.0
1407	N	6.2-15.0

Noise intrusion 18 dB, peaking to 24 dB

1426	NE	6.4-14.4
1448	N	6.0-14.0
1515	NE	6.8-14.0
1537	NE	6.0-13.8
1558	N	5.4-14.0
1616	N	5.8-11.6
1636	N	3.6-9.0
1657	NNE	4.2-9.4
1717	NNE	6.0-13.0
1730	NNE	5.2-11.0

APPENDIX 2. Observer's Field Notes.

OBSERVER REPORT PETTY-RAY GEOPHYSICAL

MEMOROUS VALUE

PAGE | 06 | PAGES

AMADOLSKA VALLEY

OBSERVER REPORT PETTY-RAY GEOPHYSICAL

Crew Work	Line No.	Study B	Arrive Camp	Leave Camp	Total Time	Down Time	Weather	Trail Conditions	Date	Day	Year	03	Client USGS	0000, Deane	PM Targets	PAGE 1 OF PAGES	
FILE NO	STA. NO	STA. NO'S (LIVE GRPS)	# OF SHTS	GAIN	SHOOTING	DAY (CLEAR, CLOUD)	DAY (CLEAR, CLOUD)	INST. SUR SOURCES	SET UP	TIME	REMARKS						
	TR TR	TR TR	TR TR	TR	MEMORY TAPE	SIZE TOP	BOT	NO CAPS UNT.	N UNITS	NO. SURVEYS							
007	141	101	220	121	340	1		4000	4886	2500	6250	611	DEMUL	4	12	80%	20465 1:00
008	141																24 AC 6-40 Hz LNS 15 TARES 39 AC R.L.
009	149																
010	149																
011	157																
012	157																
013	165	101	220	221	340	6	5000	4666									2:19 INLINE
014	165																1:12 PORTED
015	173																3:00 INLINE
016	173																3:30 PORTED
017	181																3:41 INLINE
018	181																3:53 PORTED
019	189																4:06 INLINE
020	189																4:24 PORTED
021	197																4:37 INLINE
022	197	101	220	221	340	16	4666										4:55 PORTED
	205																5:10 INLINE
	205																5:23 PORTED
	213																5:44 END OF DAY.
	213																
	221																
	221																
	229																
	229	101	220	221	340	14	4666										
	237																
	237																
	245																
	245																
	253																
	253																
	261																
	261	101	220	221	340	32	4666										

Crew No.	Line No.	Leave Party	Arrive Town/Camp	Total Time	Down Time	Weather	Trail. Conditions	Date Month	Day		Year 88	Client USA 5	OB 200/DENNY	PM TRACERS	
									TR	TR					
FILE NO.	STA. NO.	STA. NO'S (LIVE GRPS.)	C.D.P. (LIVE GRPS.)	C.D.P. (LIVE GRPS.)	POSITION REEL NO.	PAIMS TAPES	MEMORY	SIZE	TOP	BOT	NO CAPS U HT	N UNITS NO SIMS DRIVE	INST SET UP	TIME STA. OFFSET	REMARKS
23	197	101	220	221	340	466	466	75124	242	142	4	12	607	24/10/88 6:36 POTS	CHANGED 24/10/88 12:40 HR LIN. 25 TAPER 24 88. 29 AM RL
24	197													9:47 INLINE	"
25	197													10:05 POTTED	"
26	197													10:17 INLINE	"
27	197													10:30 POTTED	"
28	197													10:43 INLINE	"
29	197													11:41 POTTED	8:40HZ LIN. 25 TAPER 24 88. 39 AM RL
30	197													11:54 INLINE	"
31	197													12:05 POTTED	"
32	197													12:20 INLINE	"
33	197													12:38 POTTED	8:40 HR LIN. 25 TAPER 18 88. 33 AM RL
34	197													12:50 INLINE	"
XX	245													XX POTTED	8:40 HR LIN. 25 TAPER 24 88. 39 AM RL.
														INLINE	"
															"

OBSERVER REPORT PETTY-RAY GEOPHYSICAL

35854 2570 *Arachnida* VI

53

★ DELAYED FROM 9:56 70 FOR A
VISITOR PROBLEM

111

OBSERVER REPORT PETTY-RAY GEOPHYSICAL

CE012320 ARRESTA VANEY

PAGE 4 OF 5 PAGES

CREW NO	CARS NO	LINE NO	LEAVE TOWN	ARRIVE CAMP	DOWN TIME			WEATHER			TRAIL CONDITIONS			DATE MONTH	1 DAY	TEAR 60	CLIENT CLASS	OB SIGHT/DEADAY	FM TAPERS		
					STA. NO.	STA. NO.	NO. (LIVE GRPS)	C. D. P	DIGITAL	GAIN	PARTITY	SHOOTING	SUR. SOURCES	INST.	TIME	STA TO LINE	TIME	STA TO LINE	REMARKS		
NO	NO	NO	NO	NO	TR	TR	TR	TR	POSITION	REEL	NO.	TOP	BOT	NO CAPS	U/H/T	N UNITS	NO SAMS	DRIVE	SET UP	TO LINE	
17	47	149	101	220	221	240	340			80.2	98.6	618' ARRAY LENGTH = 251'	L.C. 100%	4	12	80%	200/605	6.12	10:00 AM	16-22 NE CAN. -25 TRAIL 24 SEC 37 SEC R.L.	DELAYED FROM 4:56 PM TO 6:12 AM SEE A VIO PROBLEM.
18	48	197	101	220	221	240						U.F. ARRAN LENGTH = 105' (STRUE)	16:02 L.C. 78.42 WING	Never out	6:42	10:00	"	"	"	"	"
19	49	197	1	1	1	1						U.B. ARRAY LENGTH = 231'			6:50	10:00	16-22 NE UN. -25 NAME	18 SEC	33 SEC R.L.		
20	50	197													7:10		END OF DAY				

OBSERVER REPORT PETTY-RAY GEOPHYSICAL

0000-2328 A 2005 के लिए

OBSERVER REPORT PETTY-RAY GEOPHYSICAL
MARLOSA VALLEY

NETTEN 3-2520 Amherst, VA

OBSERVER REPORT PETTY-RAY GEOPHYSICAL

for us to see.

GEO-252.0 *four poss.
big key*

OBSERVER REPORT PETTY-RAY GEOPHYSICAL

Franses
Haller

CEO-520

OBSERVER REPORT PETTY-RAY GEOPHYSICAL

OBSERVER REPORT PETTY-RAY GEOPHYSICAL

PAGE 4 OF 8 PAGES

GEO-252 D. AMAROCA VALLEY

OBSERVER REPORT PETTY-RAY GEOPHYSICAL

PAGE 5 OF PAGES

08-20/1965

PM TAKES

REMARKS

TRAIL CONDITIONS

DATE

MONTH

1

DAY

12

YEAR

65

CLIENT

4545

OB

08

08

08

08

08

08

08

08

08

08

08

08

08

08

08

08

08

08

08

08

08

08

08

08

08

08

08

08

08

08

08

08

08

08

08

08

08

08

08

08

08

08

08

08

08

08

08

08

08

08

08

08

08

08

08

08

08

08

08

08

08

08

08

08

08

08

08

08

08

08

08

08

08

08

08

08

08

08

08

08

08

08

08

08

08

08

08

08

08

08

08

08

08

08

08

08

08

08

08

08

08

08

08

08

08

08

08

08

08

08

08

08

08

08

08

08

08

08

08

08

08

08

08

08

08

08

08

08

08

08

08

08

08

08

08

08

08

08

08

08

08

08

08

08

08

08

08

08

08

08

08

08

08

08

08

08

08

08

08

08

08

08

08

08

08

08

08

08

08

08

08

08

08

08

08

08

08

08

08

08

08

08

08

08

08

08

08

08

08

08

08

08

08

08

08

08

08

08

08

08

08

08

08

08

08

08

08

08

08

08

08

08

08

08

08

08

08

08

08

08

08

08

08

08

08

08

08

08

08

08

08

08

08

08

08

08

08

08

08

08

08

08

08

08

08

08

08

08

08

08

08

08

08

08

08

08

08

08

08

08

08

08

08

08

08

08

08

08

08

08

08

08

08

08

08

08

08

08

08

08

08

08

08

08

08

08

08

08

08

08

08

08

08

08

08

08

08

08

08

08

08

08

08

08

08

08

08

08

08

08

08

08

08

08

08

08

08

08

08

08

08

08

08

08

08

08

OBSERVER REPORT: PETTY-RAY GEOPHYSICAL

PAGE 1 OF PAGES

OBSERVER REPORT PETTY-RAY GEOPHYSICAL

Amelosia Valley

OBSERVER REPORT PETTY-RAY GEOPHYSICAL

PAGE 3 OF PAGES

3

Amargosa Valley

CREW NO.	LINE NO.	LEAVE CAMP	ARRIVE CAMP	DOWN TIME	WEATHER	TRAIL CONDITIONS	DATE MONTH	DAY 1/4	YEAR 88	CLIENT US 95	OB J 000	PM J. Travers
FILE NO.	STA. NO.	STA. NO'S (LIVE GRPS)	TR POSITION	SHOOTING TIME	SUR. SOURCES	SUR. SOURCES	INST. NO.	TIME OF SET UP	TIME OF LINE	INST. NO.	SET UP DAY	REMARKS
FILE NO.	STA. NO.	TR 1 TR 2 TR 3	TH160 POSITION	TAPE NO. OF REEL	NO. OF CAPS	U.H.T.	IN UNITS	NO. SAMS	DRIVE	4	12 80%	2/28
24	935	889	1368	300000	200	1000	4	12 80%	10:44	2/28	2/28	start Rec 1 # 023
25	937	↓	↓	↓	↓	↓	↓	↓	↓	↓	↓	
26	939											
27	941											
28	943											
29	945											
30	947											
31	949											
32	951											
33	953											
34	955	1	1	1	1	1	1	1	1	1	1	
35	957											
36	959	999	1001	1168	50000	10000	9	12 80%	10:44	2/29		

Alasecca Valley

OBSERVER REPORT PETTY-RAY GEOPHYSICAL

PAGE	4	OF	PAGES
100		PM	J. T. Goss
100			4

OBSERVER REPORT PETTY-RAY GEOPHYSICAL

Digitized by srujanika@gmail.com

PAGE 2 OF PAGES

65

OBSERVER REPORT PETTY-RAY GEOPHYSICAL

660-23338 *Anisognathus* ussheri

PAGE 6 OF 10 PAGES

OBSERVER REPORT PETTY-RAY GEOPHYSICAL

PAGE 7 OF PAGES

CREW NO NO. 606	LINE NO.	AU-1	LEAVE CAMP	ARRIVE TOWN/CAMP	TOTAL TR. TIME			DOWN TIME			WEATHER			TRAIL CONDITIONS	DATE MONTH	1 DAY	6 DAY	YEAR	98	CLIENT USES	OB	WOOD	DESMONY	PM	TABERS
					STA. NO.	STA. NO.	ST. NO.	NO. (LIVE GRPS.)	C. D. P.	DIGITAL POSITION	REEL NO.	TAPE	MEMORY	SIZE	TOP	SHOOTING	INST.	TIME	STA.	OFF-SET	SET UP	DAY			
933	6-44	Purple			933	6-44	933	4038	4038	4038	4038	4038	4038	4038	4038	4038	4038	4038	4038	4038	4038	4038	4038	4038	4038
934-35	"	Green																							
936-39	"	DRD																							
944	"	GAIN RANGE																							
953-54	"	SUN TEST																							
932	25-44	WIRELINE SIMMS																							
77	1057	809	NO SAP	1348																					
78	1058																								
79	1058																								
80	1059																								
81	1073																								
82	1077																								
83	1081																								
84	1085																								
85	1089																								
86	1093																								
87	1097																								
88	1101																								
89	1105																								
90	1109																								
91	1113																								
92	1117																								
93	1121																								
94	1125	809	NO SAP																						
95	1129	890																							
96	1133	894																							
97	1137	898																							
98	1141	902																							
99	1145	906																							
100	1149	910																							
101	1153	914																							

7

PICKED UP CENTER OF SPREAD. ROLLING COP NOW!

wind over 10 mph

noise intrusion 12-18 dC

4 " 12-18 dC

11 " 12-18 dC

GEO-262-0
Crew No. 6806 Line AU-1 Amargosa 1/1/C

OBSERVER REPORT PETTY-RAY GEOPHYSICAL

PAGE 8 OF 8

FILE NO.	STA. NO.	STA. NO.	STA. NO. (LIVE GPS)	ARRIVE TIME	TOTAL TR. TIME	WEATHER	TRAIL CONDITIONS			DATE, MONTH	1 DAY / 6 YEARS	CLIENT USGS	OB. LOAD / Heavy	PM Tapers
							TR	TR	TR					
102	1157	918	1044	1397	030	TR	0.30	0.30	0.30	4	12	80% (044)		
103	1161	922	1401											noise reduction 12-18 dB
104	1165	926	1405											12-18 dB
105	1169	930	1409											" "
106	1173	934	1413											" "
107	1177	938	1417											" "
108	1181	942	1421											" "
109	1185	946	1425											" "
110	1189	950	1429											" "
111	1193	954	1433											" "
112	1197	958	1437	E-1	0.30									" "
113	1201	962	1441		0.31									" "
114	1205	964	1445											" "
115	1209	968	1449											" "
116	1213	972	1453											" "
														5:30 PM
														End Day!!

OBSERVER REPORT PETTY-RAY GEOPHYSICAL

Anasagosa Valley

550-252-8

PAGE 9 OF PAGES 9
Honey PM / TUES 05

OBSERVER REPORT PETTY-RAY GEOPHYSICAL

610-2520 AMARGOSA VALLEY

PAGE 10 OF 10 PAGES

OBSERVER REPORT PETTY-RAY GEOPHYSICAL

FILE NO.	STA. NO.	ARRIVE TOWN/CAMP			TOTAL TR. TIME			WEATHER			TRAIL CONDITIONS			DATE	MONTH	1 DAY 20	YEAR 28	CLIENT 4-5645	OB 2000/2001	REMARKS	
		TR	TR	GRPS.	C. D. P.	DIGITAL	POSITION REEL NO.	GAIN	PARTY	SHOOTING	SUR. SOURCES	INST.	TIME	STA.	OFF SET	SET 1 OF	DAY	TMBERS 11			
933	933	933	933	933	933	933	933	933	933	933	933	933	933	933	933	933	933	933	933	933	
934-35	"	934	935	"	934	935	935	935	935	935	935	935	935	935	935	935	935	935	935	935	935
936-59	"	936	935	"	936	935	935	935	935	935	935	935	935	935	935	935	935	935	935	935	935
944	"	944	944	"	944	944	944	944	944	944	944	944	944	944	944	944	944	944	944	944	944
953-54	"	953	954	"	953	954	954	954	954	954	954	954	954	954	954	954	954	954	954	954	954
932	932	932	932	932	932	932	932	932	932	932	932	932	932	932	932	932	932	932	932	932	932
1	1	1	1	1	1	1	1	1	1	1	1	1	1	1	1	1	1	1	1	1	1
1	154	1357	1118	NO GRP	1597	2035	PARSED											4	12	2026	11:01
2	155	1361	1122		1601																
3	156	1365	1126		1605																
4	157	1369	1130		1609																
5	158	1373	1134		1613																
6	159	1377	1138		1617																
7	160	1381	1142		1621	EDR	NO EDF'S														
8	161	1385	1146		1625	NOE	NOE														
9	162	1389	1150		1629																
10	163	1393	1154		1633																
11	164	1397	1158		1637																
12	165	1401	1162		1641																
13	166	1405	1166		1645																
14	167	1409	1170		1649																
15	168	1413	1174		1653																
16	169	1417	1178		1657																
17	170	1421	1182		1661																
18	171	1425	1186		1665																
19	172	1429	1190		1669																
20	173	1433	1194		1673	400 ²	500 ²														
21	174	1437	1198		1677	800 ²	900 ²														
22	175	1441	1202		1681																
23	176	1445	1206		1685																
24	177	1449	1210		1689																
25	178	1453	1214		1693																

OBSERVER REPORT PETTY-RAY GEOPHYSICAL

Anderson Valley

PAGE 13 OF PAGES
13 PM TABBERS / DENVER

OBSERVER REPORT PETTY-RAY GEOPHYSICAL

PAGE 14 OF 14 PAGES

Crew No.	Line No.	Leave Camp	Arrive Town/Camp	TOTAL TR. TIME			WEATHER			TRAIL CONDITIONS			MONTH	DAY	YEAR	CAMP	SUR. SOURCES	INST.	TIME	STA.	OFFSET	DAYS	SET UP	DAYS	REMARKS	
				FILE NO.	STA. NO.	NO. S (LIVE GRFS.)	C. D. P.	DIGITAL GAIN	PARITY	SHOOTING	TOP	BOT.	NO CAPS	U. H. T.	N. UNITS	NO. SUMS	DRIVE									
133	Pulse			6sec	040	400												15:57								Daily Tests
934-935	Ant																									
936-939	DRD																									
944	Gain Range																									
953-954	Sum																									
952	Wireless Similarity																									
203	1549	1310	1107 81		1789														9:20							
204	1553	1314			1793																					
205	1557	1318			1797																					
206	1561	1322			1801																					
207	1565	1326			1805	EOT																				
208	1569	1330			1809	0940																				
209	1573	1334			1813																					
210	1577	1338			1817																					
211	1581	1342			1821																					
212	1585	1346			1825																					
213	1589	1350			1829																					
214	1593	1354			1833																					
215	1597	1358			1837																					
216	1601	1362			1841																					
217	1605	1366			1845																					
218	1609	1370			1849																					
219	1613	1374			1853																					
220	1617	1378			1857	EOT																				
221	1621	1382			1861	0942																				
222	1625	1386			1865																					
223	1629	1390			1869																					
224	1633	1394			1873																					
225	1637	1398			1877																					
226	1641	1402			1881																					
227	1645	1406			1885																					

Ames/059 Valley

OBSERVER REPORT PETTY-RAY GEOPH' ZAL

PAGE 5 OF 15

FILE NO.	LINE NO.	AV/1	TOWN/CAMP	ARRIVE		TOTAL TR. TIME		WEATHER		SHOOTING		TRAIL CONDITIONS		DATE MONTH	STA. NO.	SUR. SOURCES	CLIENT USGS	OB	Load	Dense	Pg. 15
				STA. NO.	NO'S (LIVE GRPS)	C. D. P.	DIGITAL POSITION	PANS	GAIN	PARTY	TOP	BOT.	NO CAPS	U.H.T.	N. UNITS	NO. SUNS	DRIVE	INST. SET UP	TIME DAY	STA. TO LINE	REMARKS
228	1649	1410	1409	1389	042	042	042	042	042	042	042	042	042	042	042	042	042	042	042	042	
229	1653	1414	1413	1897																	
230	1657	1418	1417																		
231	1661	1422	1421																		
232	1665	1426	1425																		
233	1669	1430	1429																		
234	1673	1434	1433																		
235	1677	1438	1437																		
236	1681	1444	1443																		
237	1685	1446	1445																		
238	1689	1450	1449																		
239	1693	1454	1453																		
240	1697	1458	1457																		
241	1701	1462	1461																		
242	1705	1466	1465																		
243	1709	1470	1469																		
244	1713	1474	1473																		
245	1717	1478	1477																		
246	1721	1482	1481																		
247	1725	1486	1485																		
248	1729	1490	1489																		
249	1733	1494	1493																		
250	1737	1497	1496																		

OBSERVER REPORT PETTY-RAY GEOPHYSICAL

PAGE 16 OF 16 PAGES

GEO 2500D Amaracosa Valley

CREW NO.	FILE NO.	LINE NO.	A.U. NO.	LEAVE TOWN	ARRIVE CAMP	TOTAL TIME	WEATHER	TRAIL CONDITIONS		DATE MONTH	1 DAY 23	YEAR 89	CLIENT USES	OB. NO. / DECODED	PM TAPERS	
								C. D. P.	DIGITAL POSITION							
NO.	TR	TR	TR	TR	TR	NO. REEL	NAME	MEMORY	SIZE	TOP	BOT.	NO. CAPS	U.H.T.	N. UNITS	NO. SUMS DRIVE	REMARKS
933	600	700	700	700	700	4	044	400								
934-35	"	DRD														
934	"	GAIN RANGE														
953-54	"	SWIM TEST														
932	20 sec	WIRELINE SIMILARITY				124	10 441E LIN.	24 sec				4	1			
251	1790	1390	NO GAP	1975	400F	RECORDED	RECORDED	200F	162'	250'	4	U.H. CH 4-40	1836	10/20		
1	252	1741	1502			1975						4	12	802	1836	10/20
2	253	1745	1526													REMARKS. END OF LINE ST # 1035.
3	254	1749	1510													
4	255	1753	1514													
5	256	1757	1518													
6	257	1761	1522			400F	400F	400F	400F	400F	400F					
7	258	1765	1526													
8	260	1769	1520													
9	261	1773	1524													
10	262	1777	1528													
11	263	1781	1532													
12	264	1785	1546													
13	265	1789	1550													
14	266	1793	1554													
15	267	1797	1558													
16	268	1801	1562													
17	269	1805	1566													
18	270	1809	1570													
19	271	1813	1574													
20	272	1817	1578													
21	273	1821	1582													
22	274	1825	1586													
23	275	1829	1590													
24	276	1833	1594													
																50' S UP 1013 OFFSET SOUTH.
																3:20

OBSERVER REPORT PETTY-RAY GEOPHYSICAL

Marsossaïscher

OBSERVER REPORT PETTY-RAY GEOPHYSICAL

PAGE 18 OF 19 PAGES

Geophysical Survey
Date 8/26 June 1961
No. 76-1 Town Camp

FILE NO.	STA. NO.	ARRIVE CAMP		TOTAL TIME	WEATHER		TRAIL CONDITIONS	DATE	MONTH	DAY 24 YEARS 88	CLIENT USES	OB	4000/10000	PM / AM	REMARKS						
		STA. NO'S (LIVE GRPS.)	TR		C. D. P.	DIGITAL															
FILE NO.	STA. NO.	TR	TR	TR	TR	TR	POSITION	REEL NO.	PADS	TAPE	MEMORY	SIZE	TOP	BOT	NO CAPS	U.H.T. N.	UNITING SUMS	DRIVE	SET UP	TIME	STA.
933	Pulse						6sec	48													Daily Tests
934-2	Env																				↓
936-3	ARD																				
944	Can Reg																				
953-4	Sun 15																				
932	Wilhelms Sim						25sec		EOF												
295	1881	1692	Playoff	1975	Polo																
296	1883	1644																			
297	1885	1696																			
298	1887	1648																			
299	1889	1650																			
300	1891	1652																			
301	1893	1654																			
302	1895	1656																			
303	1897	1658																			
304	1899	1660																			
305	1901	1662																			
306	1903	1664																			
307	1905	1666							EOF	0.49											
308	1907	1668																			
309	1909	1670																			
310	1911	1672																			
311	1913	1674																			
312	1915	1676																			
313	1917	1678																			
314	1919	1680																			
315	1921	1682																			
316	1923	1684																			
317	1925	1686																			
318	1927	1688																			
319	1929	1690																			

NOISE = 18 db OUTST 35% @ 24db (FAR TOWERS ON WEST END)

STANDING BY FOR WIND NOISE INTRUSION OF 24db.

BACK TO WORK - WIND INTRUSION 18 db, LESS THAN

30% @ 24db.

NOISE INTRUSION = 18 db.

Amarosa Valley

OBSERVER REPORT PETTY-RAY GEOPHYSICAL

PAGE 19 OF 19 PAGES

19

Crew No.	Line No.	AV-1	Leave Camp	Arrive Camp	TOTAL TIME	WEATHER	TRAIL CONDITIONS	DATE	DAY 24		YEAR 88		CLIENT LESSONS	OB GEOGRAPHY	PM TRACES			
									NO.	STA. NO.	STA. NO.	NO. (LIVE GRPS.)	C. D. P.	WEIGHT	SHOOTING	SUR. SOURCES	INST.	TIME
NO.	TR	TR	TR	TR	POSITION	REEL NO.	MEMORY	SIZE	TOP	BOT	NO. CAPS	U. H. T.	IN UNITS	SHO.	DRIVE	SET	UP	DAY
320	1931	1692	ND	ND	ND	ND	ND	ND	ND	ND	ND	ND	ND	ND	ND	4	12	80%
321	1933	1694																
322	1935	1696																
323	1937	1698																
324	1939	1700																
325	1941	1702																
326	1943	1704																
327	1945	1706																
328	1947	1708																
329	1949	1710																
330	1951	1712																
331	1953	1714																
332	1955	1716																
333	1957	1718																
334	1959	1720																
335	1961	1722																
336	1963	1724																
337	1965	1726																
338	1967	1728																
339	1969	1730																
340	1971	1732																
341	1973	1734																
342	1975	1736	ND	ND	ND	ND	ND	ND	ND	ND	ND	ND	ND	ND	ND	4	12	80%

Noise intrusion 12-18-86

APPENDIX 3: Processing Scheme for Line AV-1

LINE AV-1 Processing Flow for 5.0 second Relative Amplitude Stack, 4.0 ms. Sample Rate

<u>Process</u>	<u>Program Name</u>
1) SEGD to SEGY Conversion Vibroseis Correlation	FPT-32 Field Unit
2) Sort to CDP Order Account for Acquisition Geometry Trace Edit	LANDSORT
3) ABC Scaling to Correct for Transmission Loss and Spherical Divergence Gain (t) = $A*t + B*20 \log(t) + C$	ABCSCL
4) Apply Datum Statics - Floating Velocity = 6000 ft/sec	CORRECT
5) Detailed Refraction Statics Analysis and Application. Short Period Solution Applied.	TIMEPIK DRMLMO
6) Velocity Analysis. Constant Velocity Stacks. One per mile for Brute Stack.	CVSTACK
7) Surface Consistent Deconvolution. Operator: 360 ms. long.	SCDECON
8) Mute Analysis and Gathers Display	STACK
9) Velocity Analysis. Constant Velocity Stacks. Continuous Analysis, one per half mile Application on Final Stack.	CVSTACK
10) Surface Consistent Residual Statics (Statics derived from 15.0 second data set)	STATA
11) Surgical Mute to Remove Airblast	CORRECT
12) Final NMO Correction and Mute Application	STACK

13) CDP Stack, Average Fold is 60 STACK

14) Bandpass Filter Applied

Time	<u>Filter (Hz)</u>	TMOD
0000 ms	6, 10, 44, 52	
2500 ms	6, 10, 38, 46	
4000 ms	6, 10, 30, 35	

15) Shift to Flat Datum, 825 meters (2700 feet) DSHIFT

16) Film Display - Normal Polarity SSD

FOR MIGRATED 5.0 Second Stack change to:

16) Post-Stack Migration, 15° Finite Difference Approximation WAVEMIGR

17) Film Display - Normal Polarity SSD

LINE AV-1 Processing Flow for 15.0 Second Relative Amplitude Stack, 8.0 ms Sample Rate

Process

1) SEGD to SEGY Conversion

Vibroseis Correlation

2) Sort to CDP Order

Account for Acquisition Geometry

Trace Edit

3) ABC Scaling to Correct for Transmission Loss and Spherical Divergence

Gain (t) = A*t + B* 20 Log (t) + C

4) Apply Datum Statics-Floating Velocity = 6000 ft/sec

5) Detailed Refraction Statics Analysis and Application. Short Period Solution Applied.

6) Velocity Analysis. Constant Velocity Stacks. One per mile for Brute Stack.

7) Mute Analysis and Gathers Displays

8) Velocity Analysis. Constant Velocity Stacks, Continuous Analysis. One per Half Mile Application on Final Stack.

9) Surface Consistent Residual Statics. (Statics derived from 15.0 second data set)

10) Surgical Mute to remove Airblast

11) Final NMO Correction and Mute Application

12) Resample to 8.0 msec sample rate

13) CDP Stack, Average 60 fold

Program Name

FPT-32 Field Unit

LANDSORT

ABCSCALE

CORRECT

TIMEPIK
DRMLMO

CVSTACK

STACK

CVSTACK

STATA

CORRECT

STACK

CORRECT

STACK

14) Bandpass Filter Applied TMOD

Time	Filter (Hz)
0000 ms	6, 10, 44, 52
2500 ms	6, 10, 38, 46
4000 ms	6, 10, 30, 35
8000 ms	6, 10, 25, 30

15) Shift to Flat Datum, 825 m DSHIFT
(2700 ft.)

16) Film Display - Normal Polarity SSD

LINE AV-1 Processing Flow for 15.0 second Automatic
Gain Control Stack, 8.0 ms. Sample Rate

<u>Process</u>	<u>Program Name</u>
1) SEGD to SEGY Conversion Vibroseis Correlation	FPT-32 Field Unit
2) Automatic Gain Control Scaling, 1500 ms. window	SCALE/XSS
3) Bandpass Filter - 6/10 to 44/54 Hz	FILTER/XSS
4) Resample to 8 msec.	CORRECT
5) Sort to Shot Station Location Trace Edit	LANDSORT
6) Velocity Filter to Attenuate Linear Noise. Window removed 300-2500 m/sec (1000-8000 ft/sec)	FANFILT
7) Sort to CDP order Account for Acquisition Geometry	LANDSORT
8) Apply Datum Statics - Floating Velocity = 6000 ft/sec.	CORRECT
9) Detailed Refraction Statics Analysis and Application. Short Period Solution Applied.	TIMEPIK DRMLMO
10) Velocity Analysis, Constant Velocity Stacks. One Per Mile for Brute Stack.	CVSTACK

11) Mute Analysis and Gathers Display STACK

12) Velocity Analysis. Constant Velocity Stacks. Continuous Analysis. One per Half mile Application on Final Stack CVSTACK

13) Surface Consistent Residual Statics. STATA

14) Final NMO Correction and Mute Application STACK

15) CDP Stack. Average 60 fold. STACK

16) Bandpass Filter Applied
Time Filter (z)
0000 ms 6, 10, 44, 52
2500 ms 6, 10, 38, 46
4000 ms 6, 10, 30, 35
8000 ms 6, 10, 25, 30 TMOD

17) Shift to flat Datum, 825 m (2700 feet) DSHIFT

18) Film Display - Normal Polarity SSD

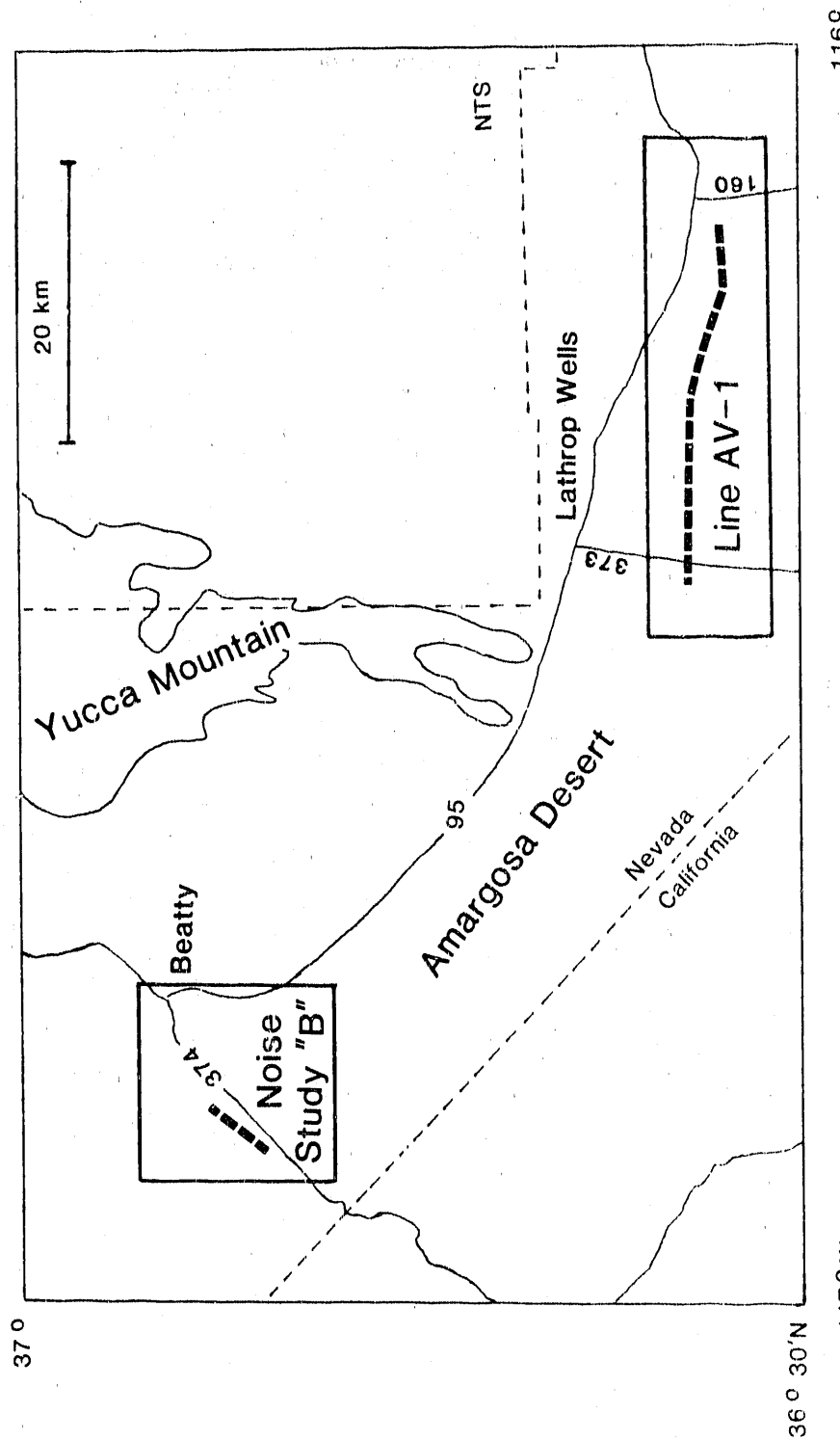
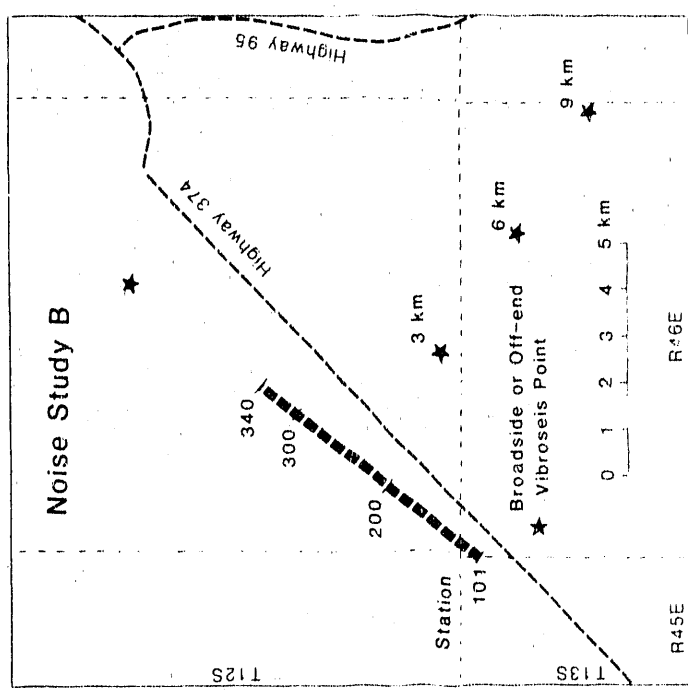


Figure 1a

Figure 1b



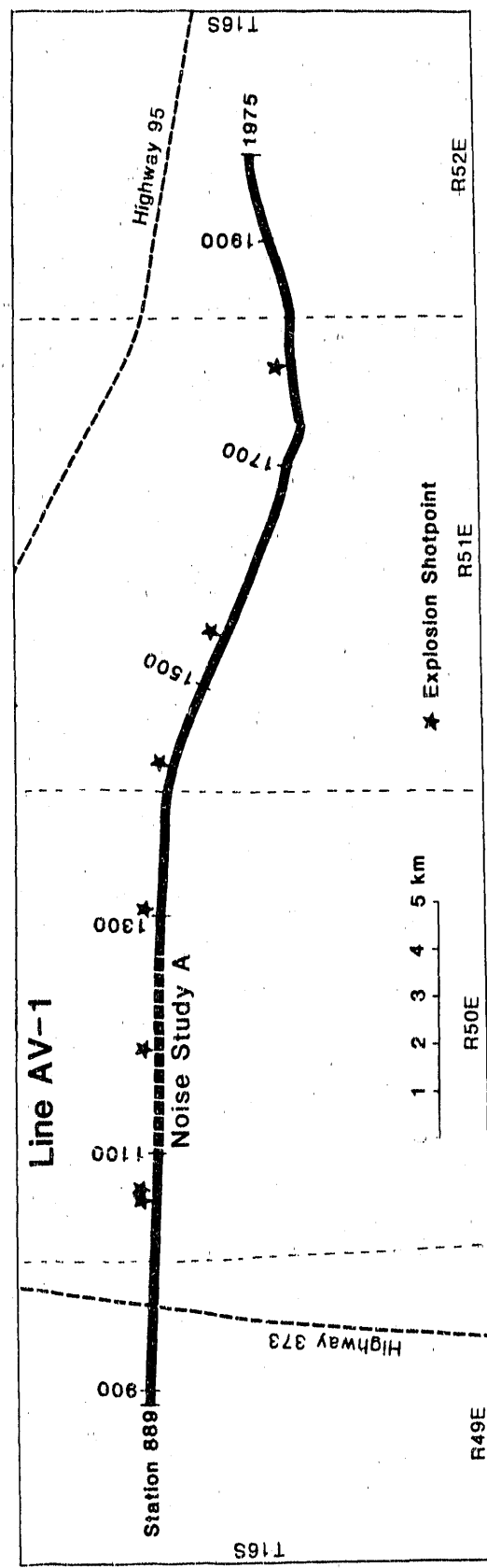


Figure 1c

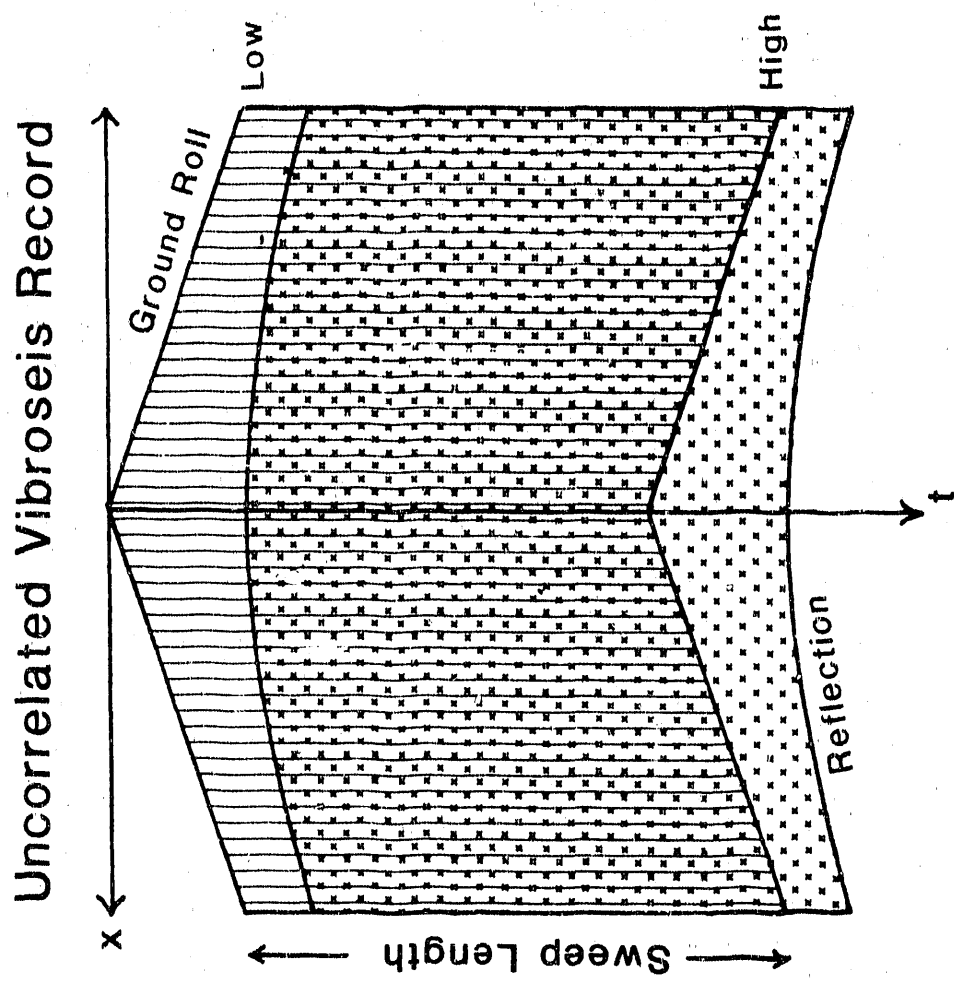


Figure 2

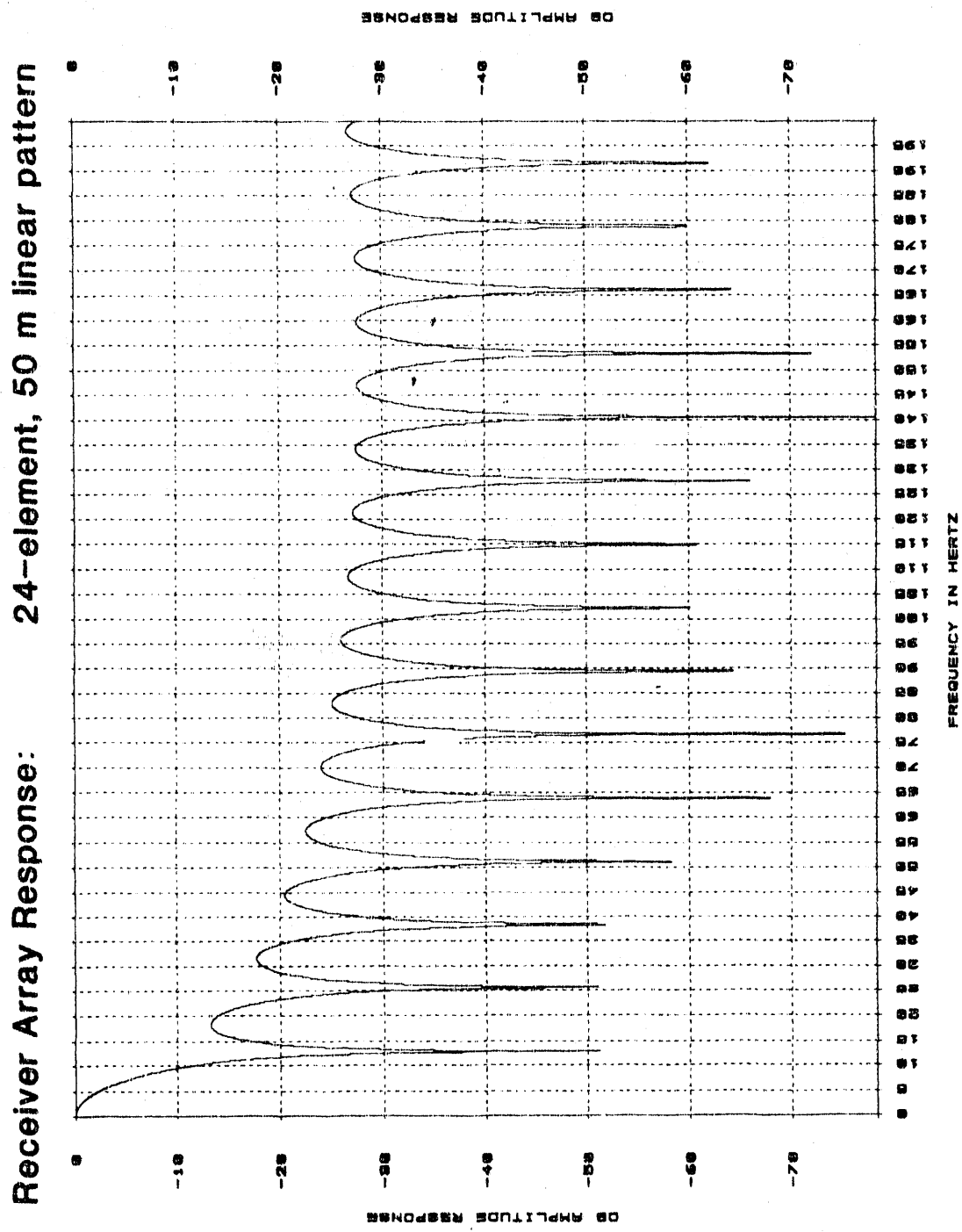


Figure 3a

Receiver Array Response: 24-element, 50 m weighted pattern

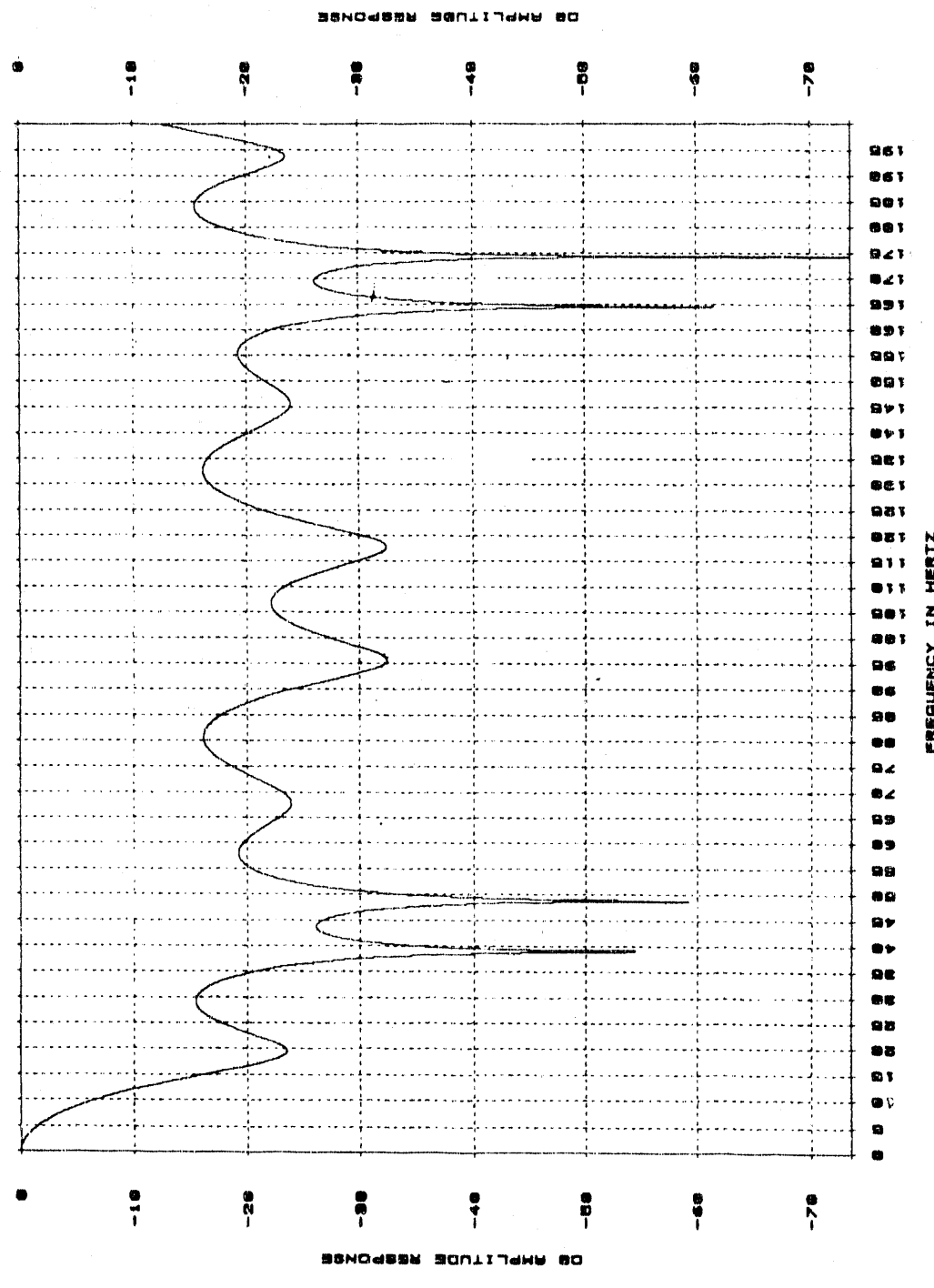


Figure 3b

Source Array Response:

24-element, 50 m linear pattern

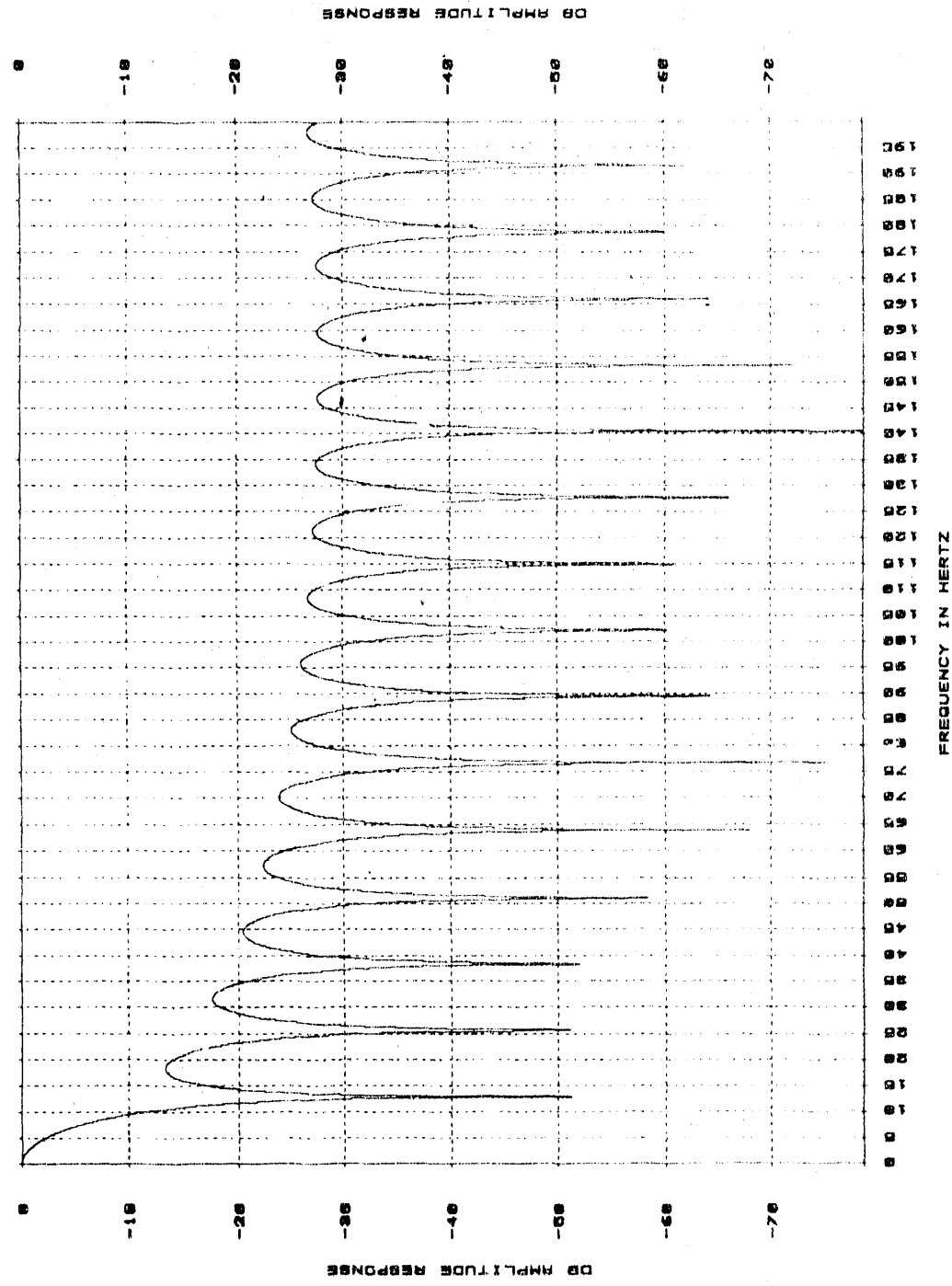


Figure 4a

Source Array Response:
30-element, 70 m weighted pattern

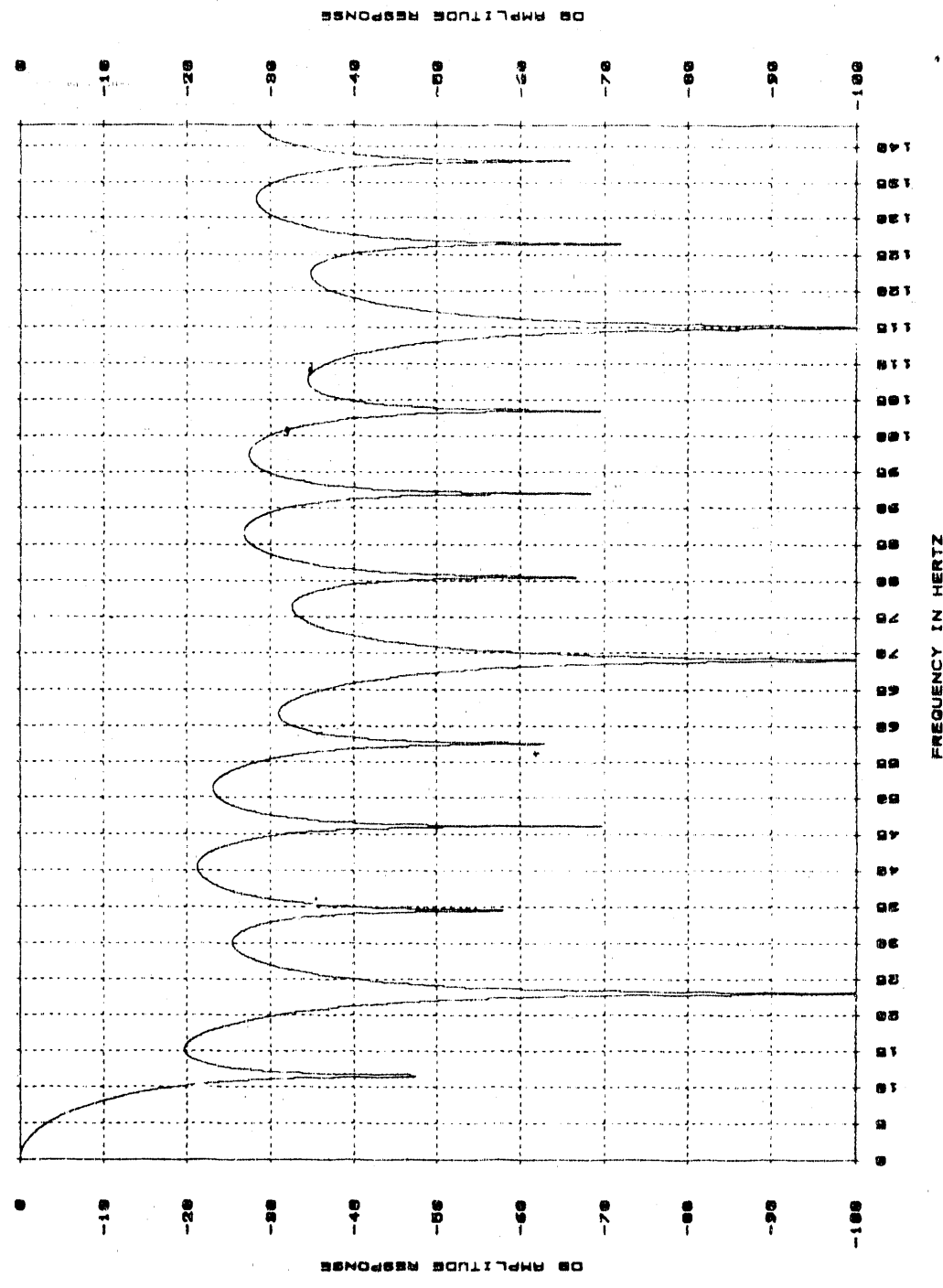


Figure 4b

Combined Array Response:
both 24-element, 50 m linear patterns

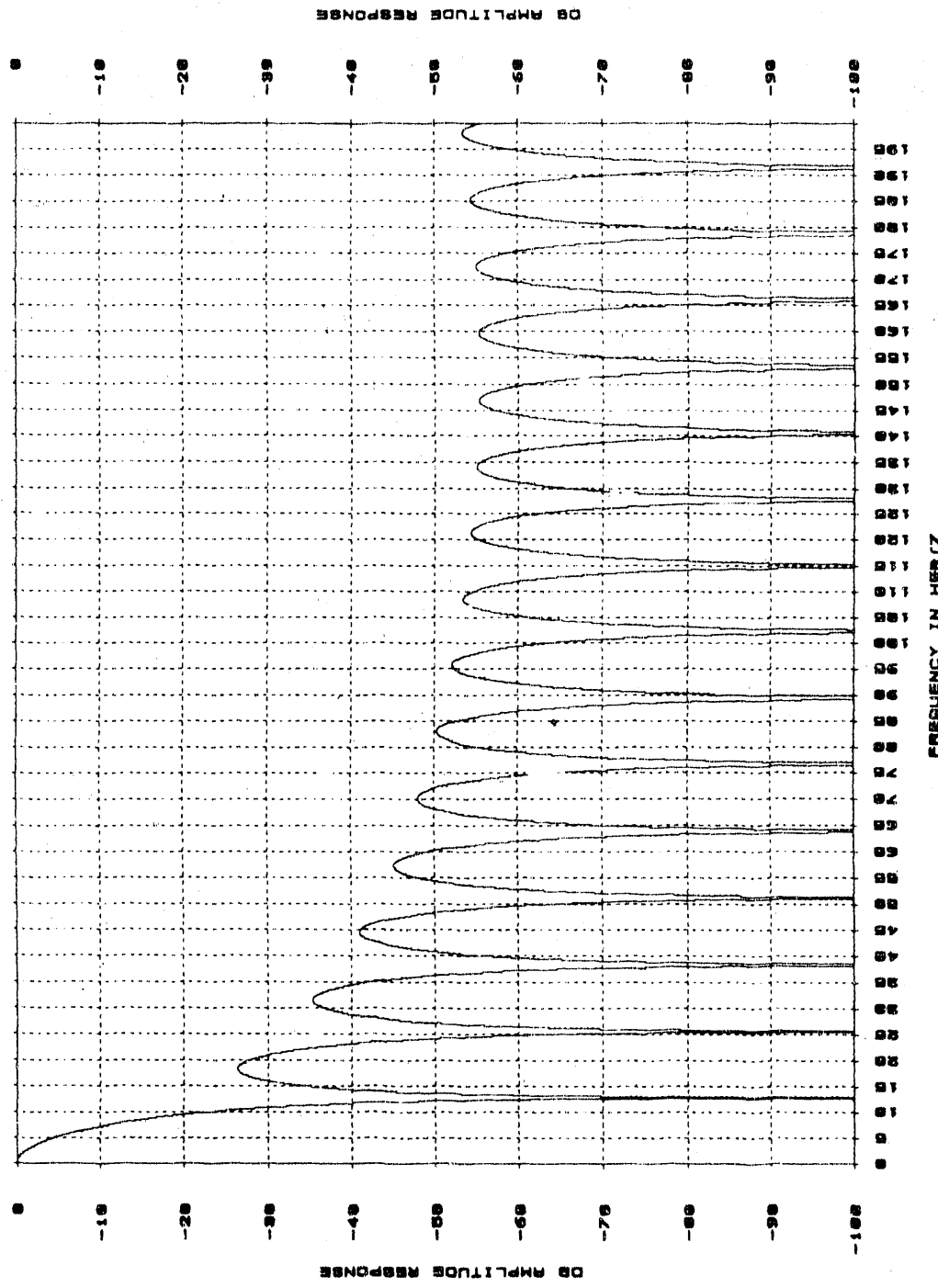


Figure 5a

Combined Array Response:
70 m source, 50 m linear receiver patterns

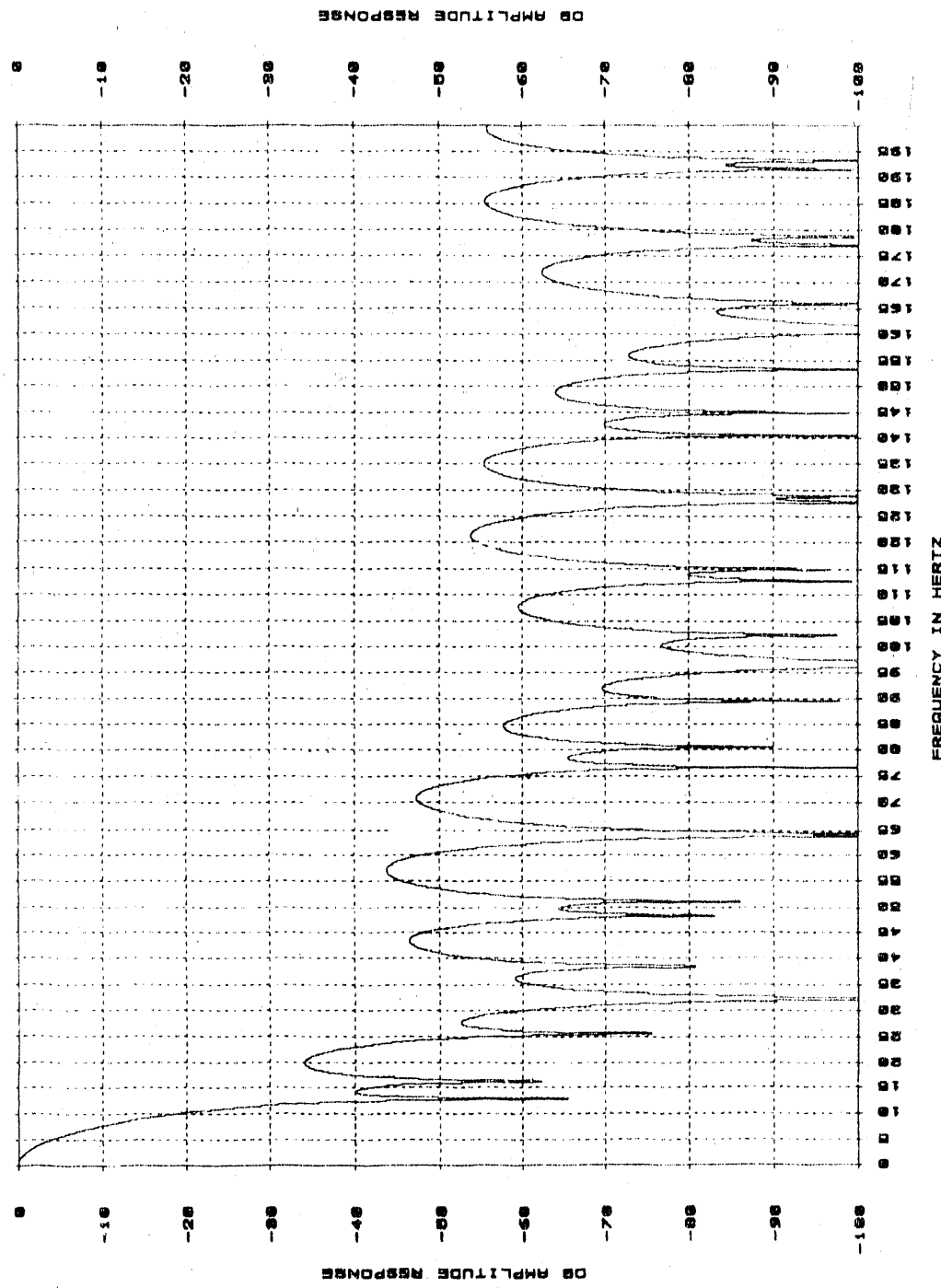


Figure 5b

Combined Array Response:

70 m source, 50 m weighted receiver patterns

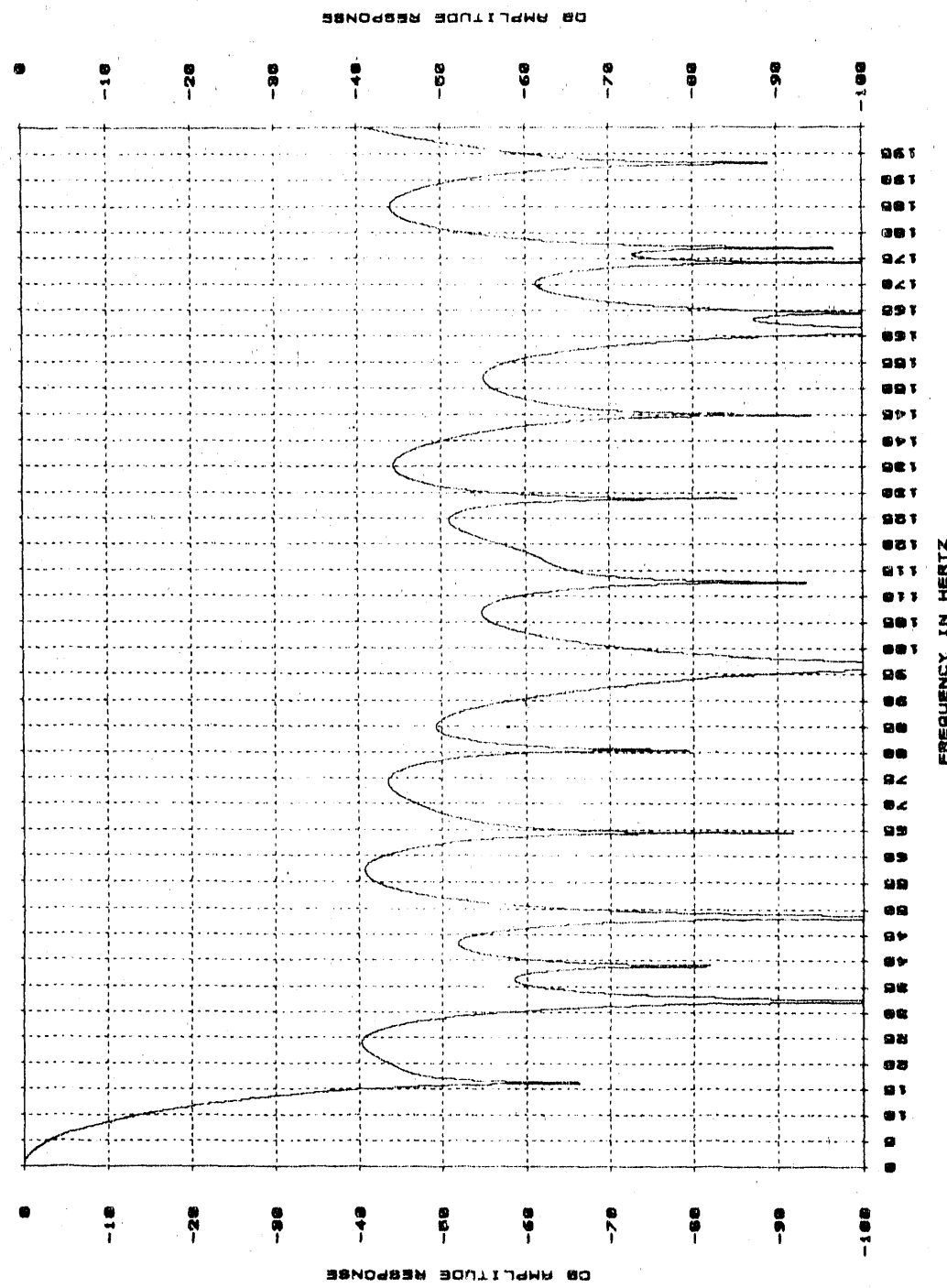


Figure 5c

24-element, 50 m weighted receiver pattern

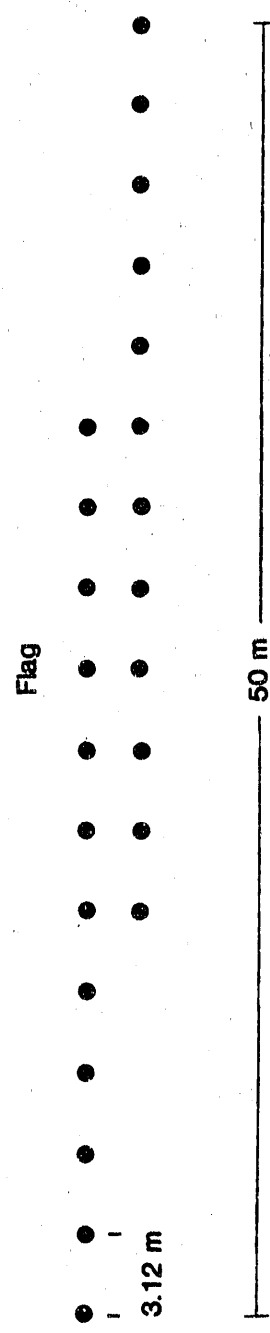


Figure 6a

50-m-long Vibroseis Array Pattern

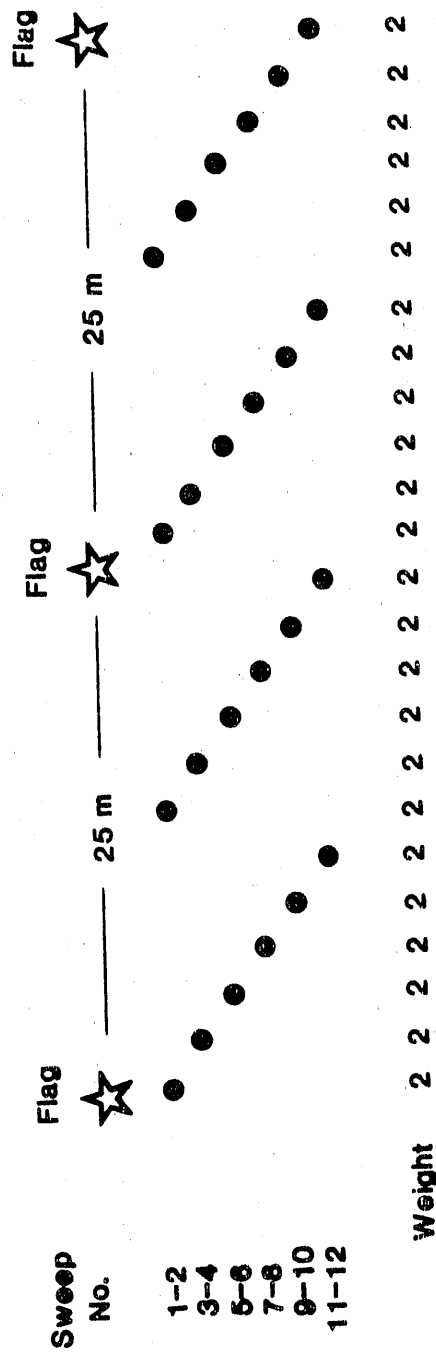


Figure 6b

70-m-long Vibroseis Array Pattern

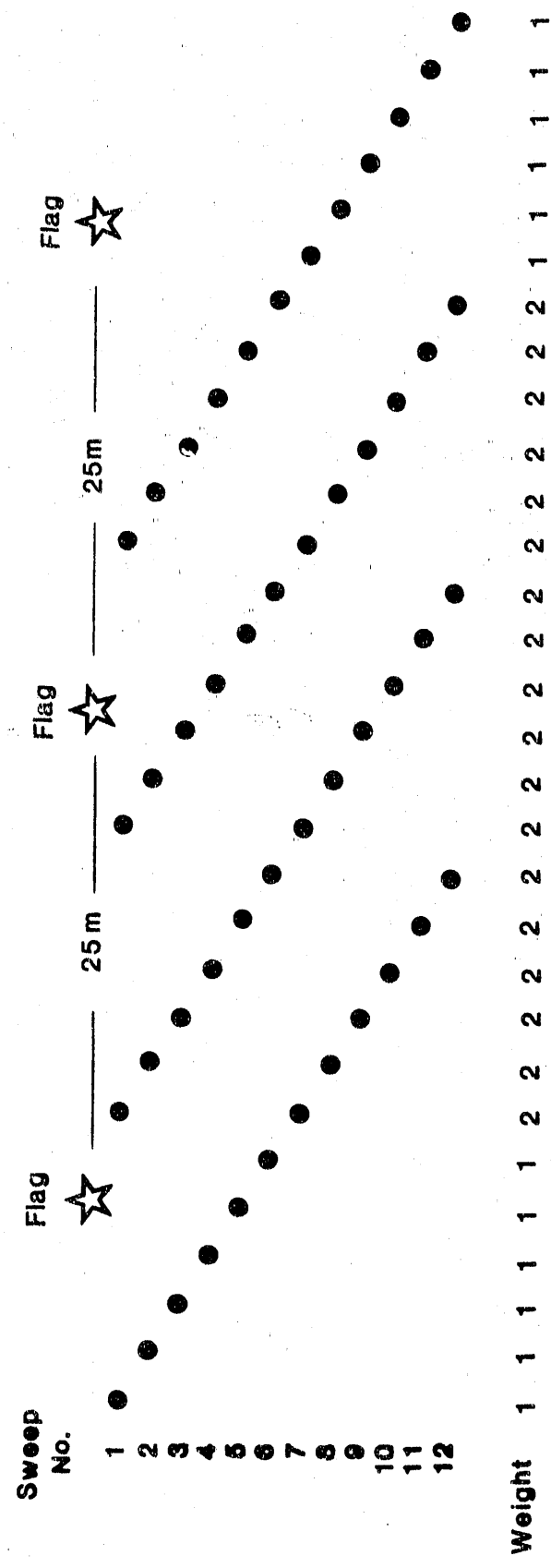
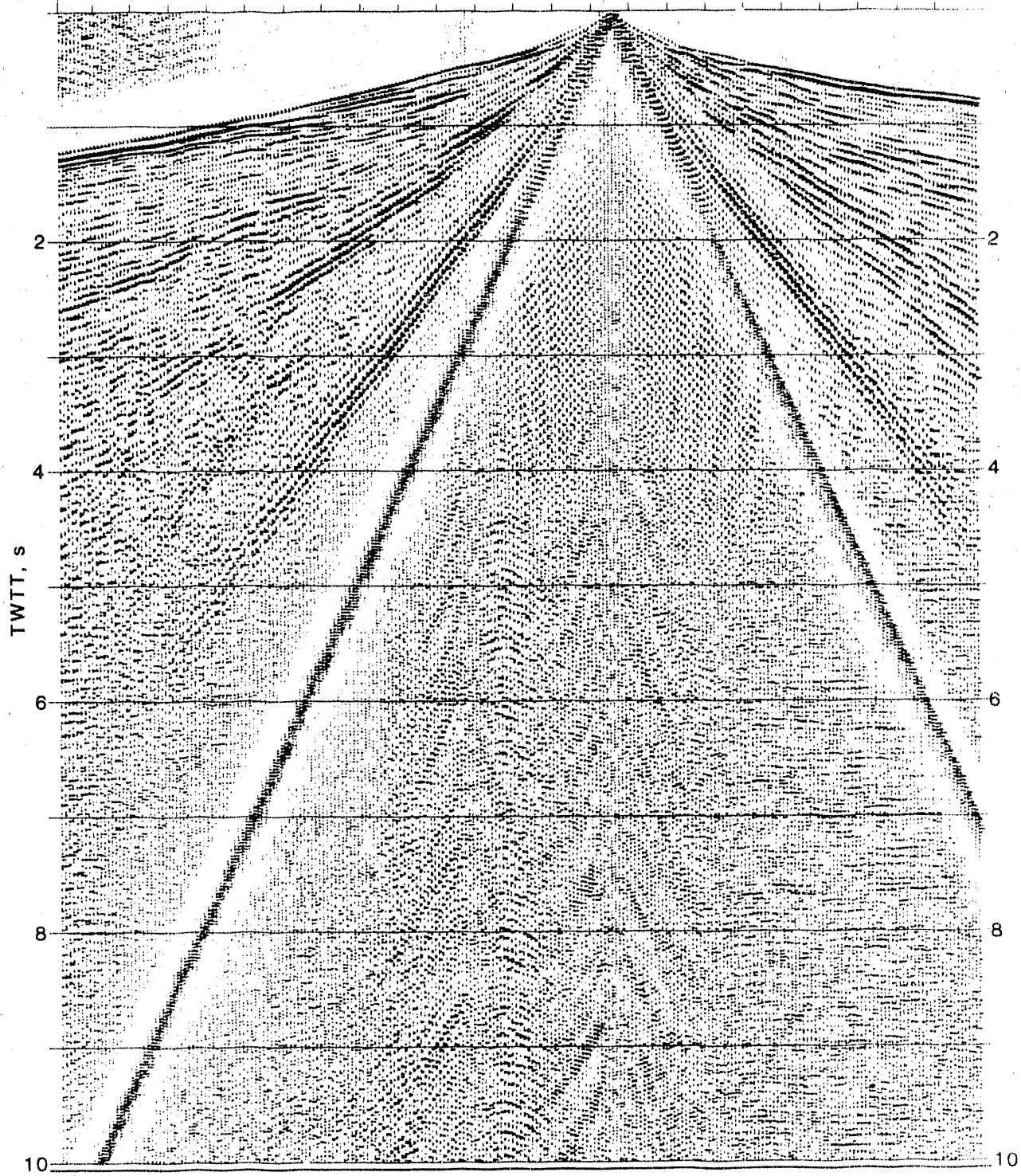
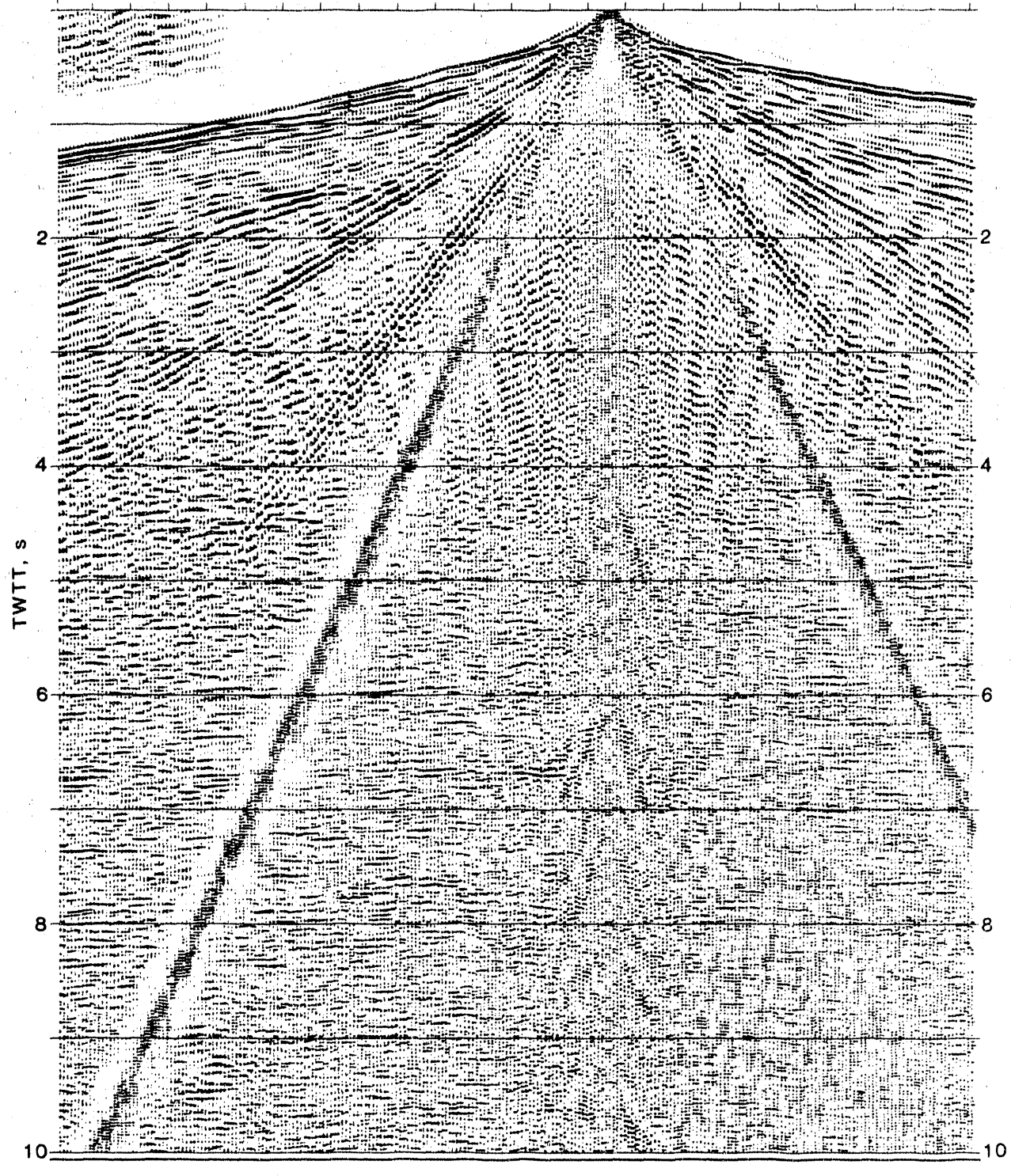


Figure 6c

8-40 HZ, VIB ARRAY = 108°, REC ARRAY = POTTED

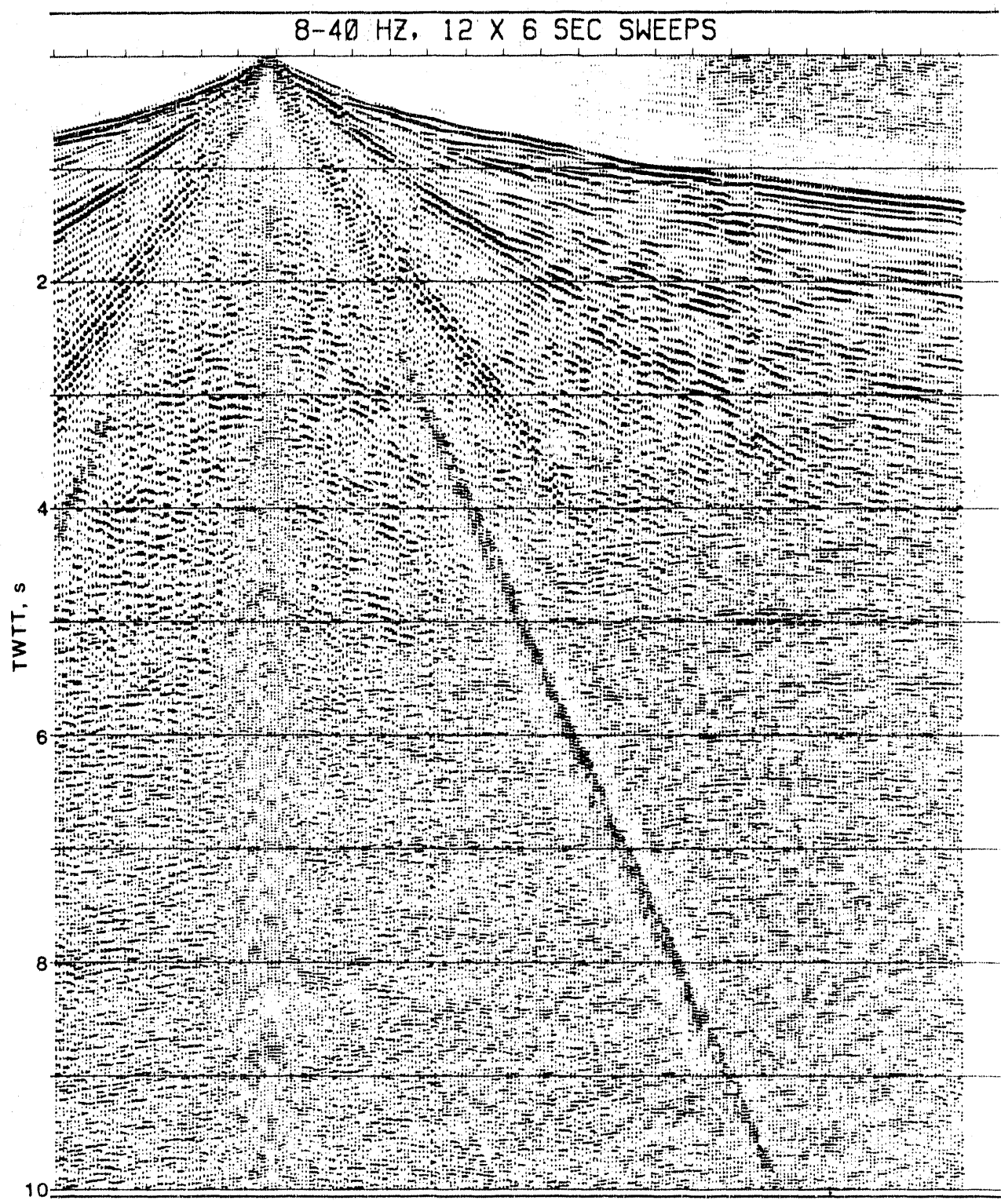


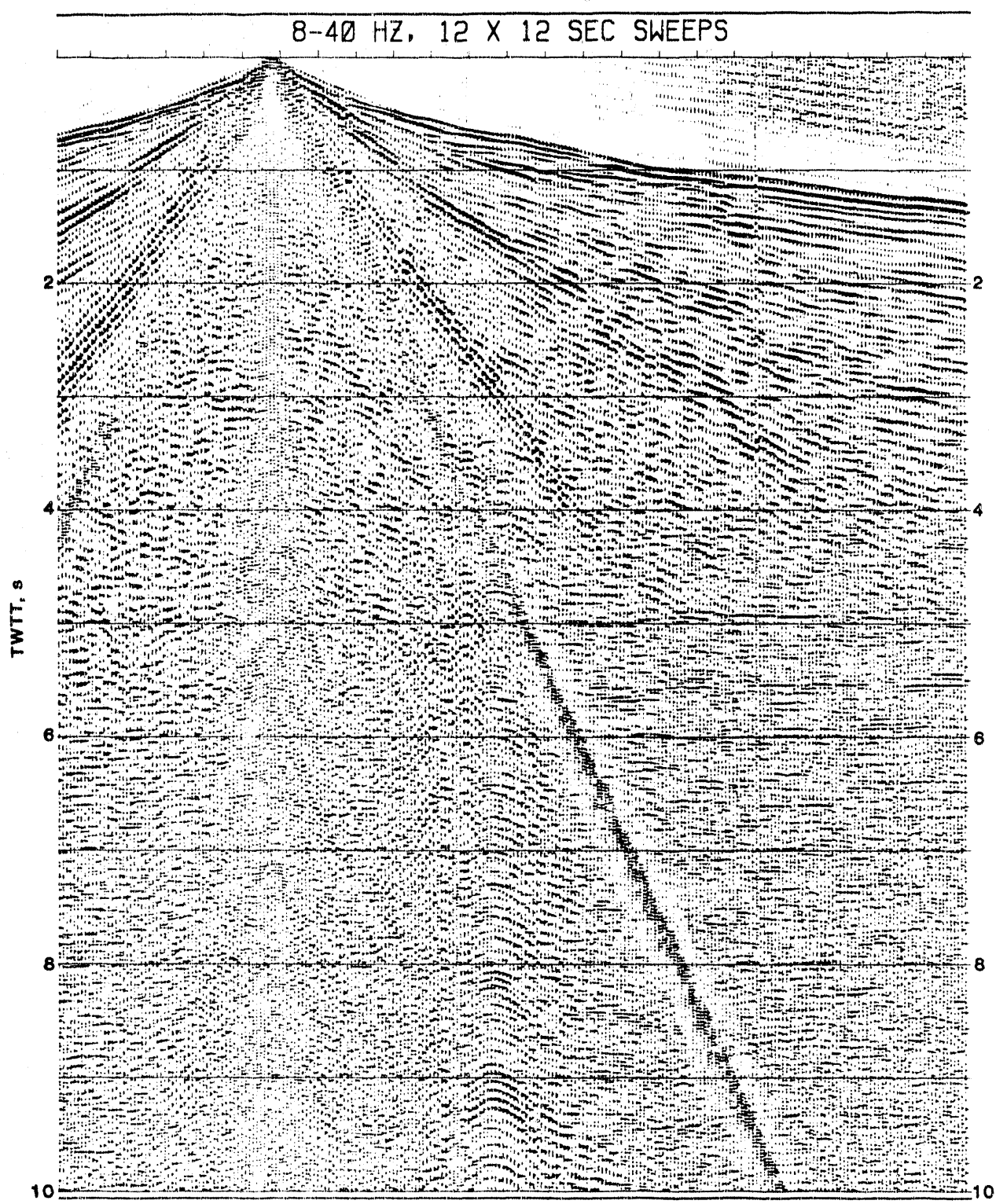
8-40 HZ, VIB ARRAY = 108', REC ARRAY = 165'

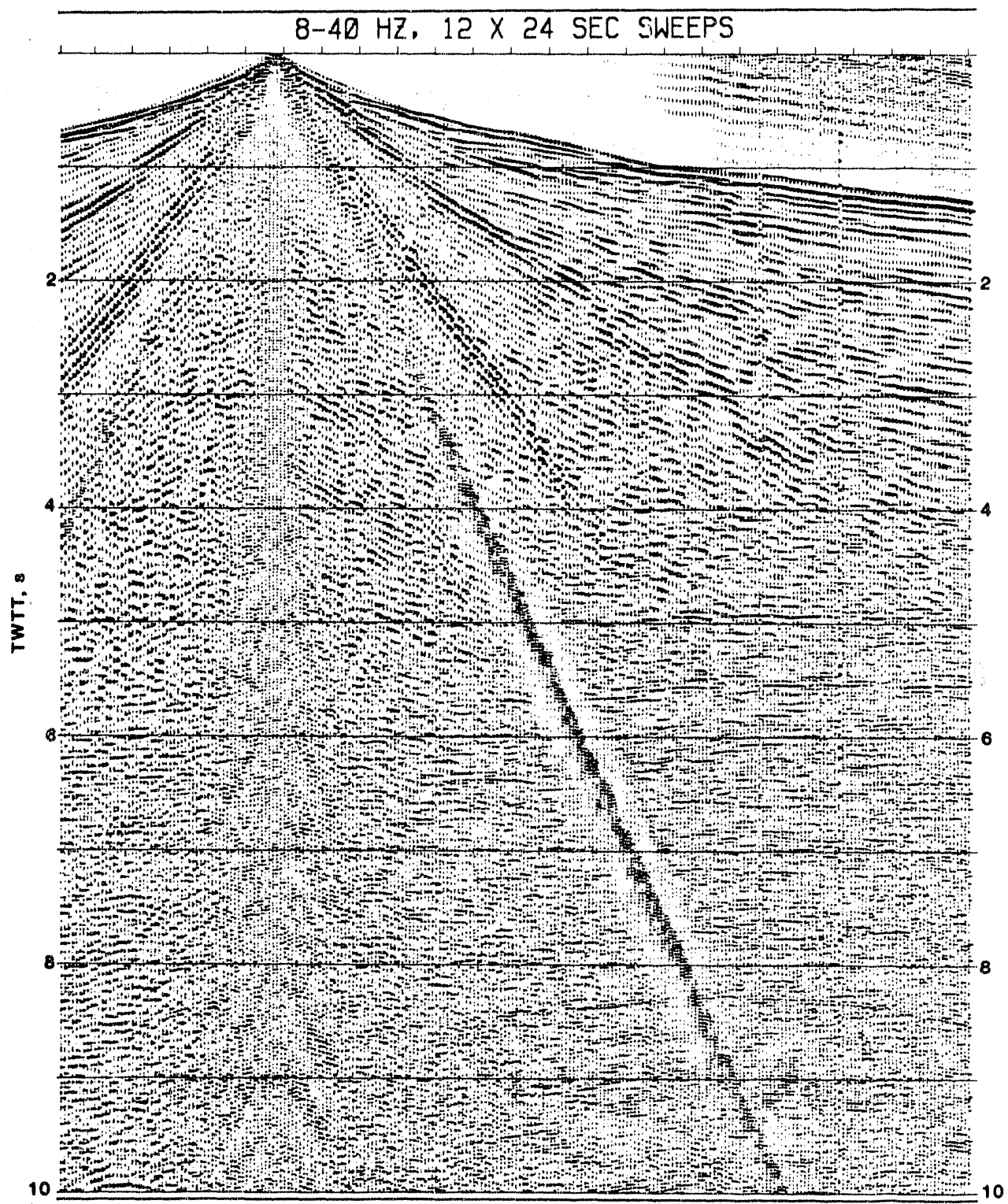


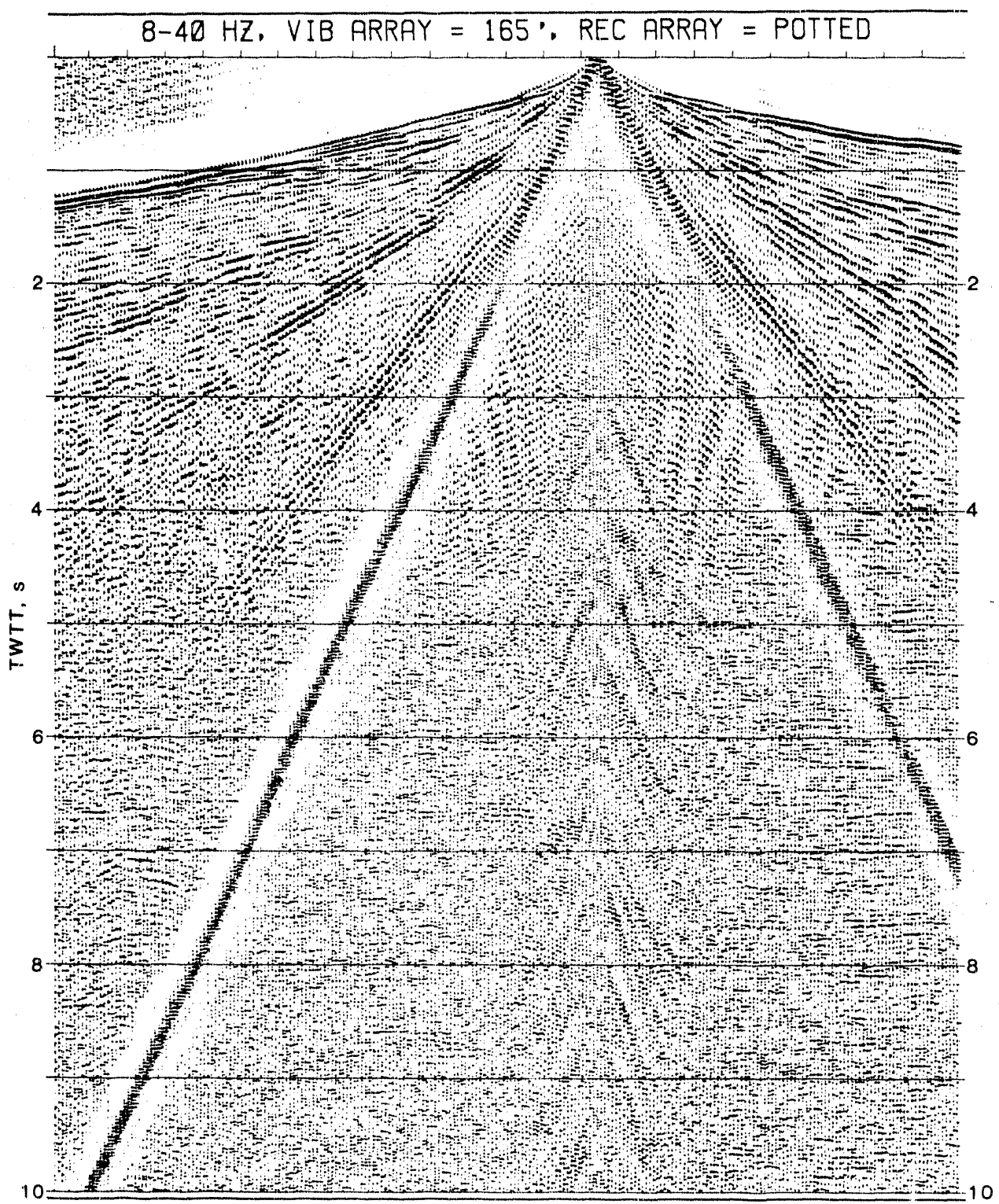
100

Figure 8









8-40 HZ, VIB ARRAY = 231', REC ARRAY = POTTED

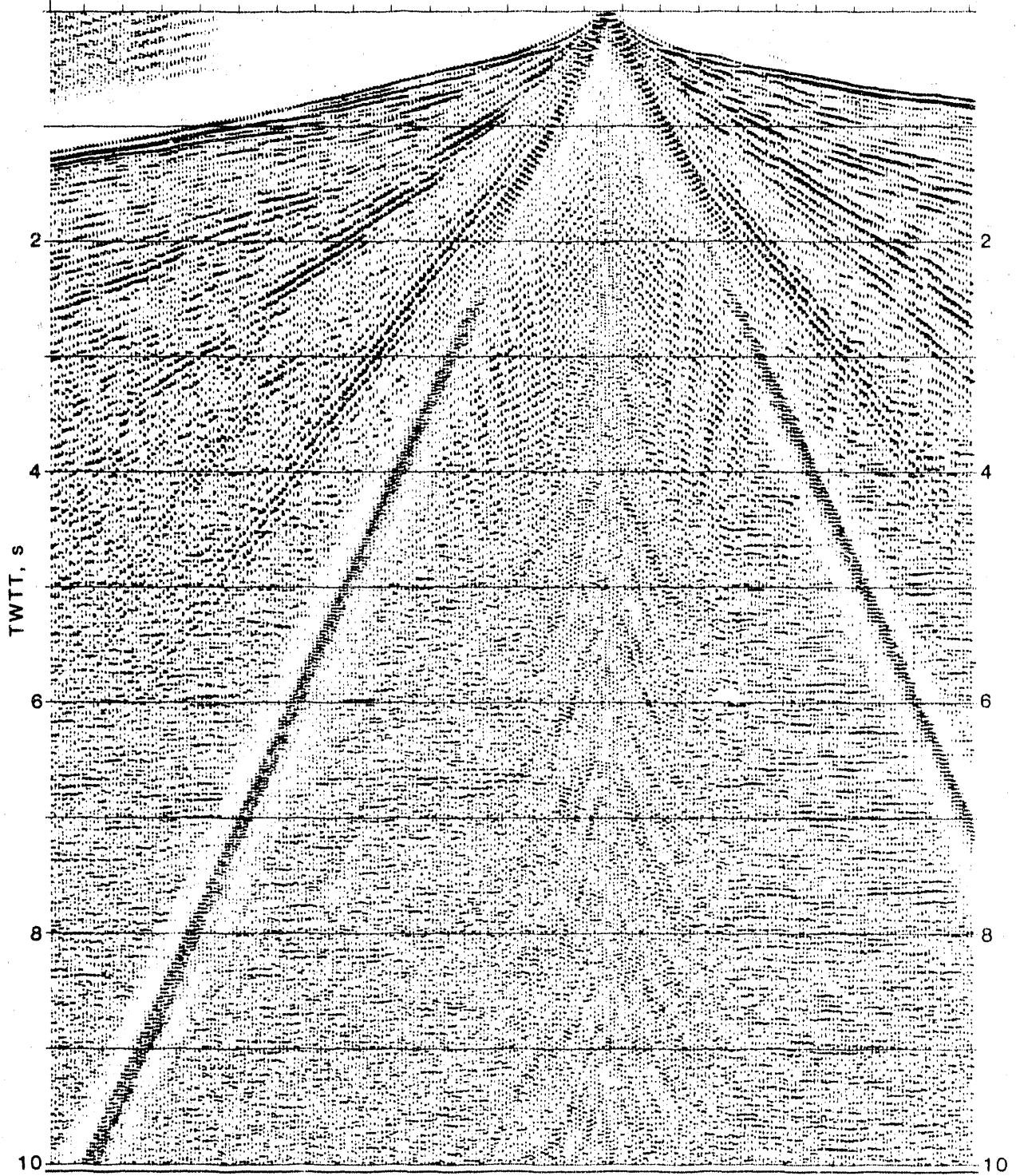
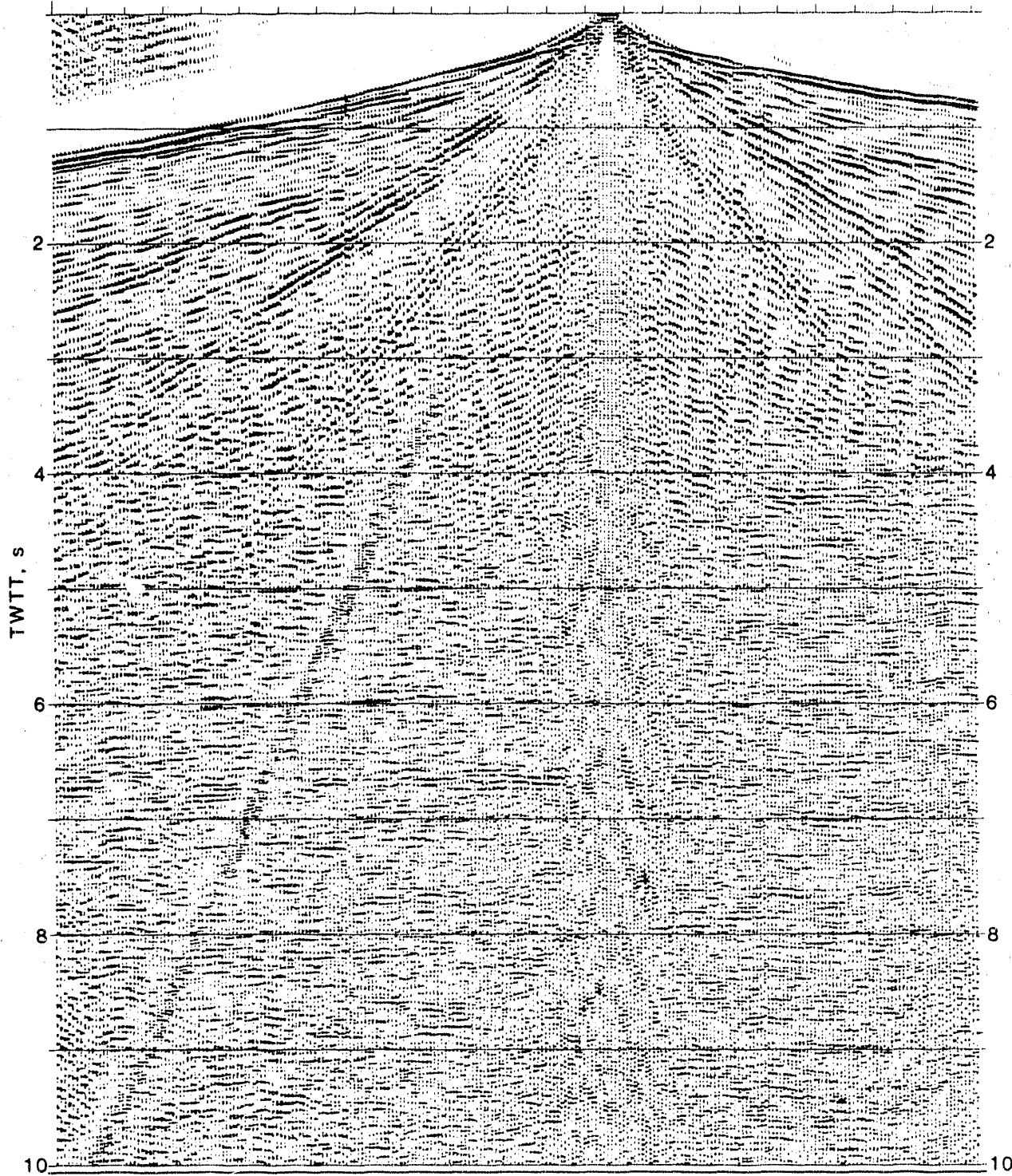
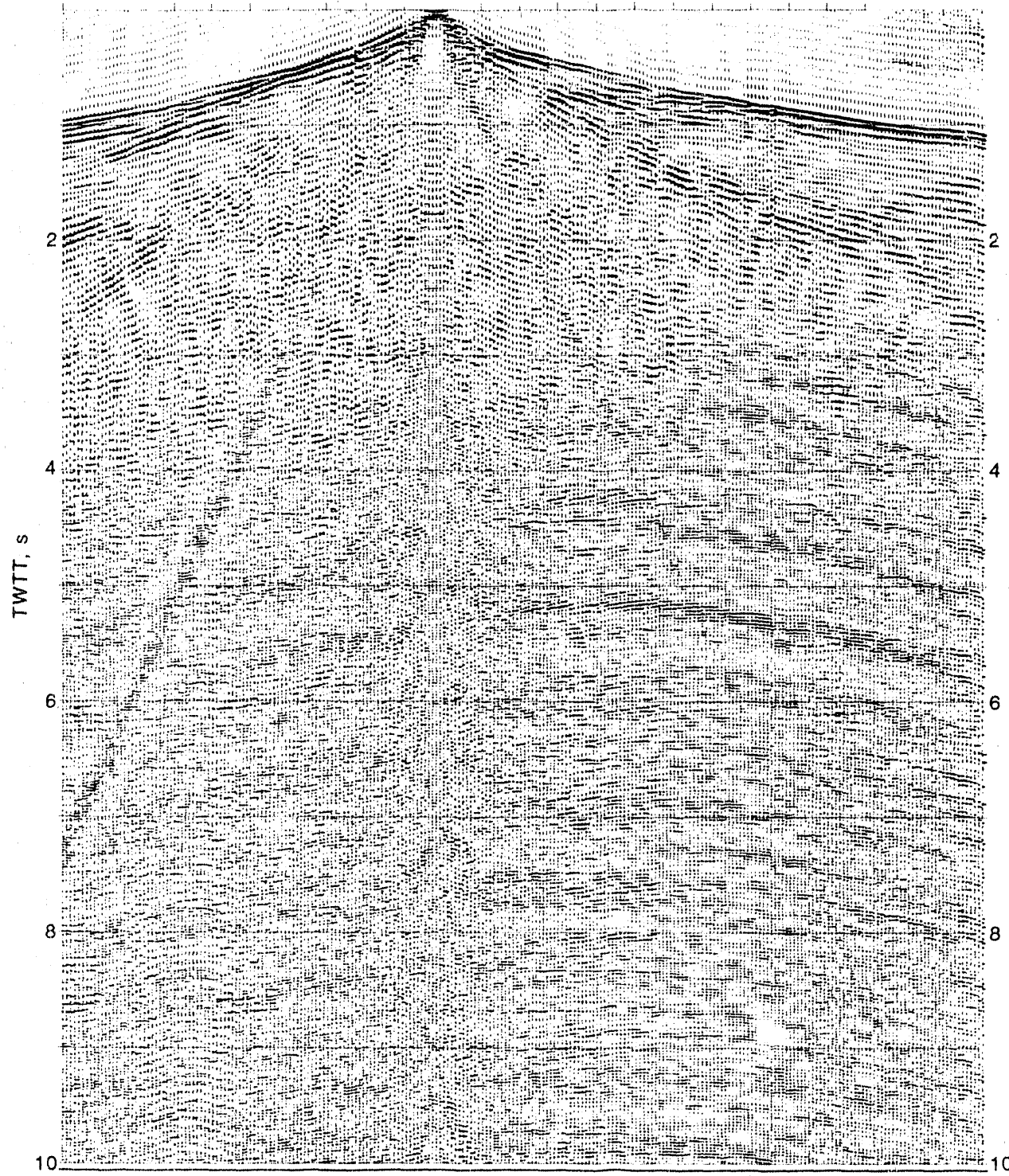


Figure 11

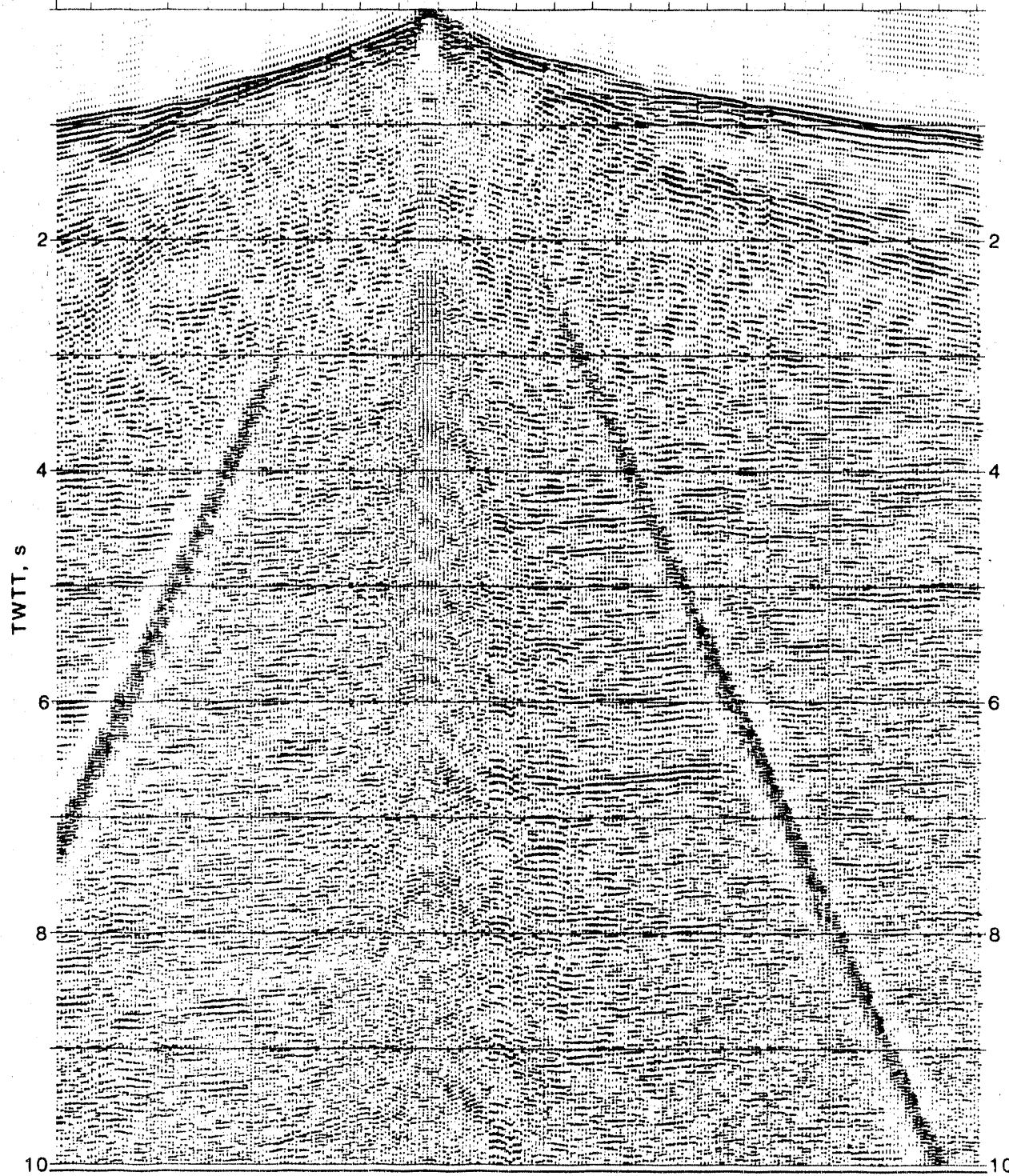
8-40 HZ, VIB ARRAY = 231', REC ARRAY = 165'



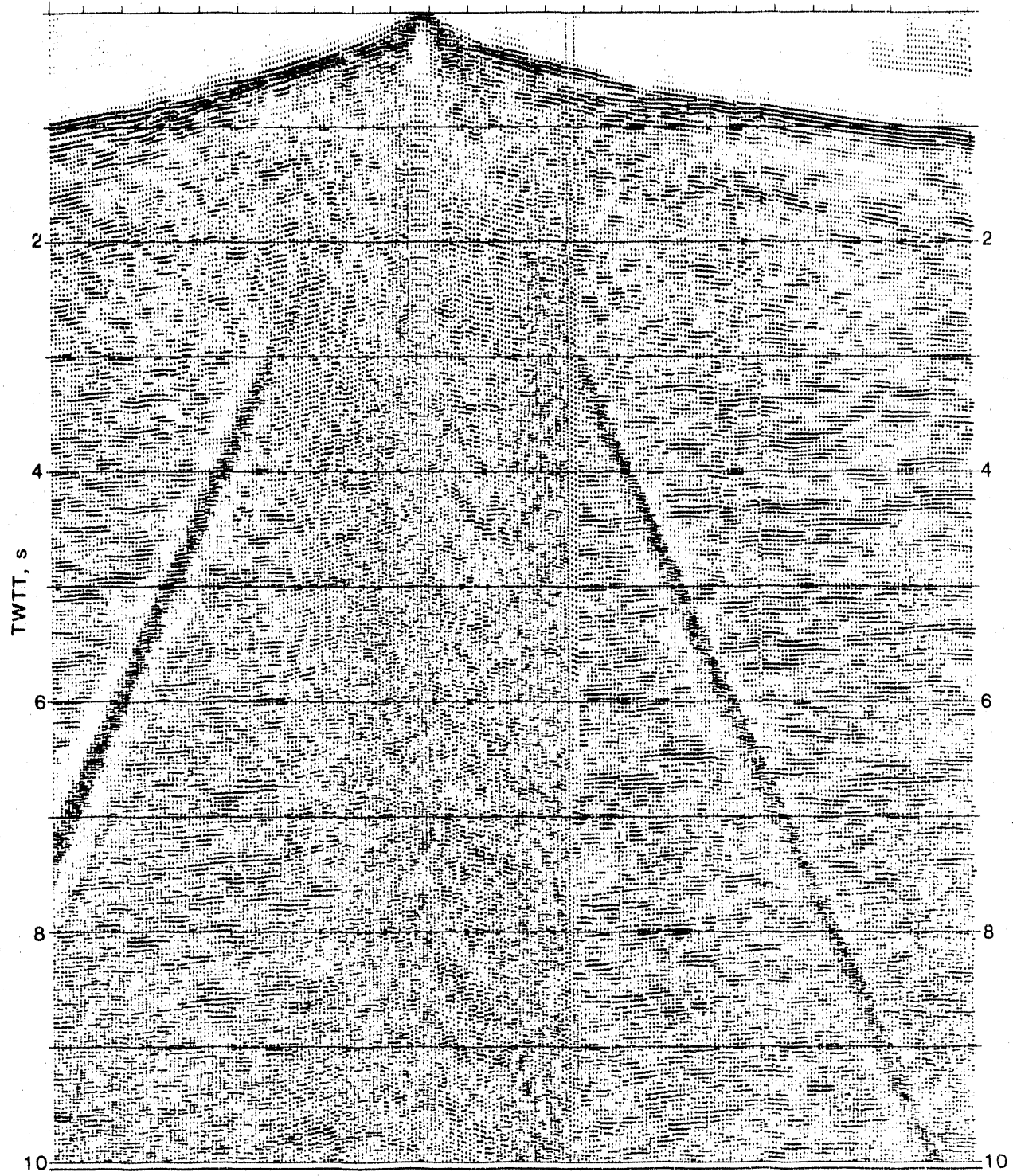
12-48 HZ, VIB ARRAY = 231°, REC ARRAY = 82°



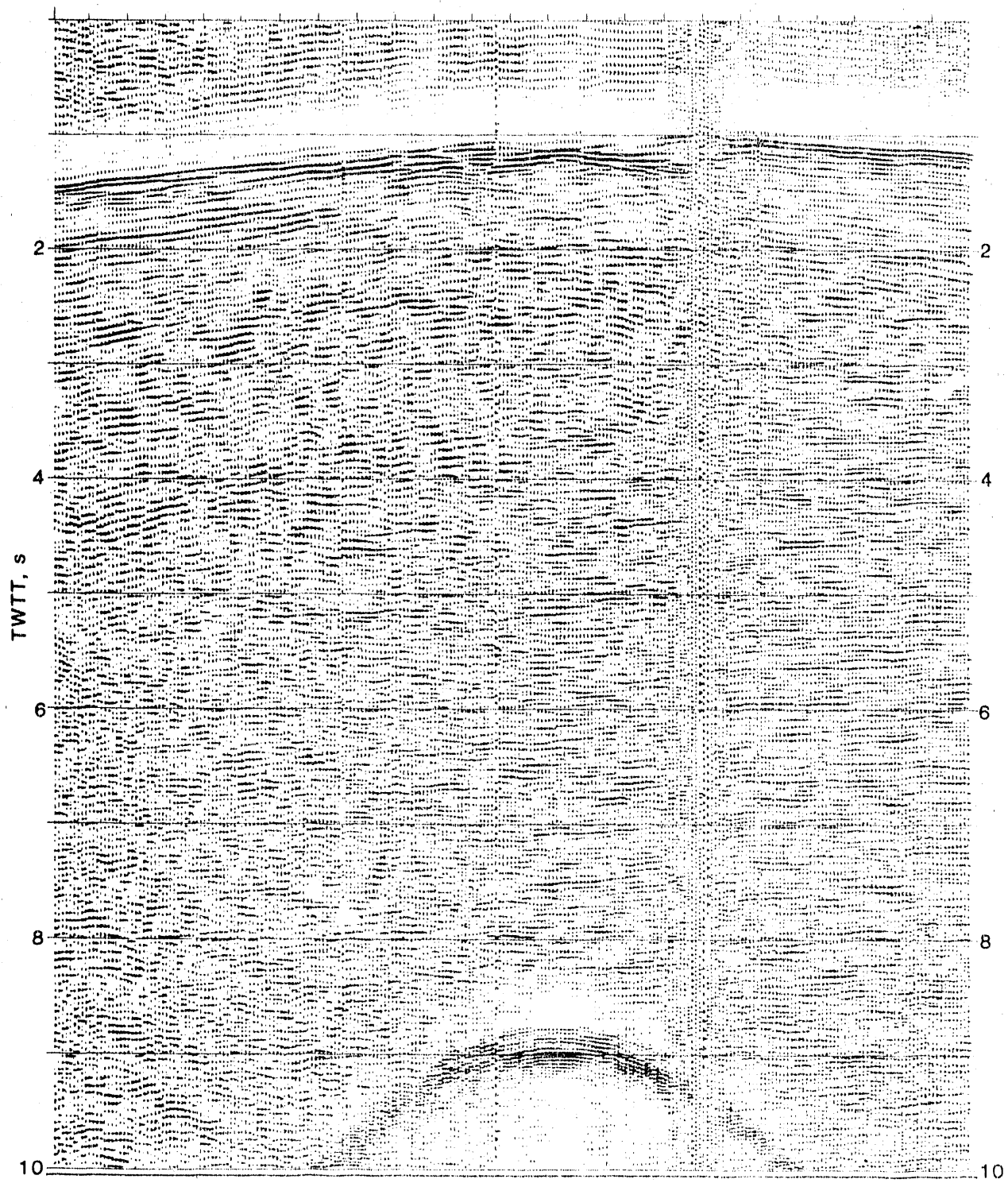
14-56 HZ, VIB ARRAY = 231', REC ARRAY = 165'



18-72 HZ NON-LIN. VIB ARRAY = 231', REC ARRAY = 165'

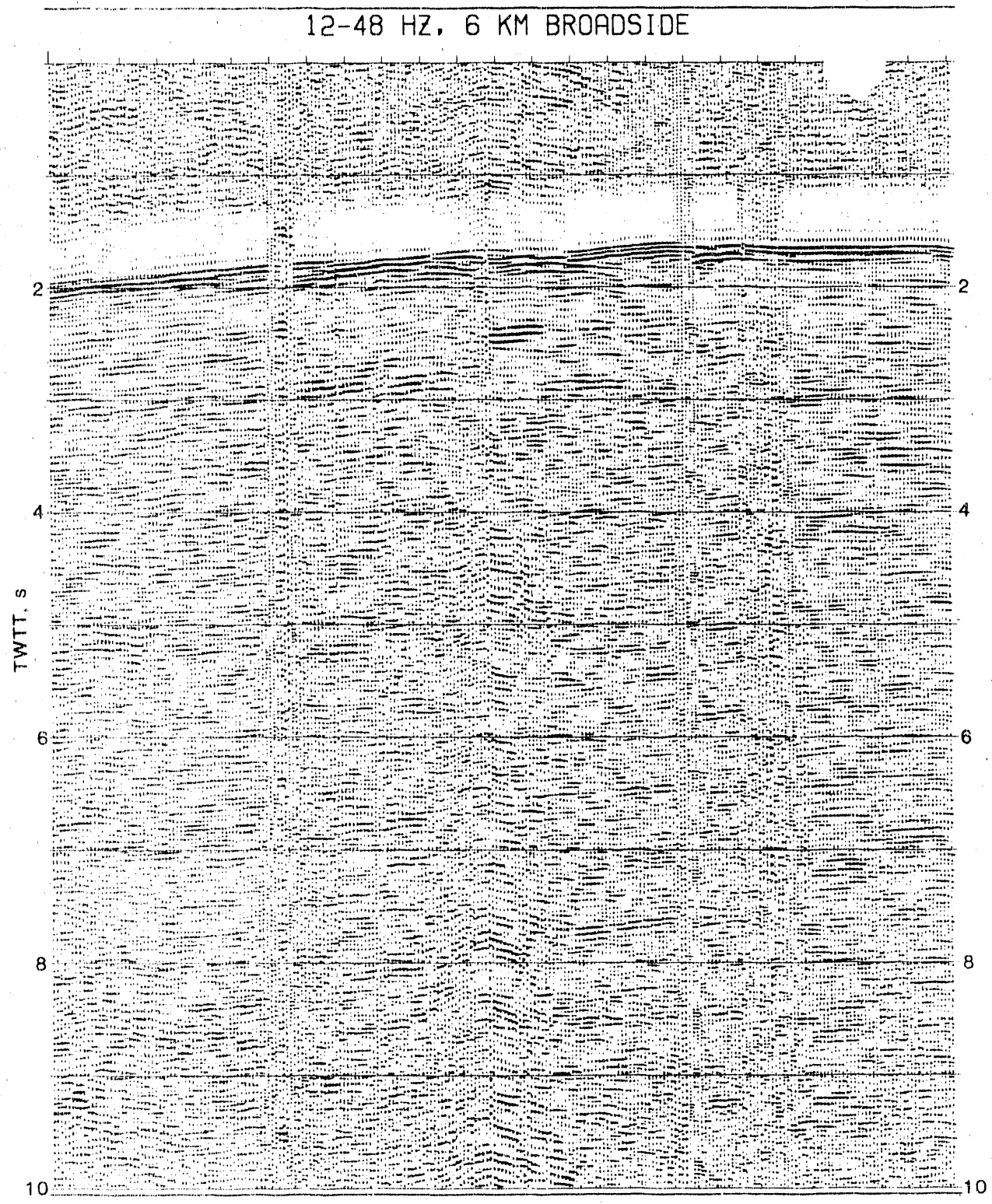


12-48 Hz, 3 km broadside

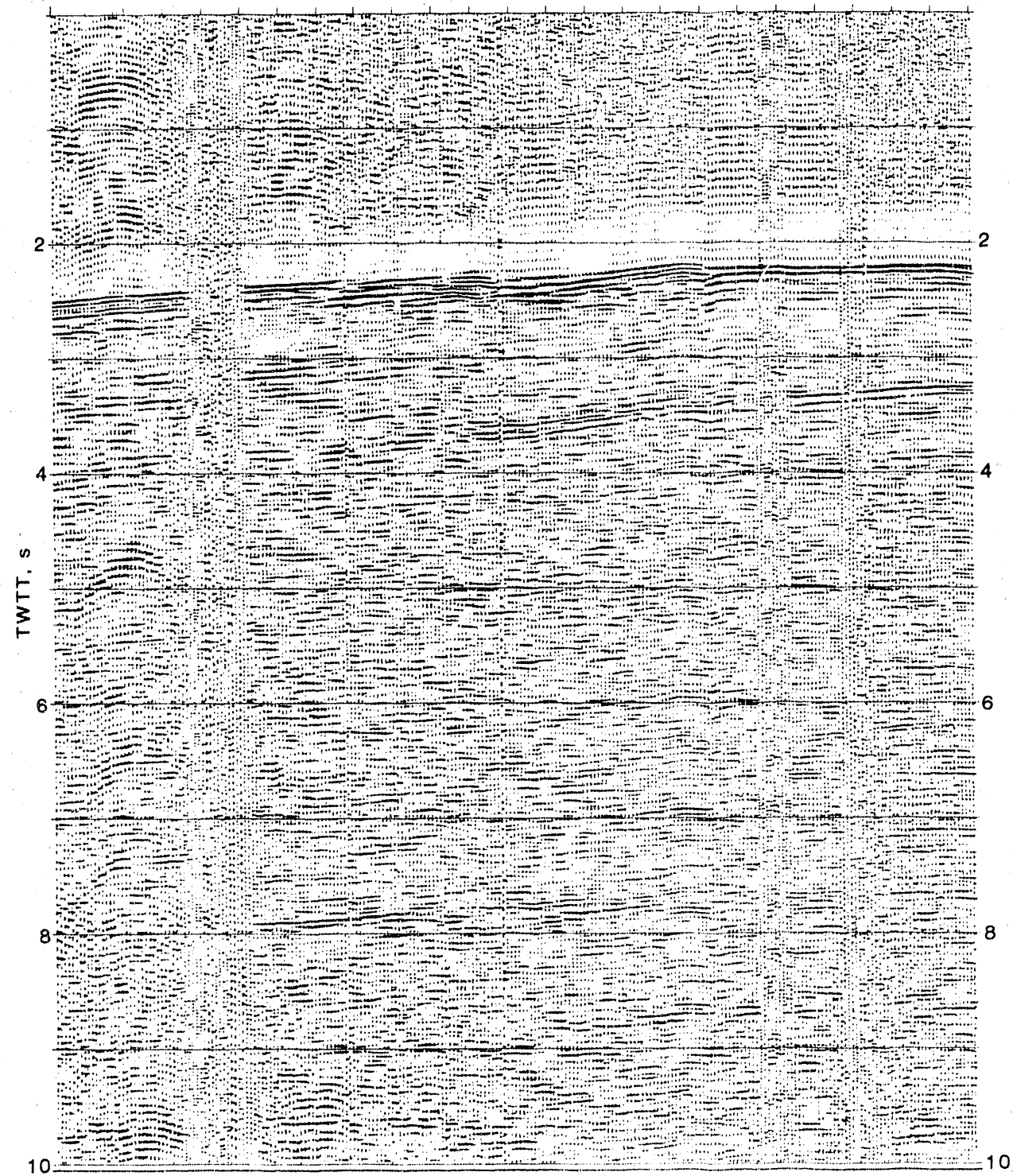


110

Figure 14a

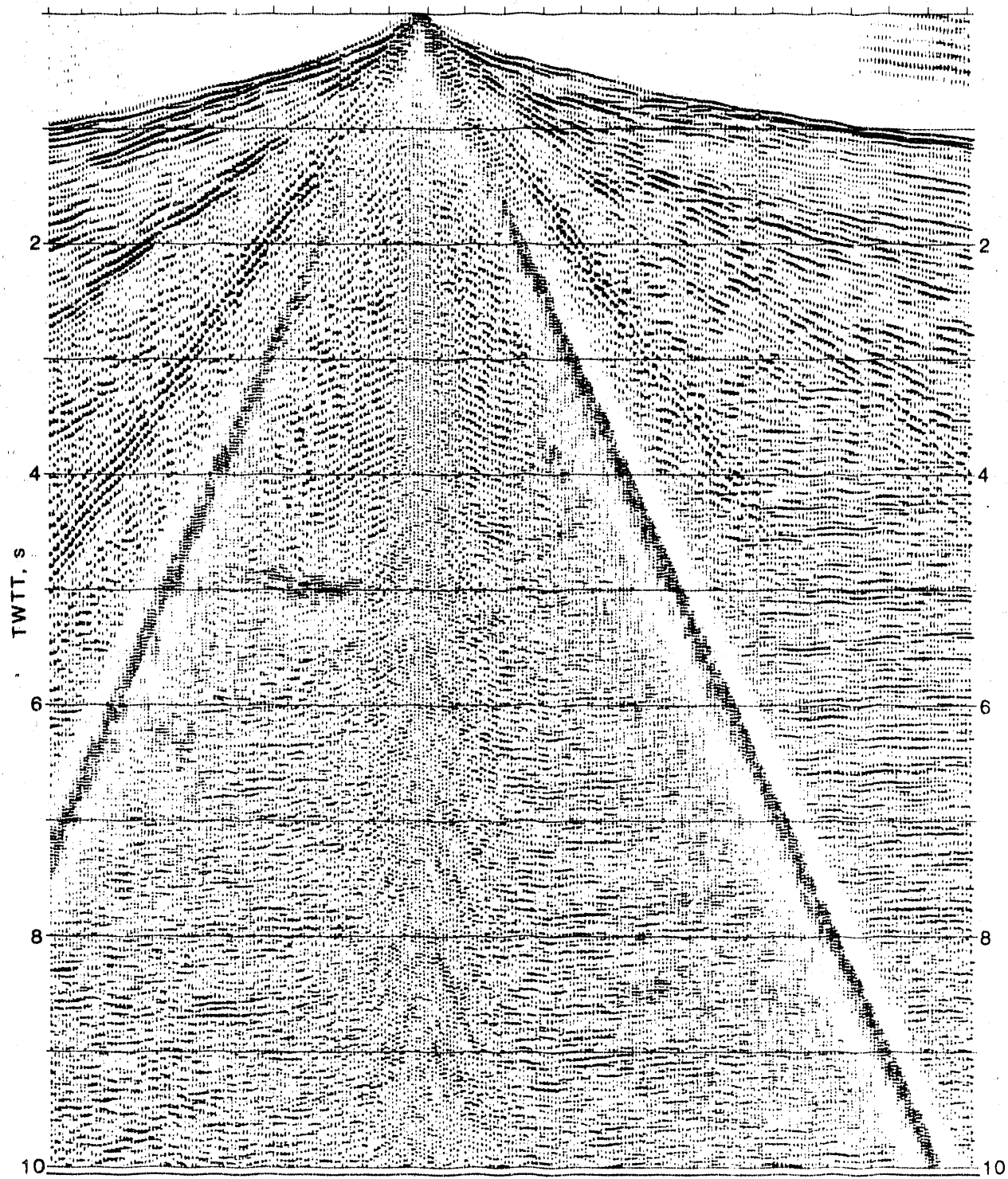


12-48 HZ, 9 KM BROADSIDE



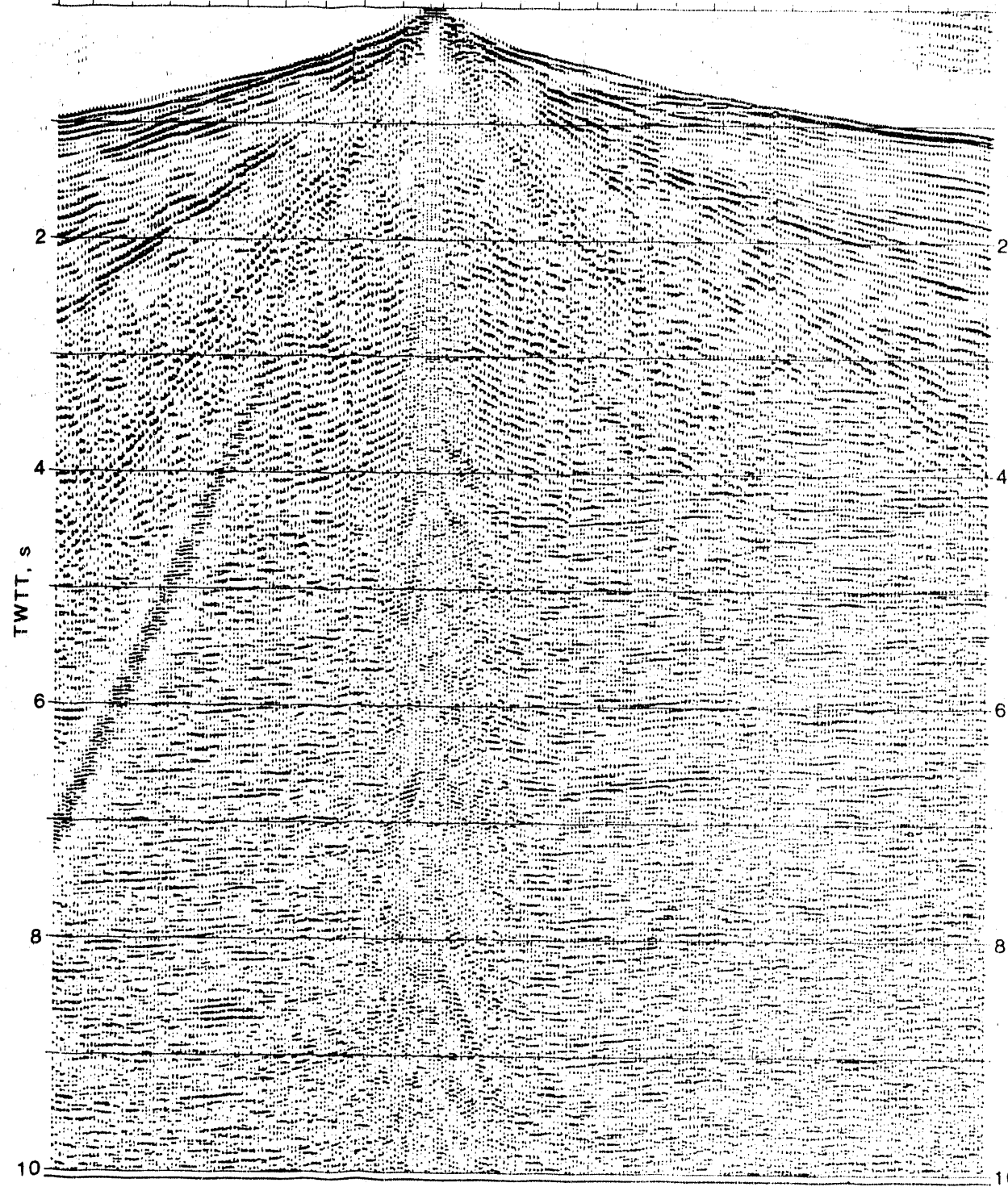
Windspeed 2 mph

8-40 HZ, VIB ARRAY = 108', REC ARRAY = 165'



Windspeed 5-8 mph

8-40 Hz, VIB ARRAY = 231', REC ARRAY = 165'



8-40 HZ, VIB ARRAY = 108', REC ARRAY = POTTED

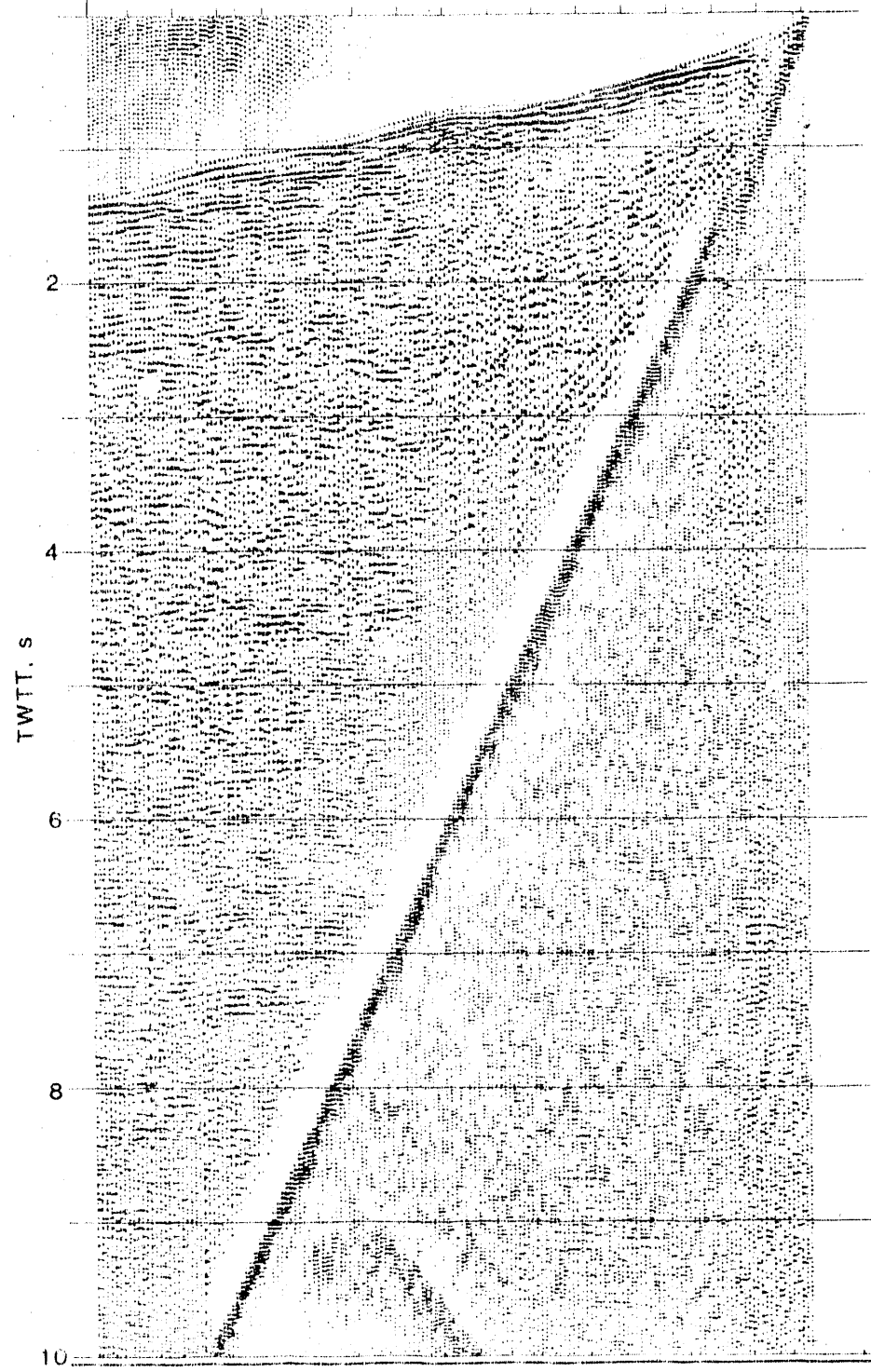


Figure 16

REC ARRAY LINEAR

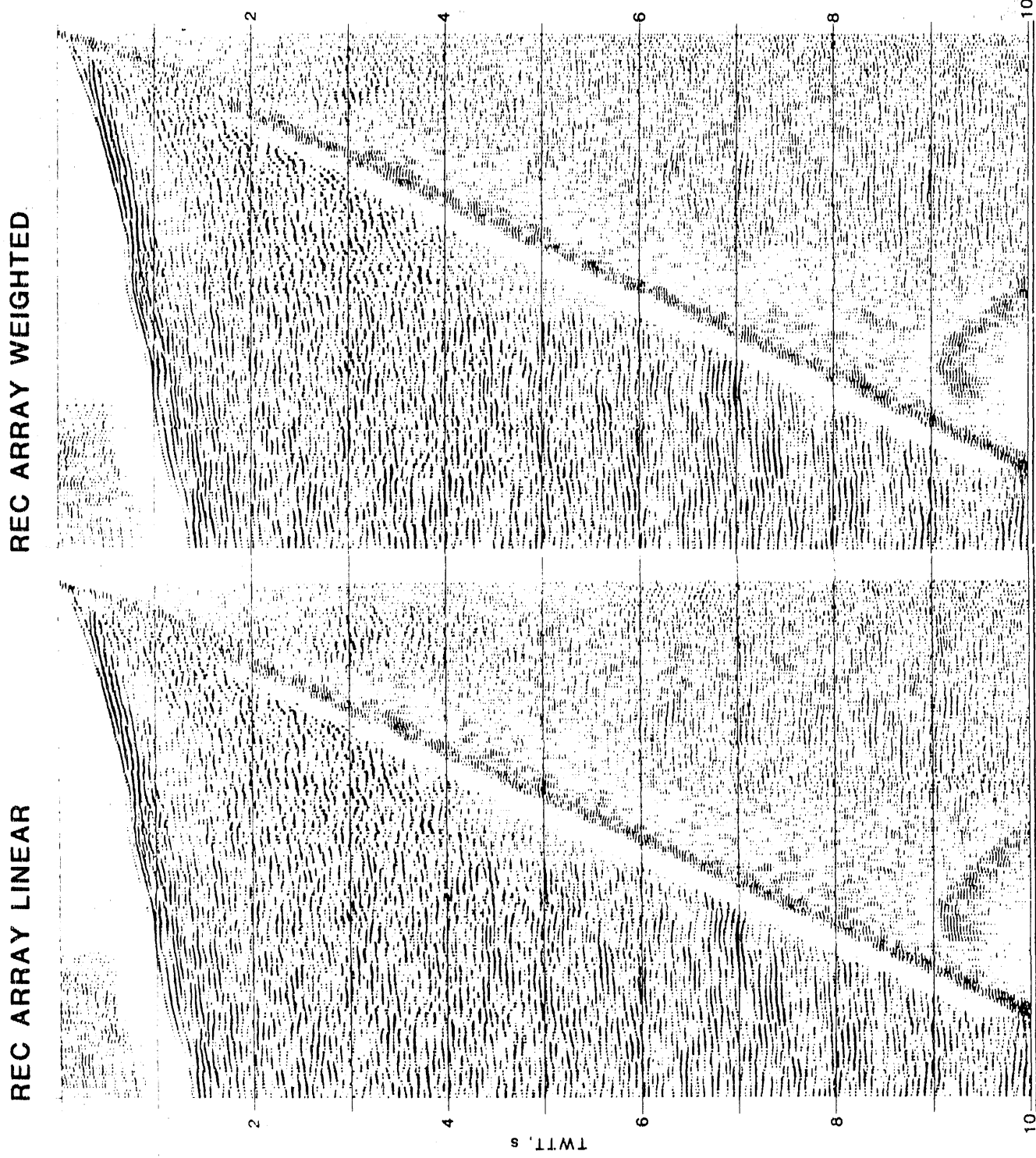


Figure 17

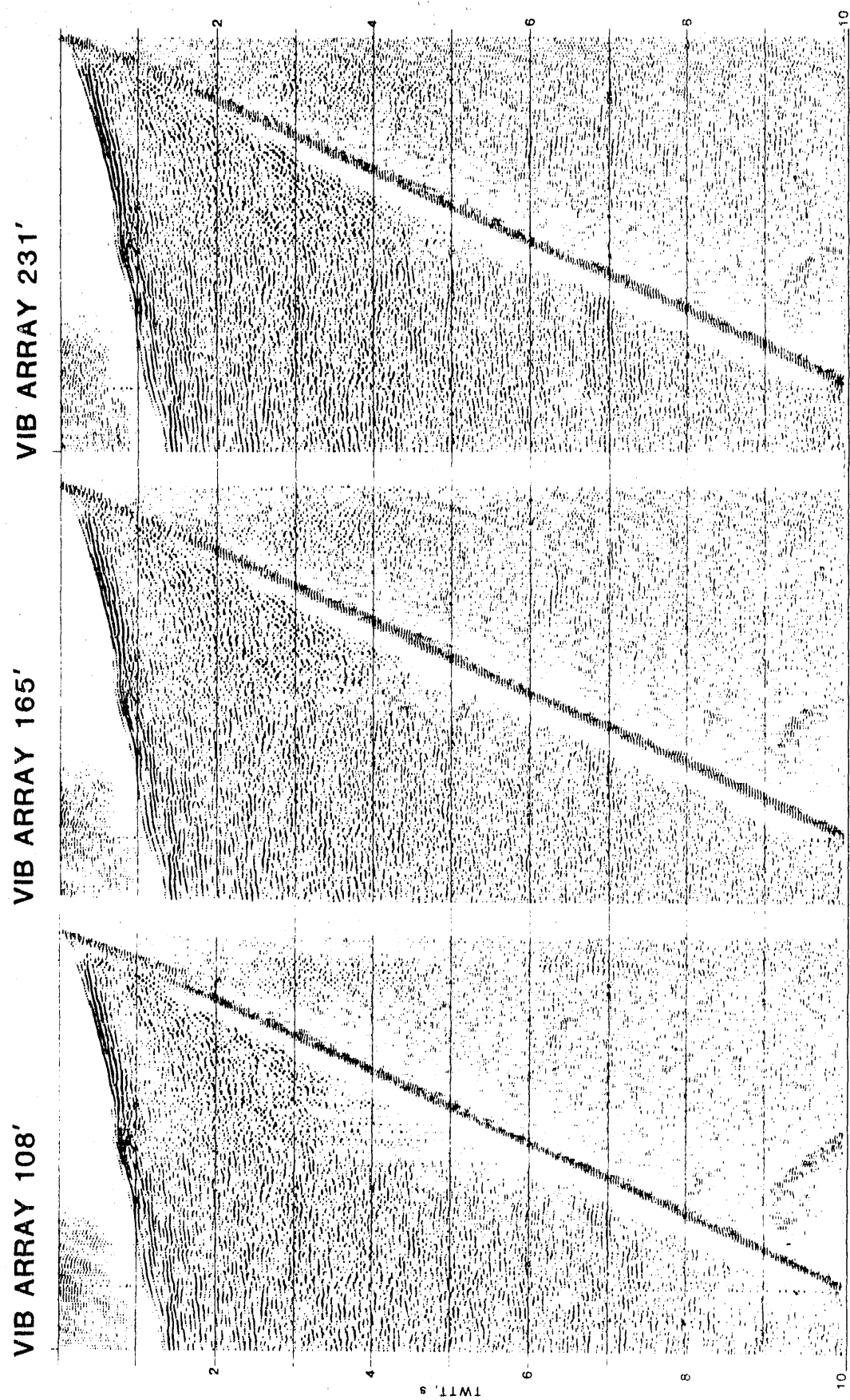
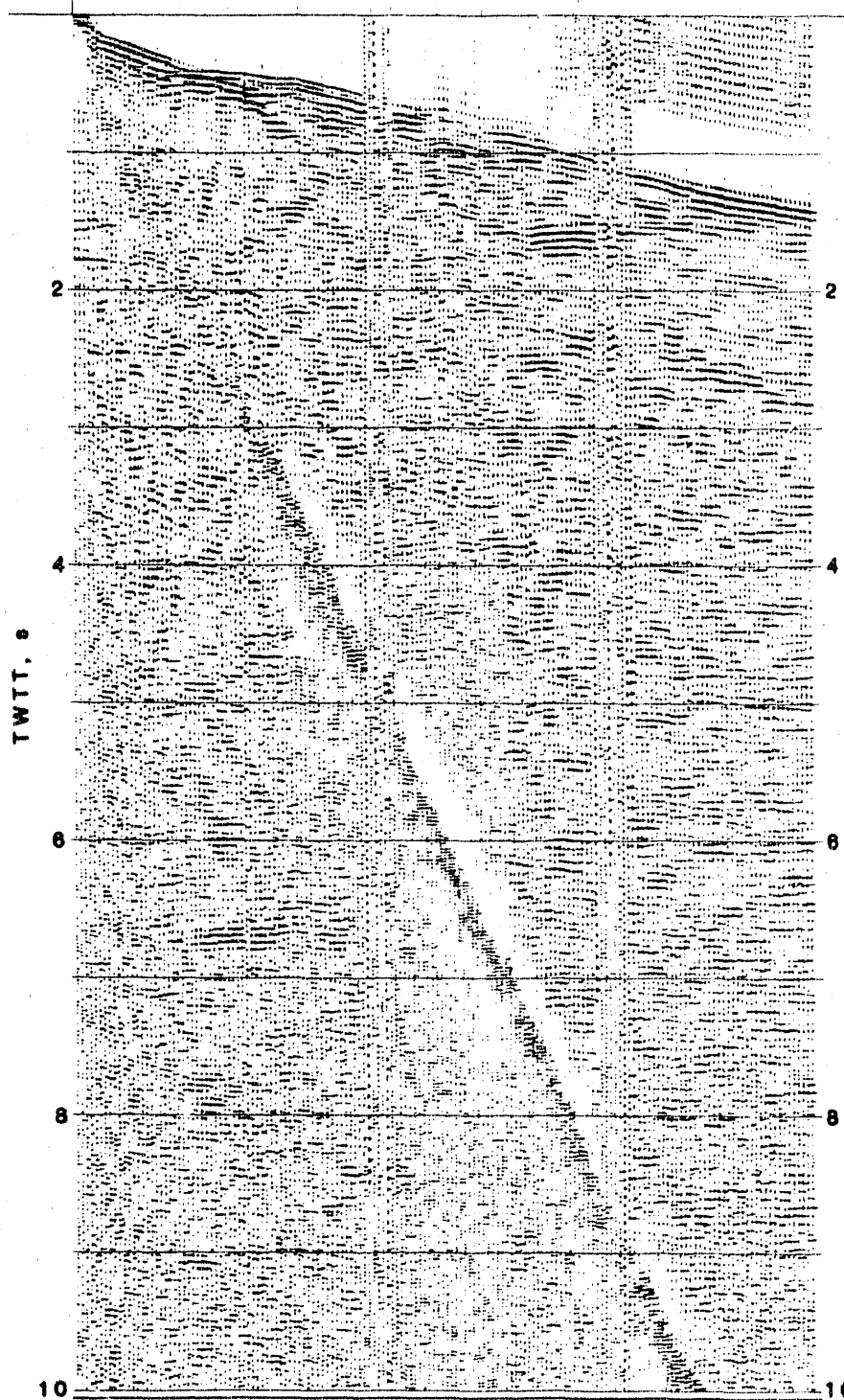
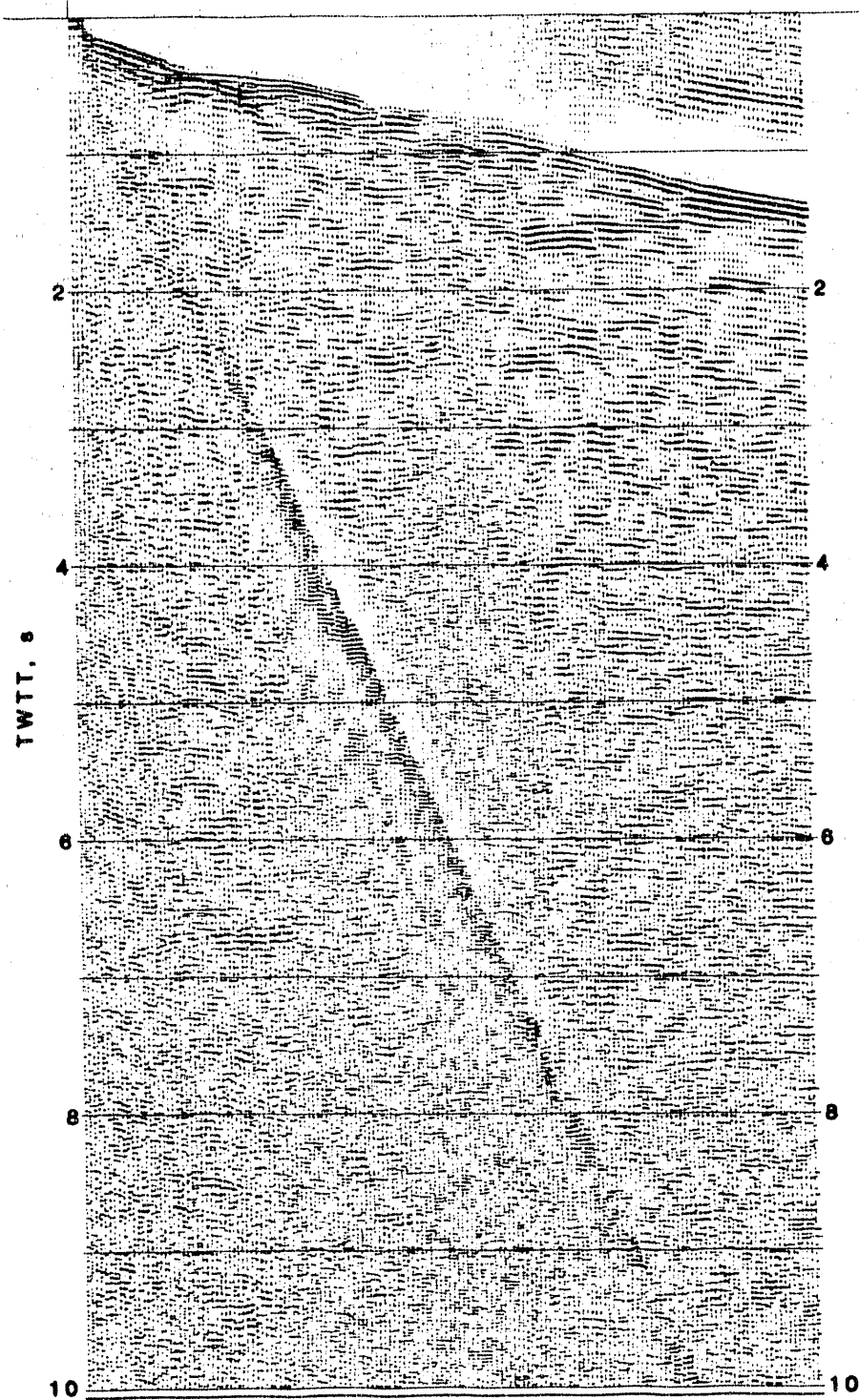


Figure 18

12-48 HZ, VIB ARRAY = 231', REC ARRAY = WEIGHTED



14-56 HZ, VIB ARRAY = 231, REC ARRAY = WEIGHTED



16-64 HZ, V1B ARRAY = 231', REC ARRAY = WEIGHTED

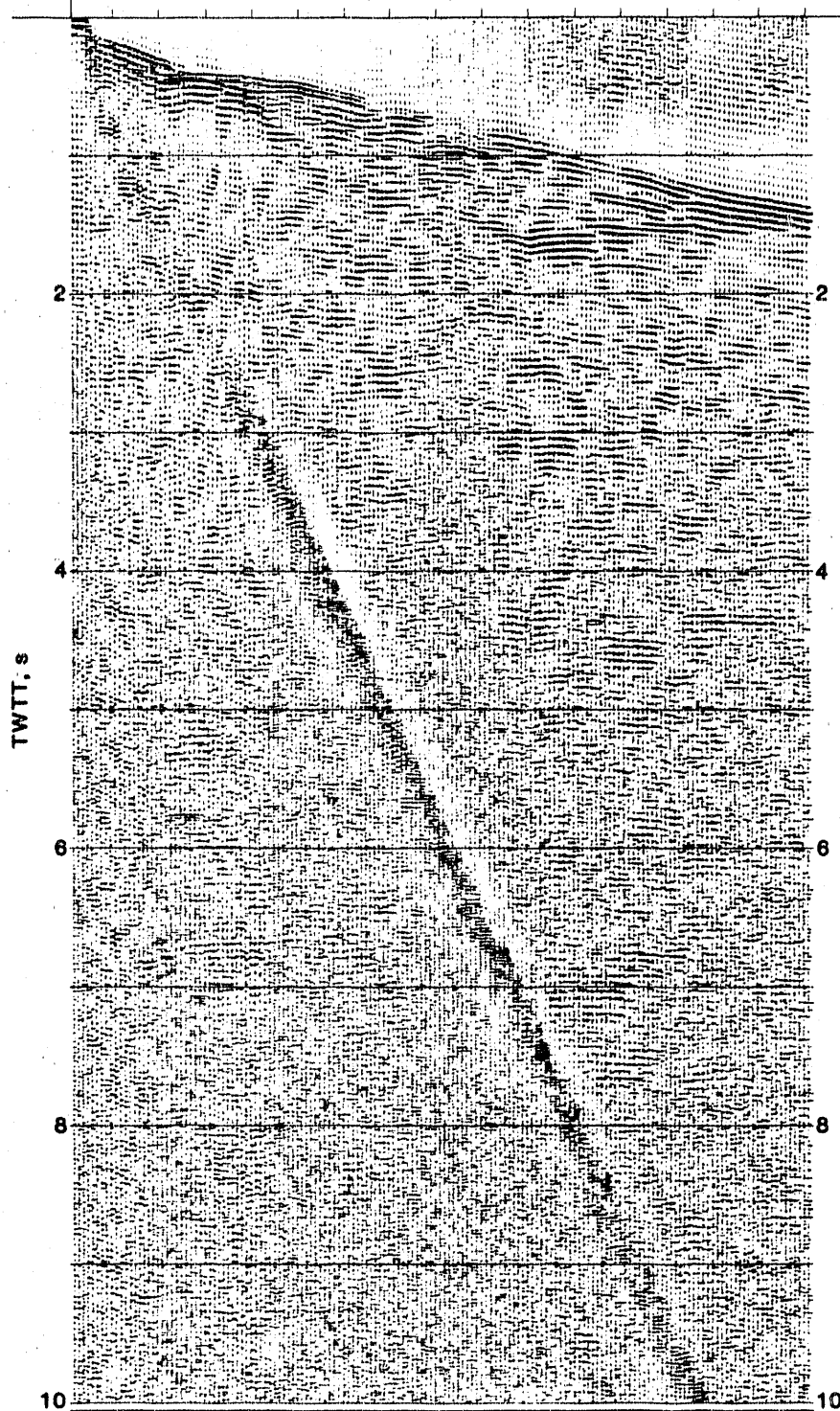
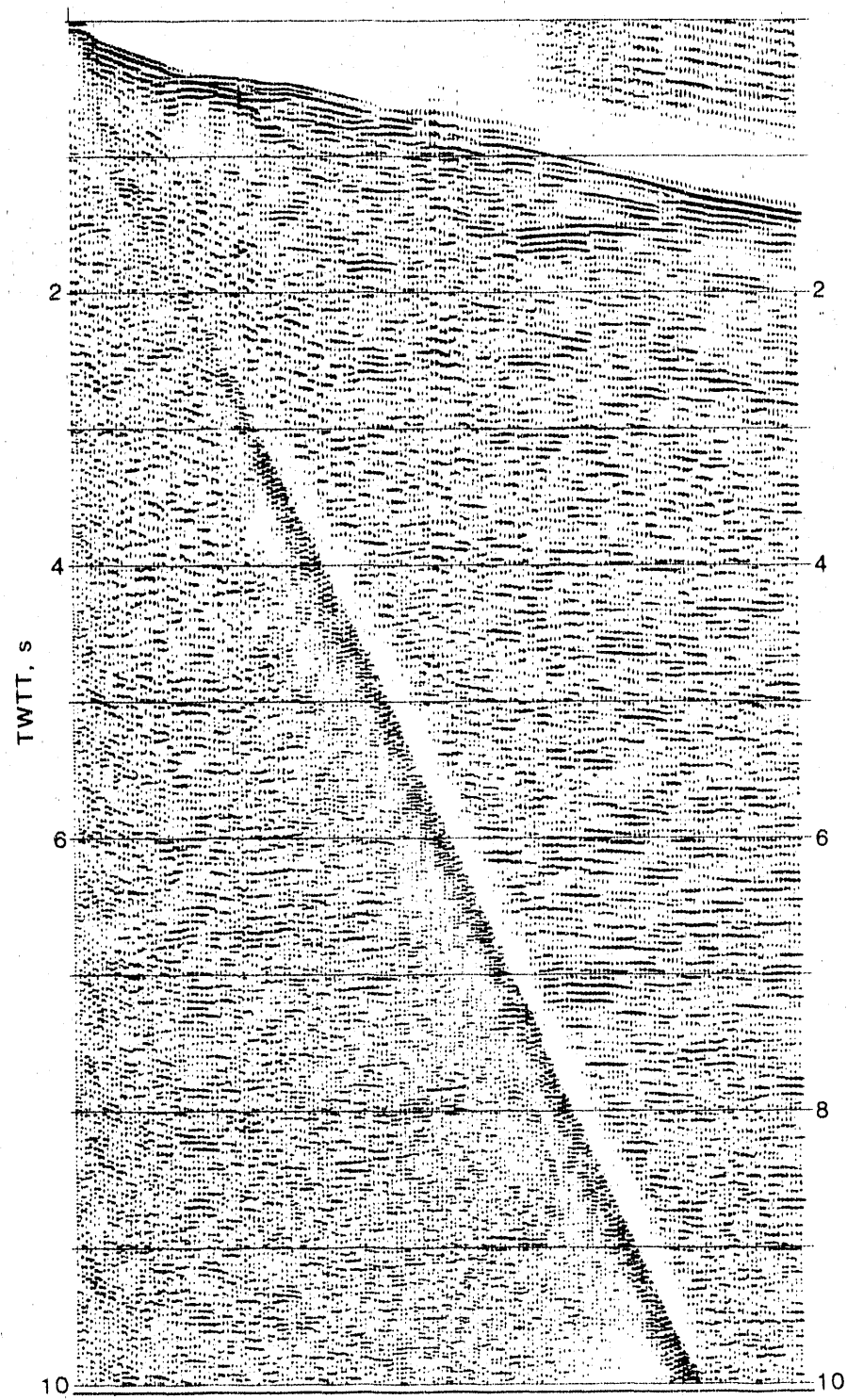


Figure 19c

10-44 Hz, VIB ARRAY IS 231', REC ARRAY IS WEIGHTED



8-40 Hz, VIB ARRAY = 231', REC ARRAY = WEIGHTED

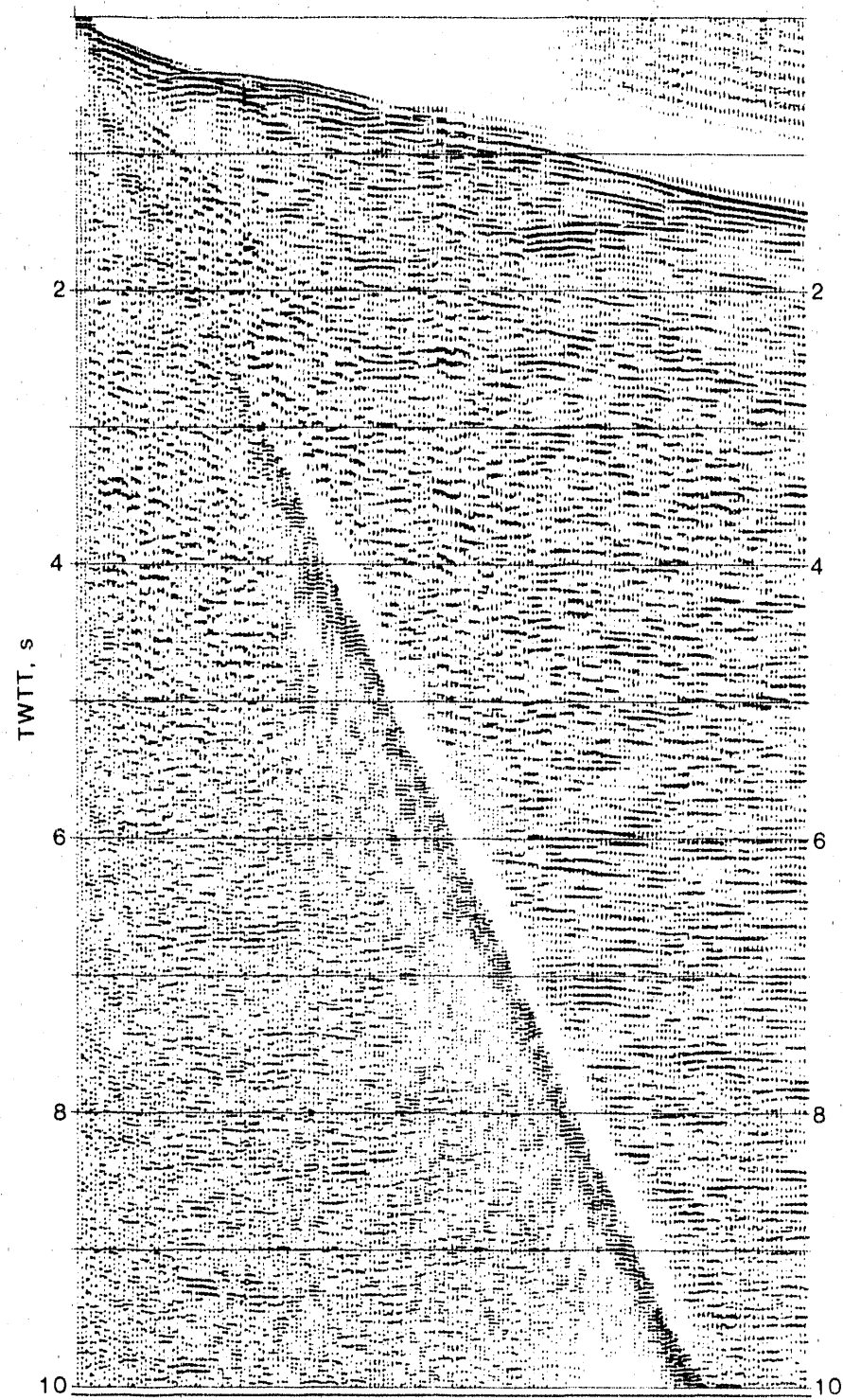
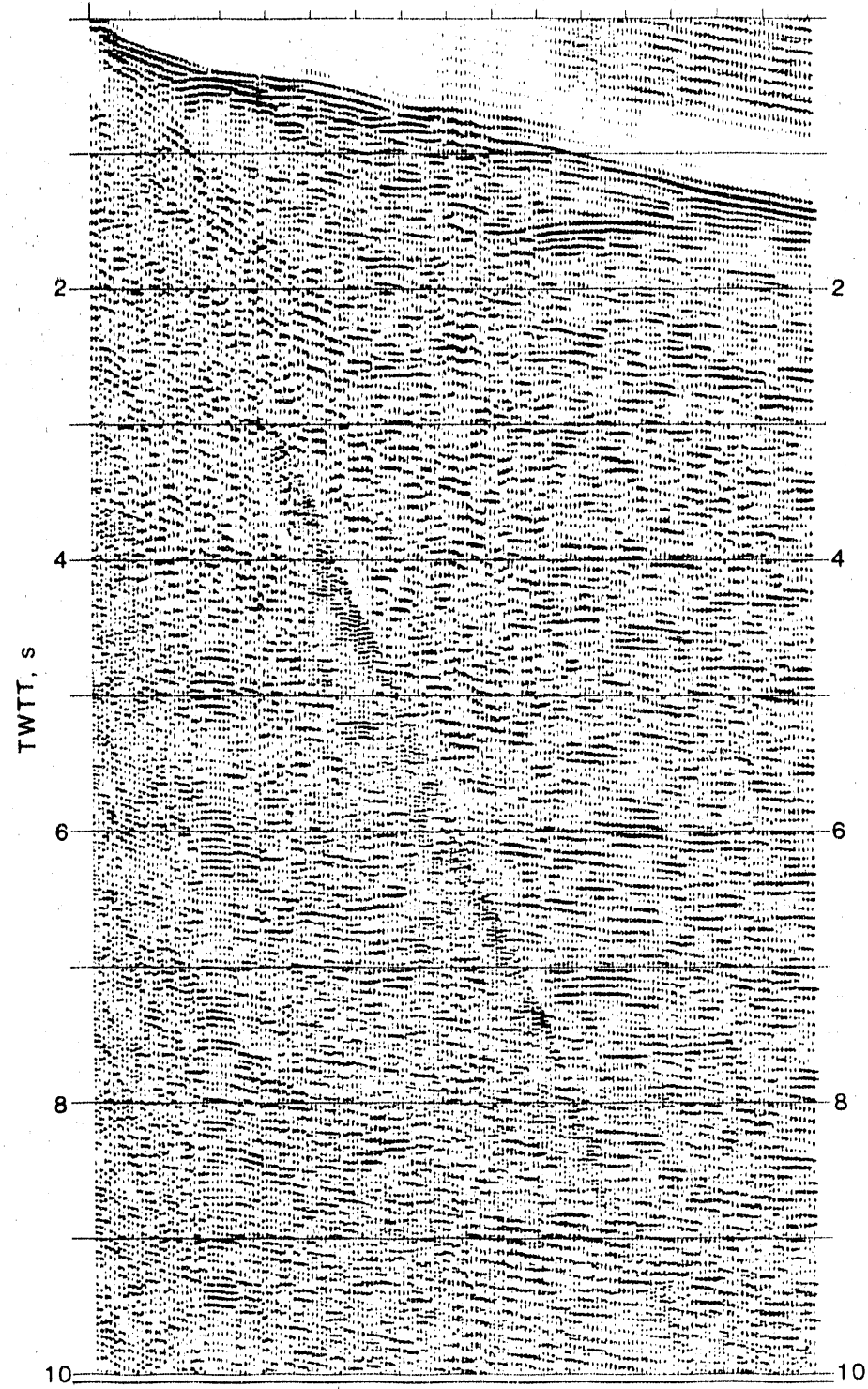


Figure 20b

14-56 HZ NON-LINEAR, VIB ARRAY 231', REC ARRAY WEIGHTED



Windspeed 6-8 mph

14-56 Hz, VIB ARRAY = 231', REC ARRAY = WEIGHTED

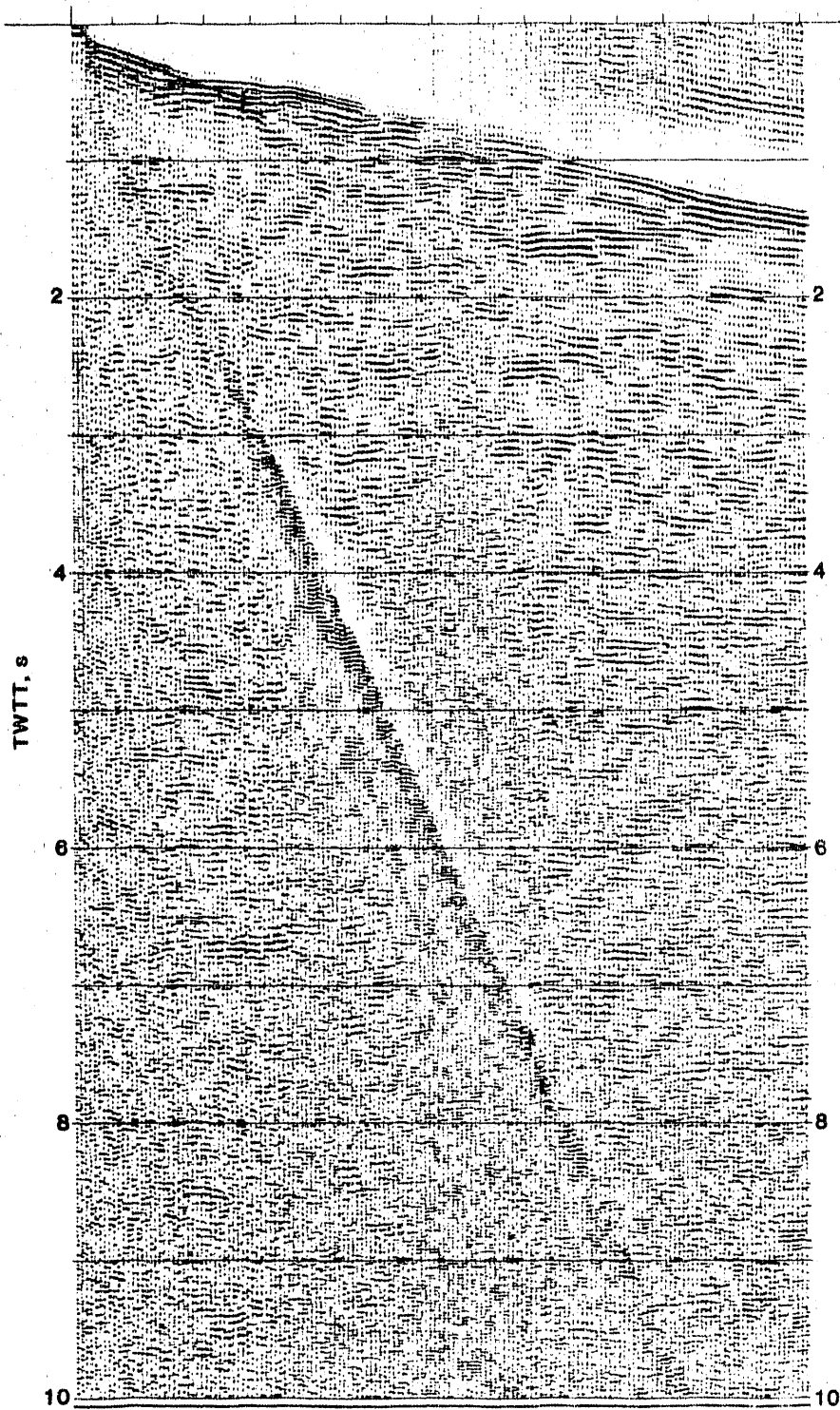
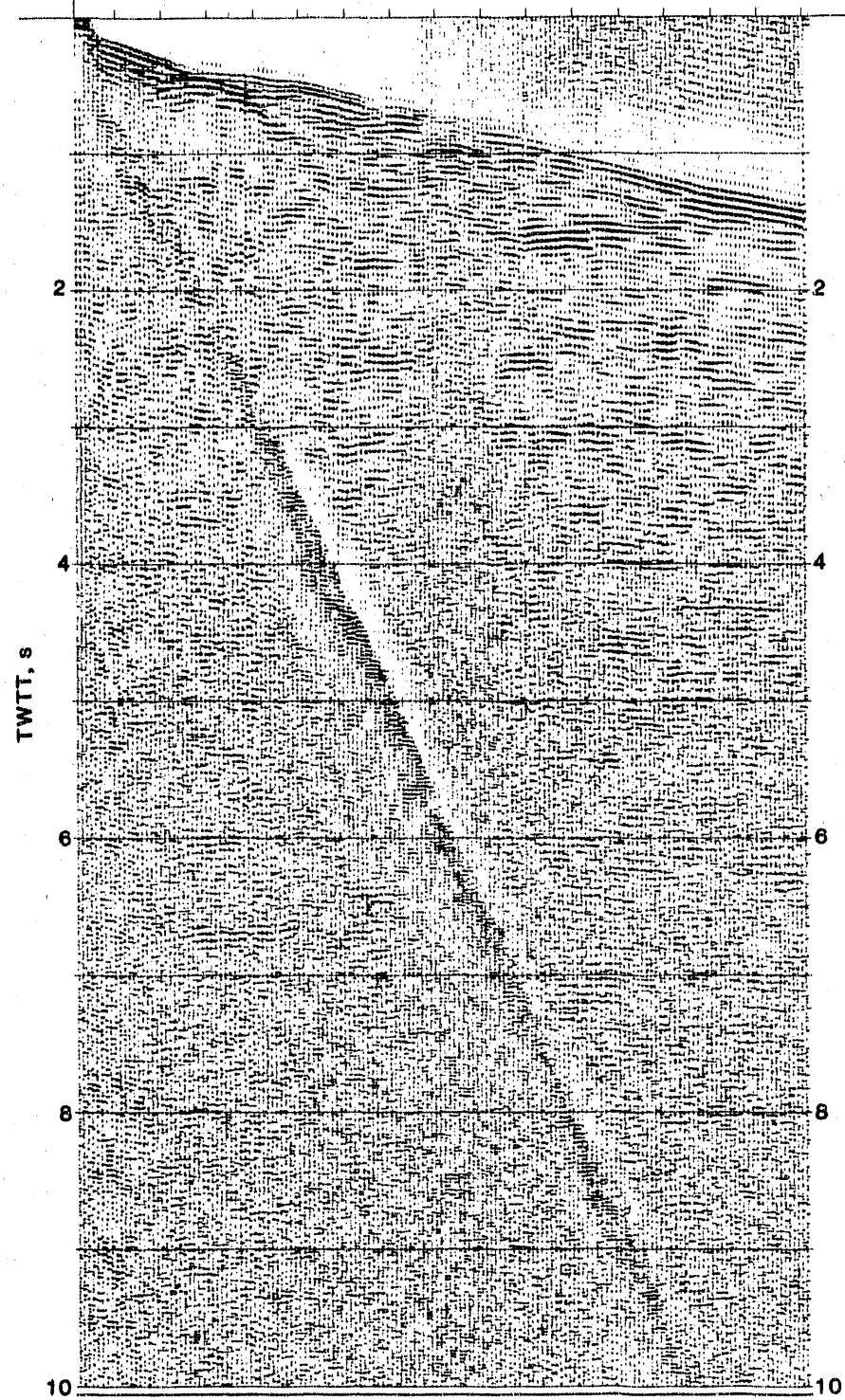


Figure 22a

Windspeed 12-14 mph

14-56 Hz, VIB ARRAY = 231', REC ARRAY = WEIGHTED



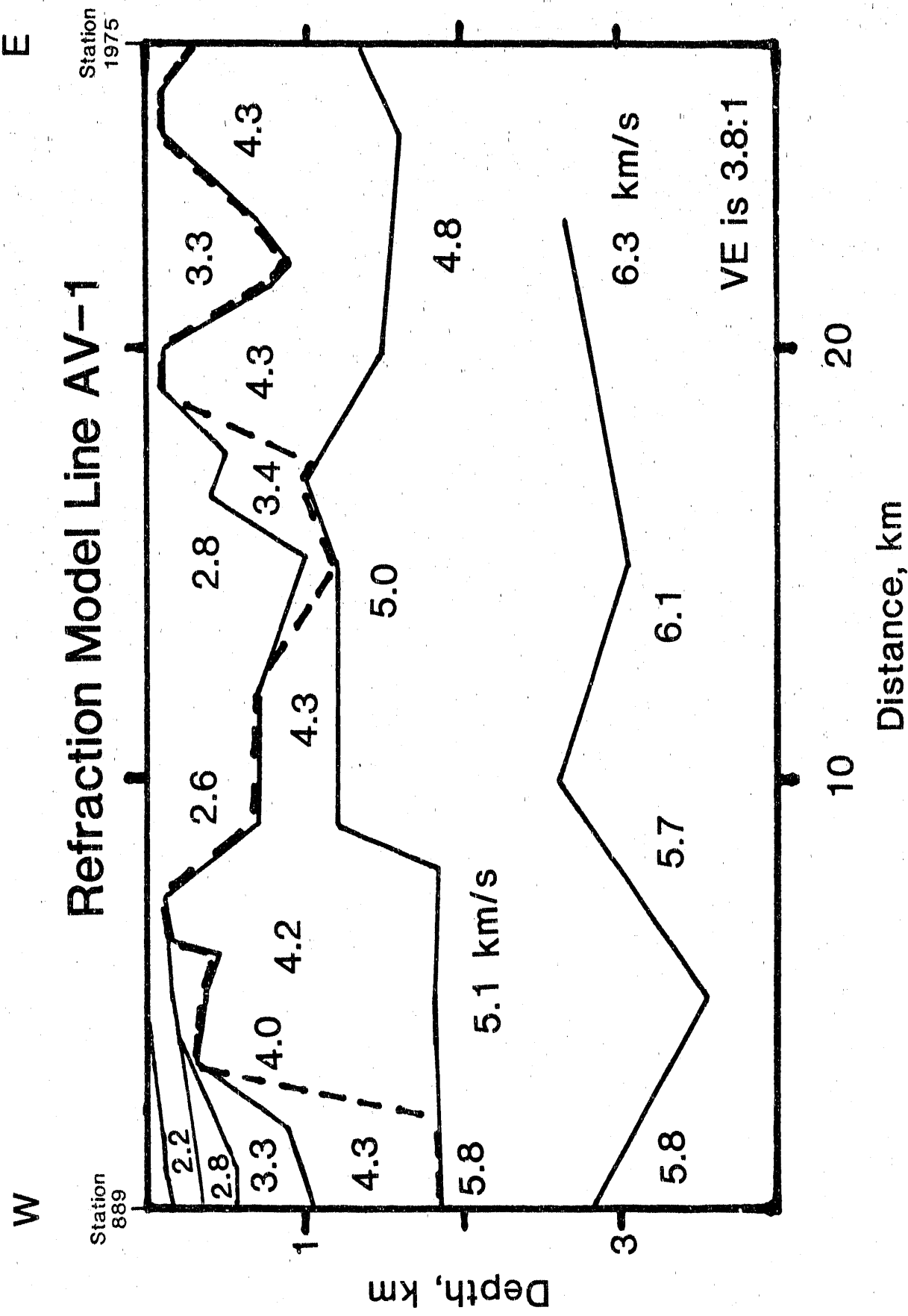


Figure 23

EXPLOSIVE SOURCE

Station 1069

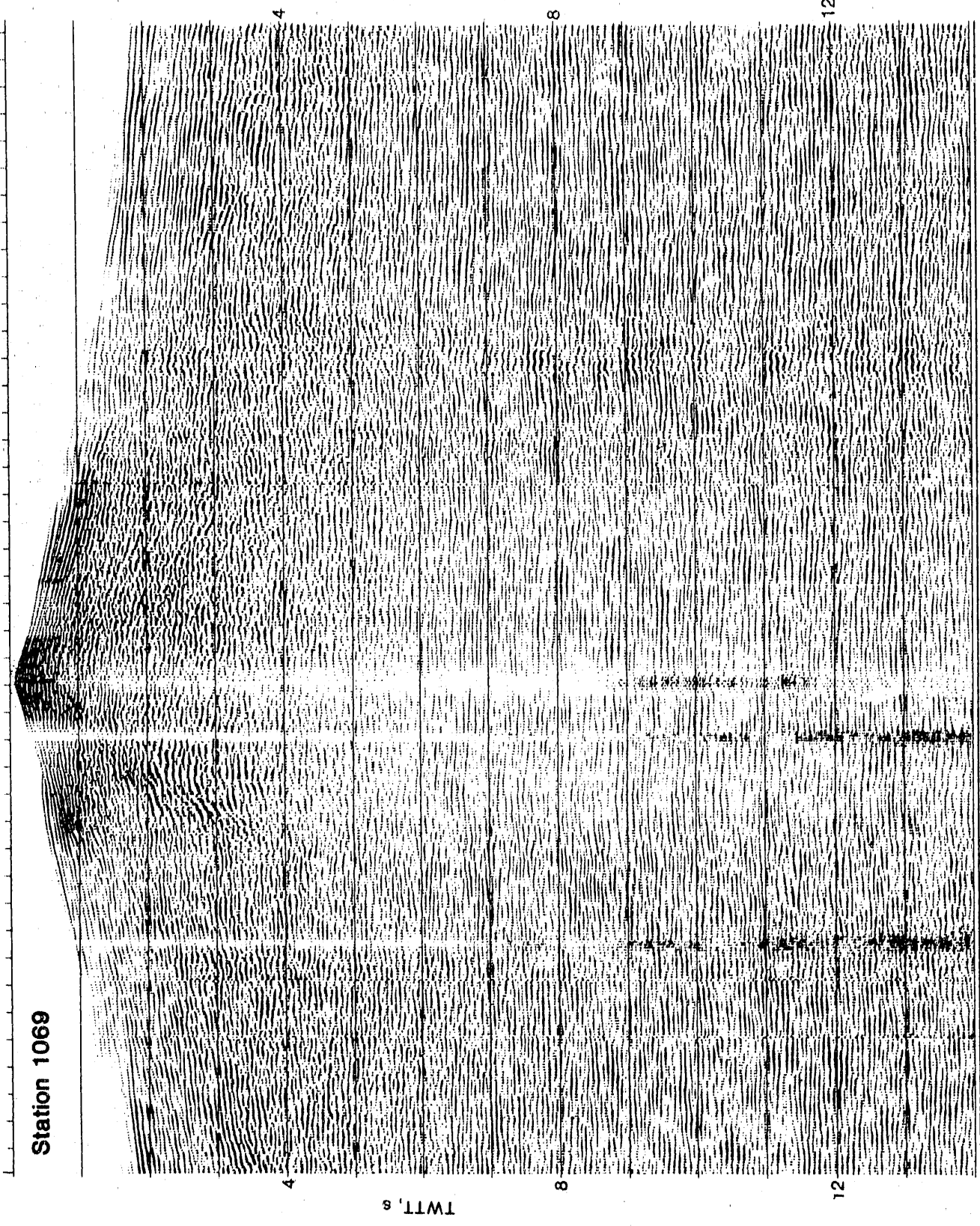


Figure 24a

VIBROSEIS SOURCE

Station 1069

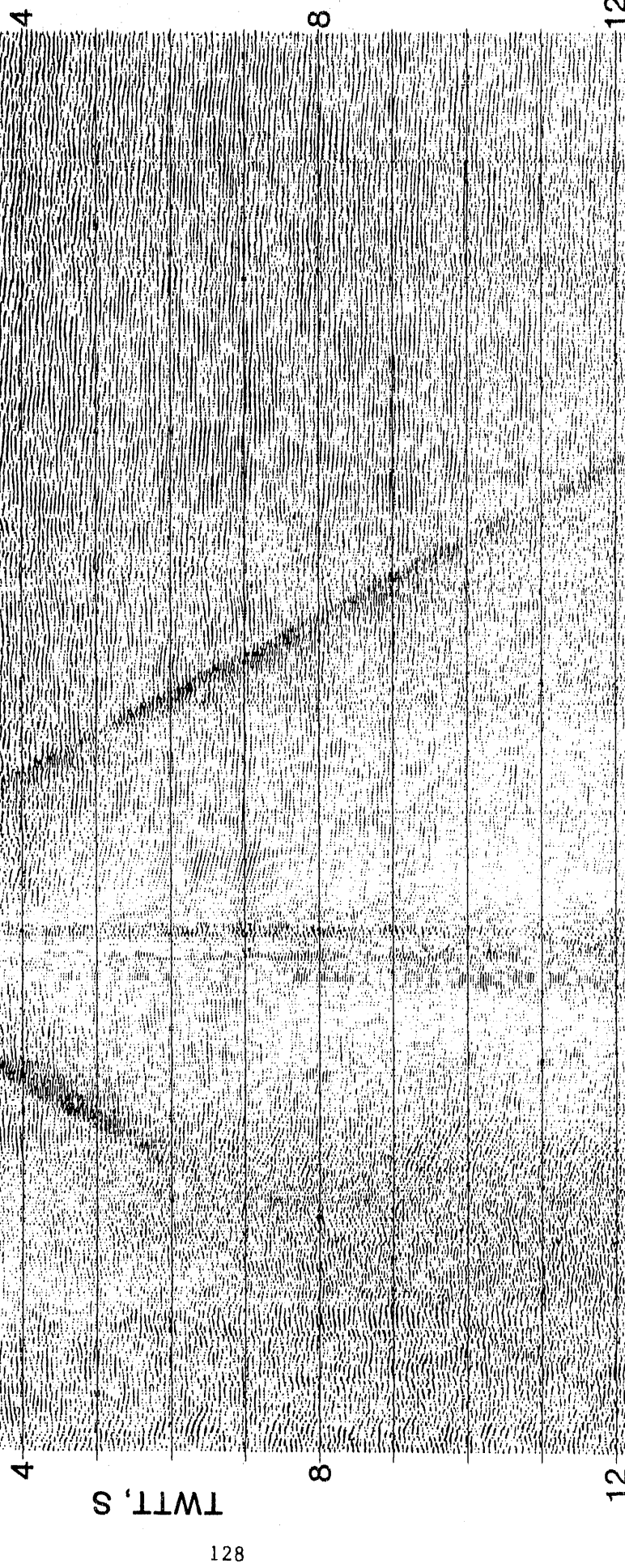
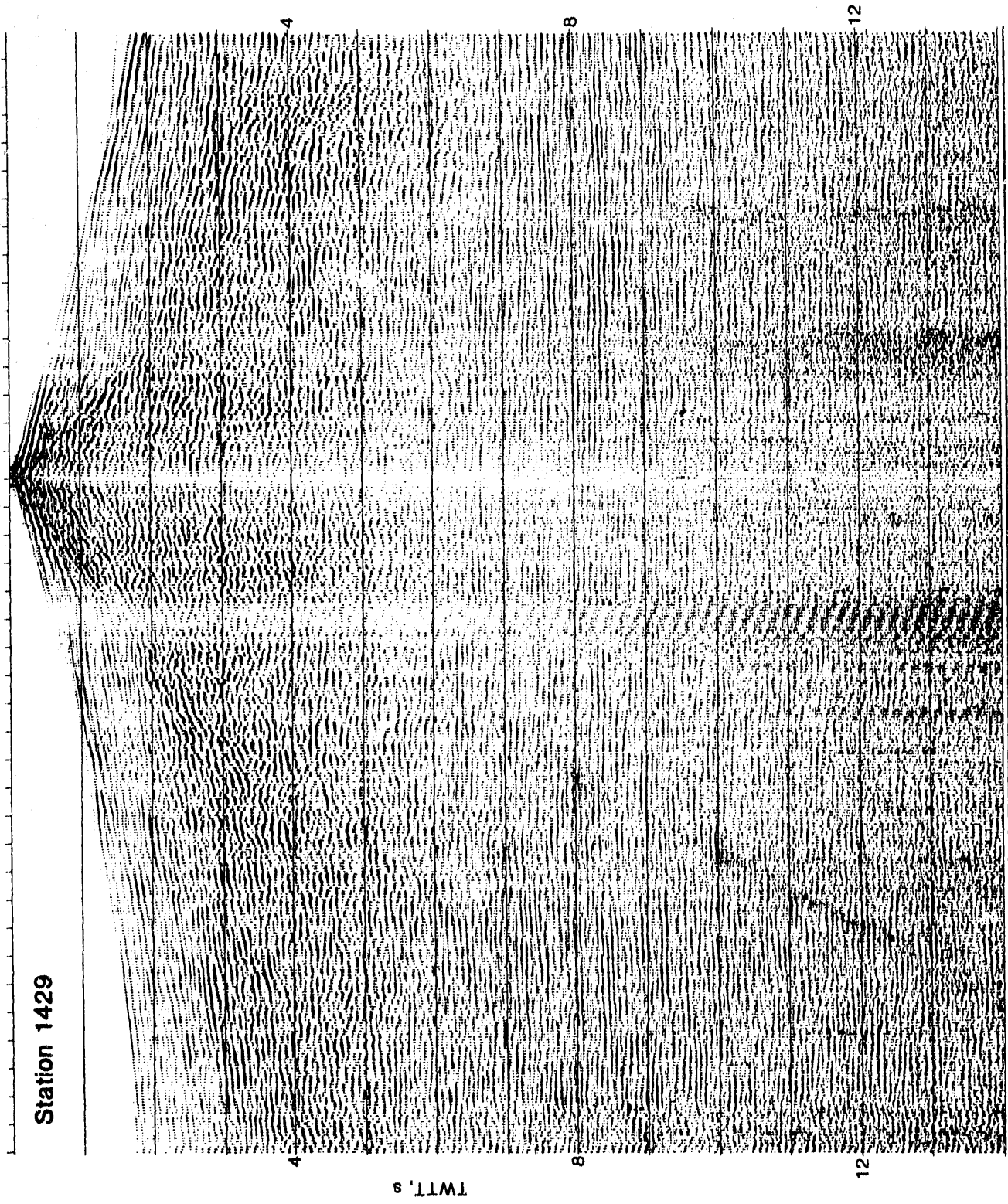


Figure 24b

EXPLOSIVE SOURCE

Station 1429



VIBROSEIS SOURCE

Station 1429

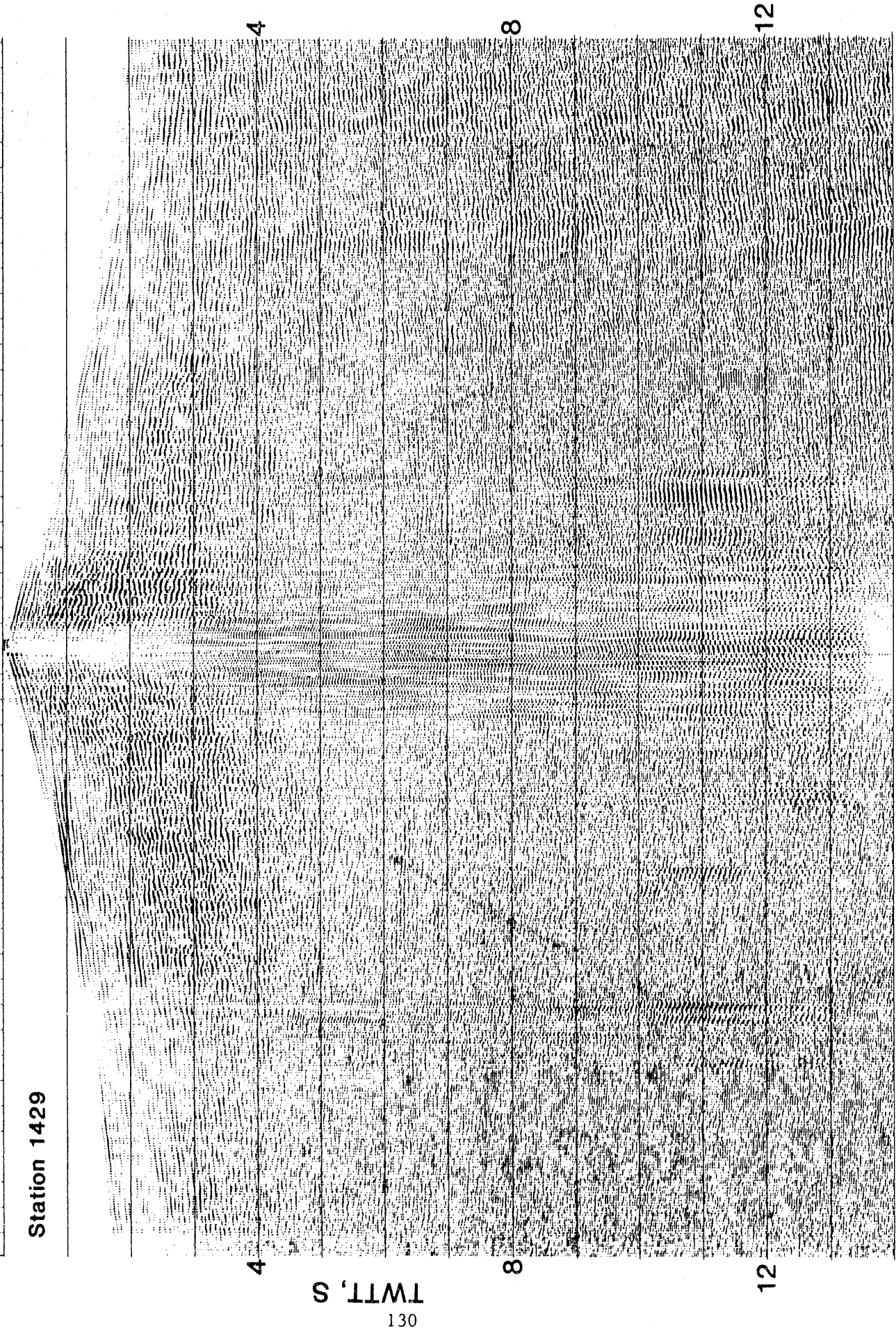


Figure 24d

EXPLOSIVE SOURCE

Station 1789

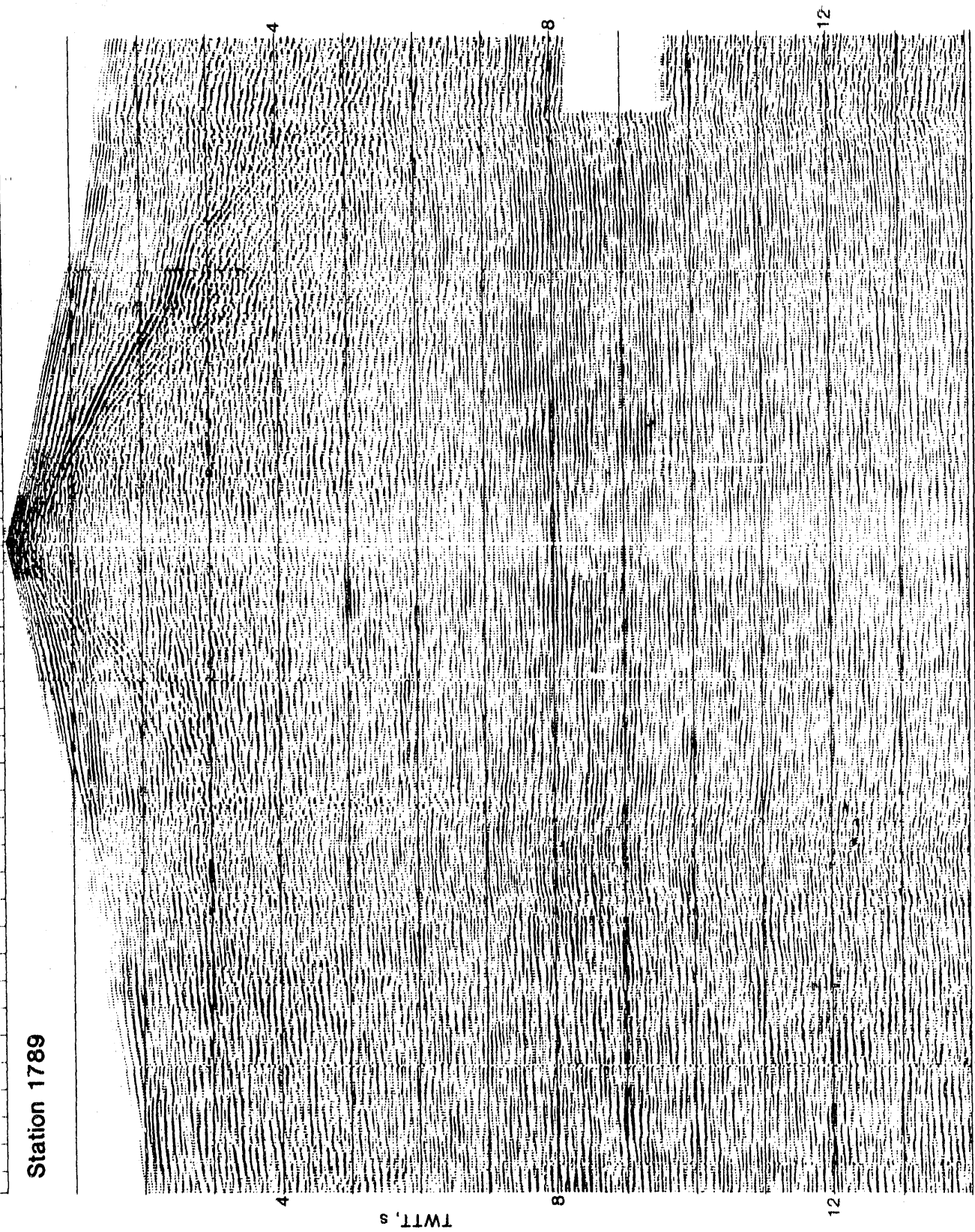


Figure 24e

VIBROSEIS SOURCE

Station 1789

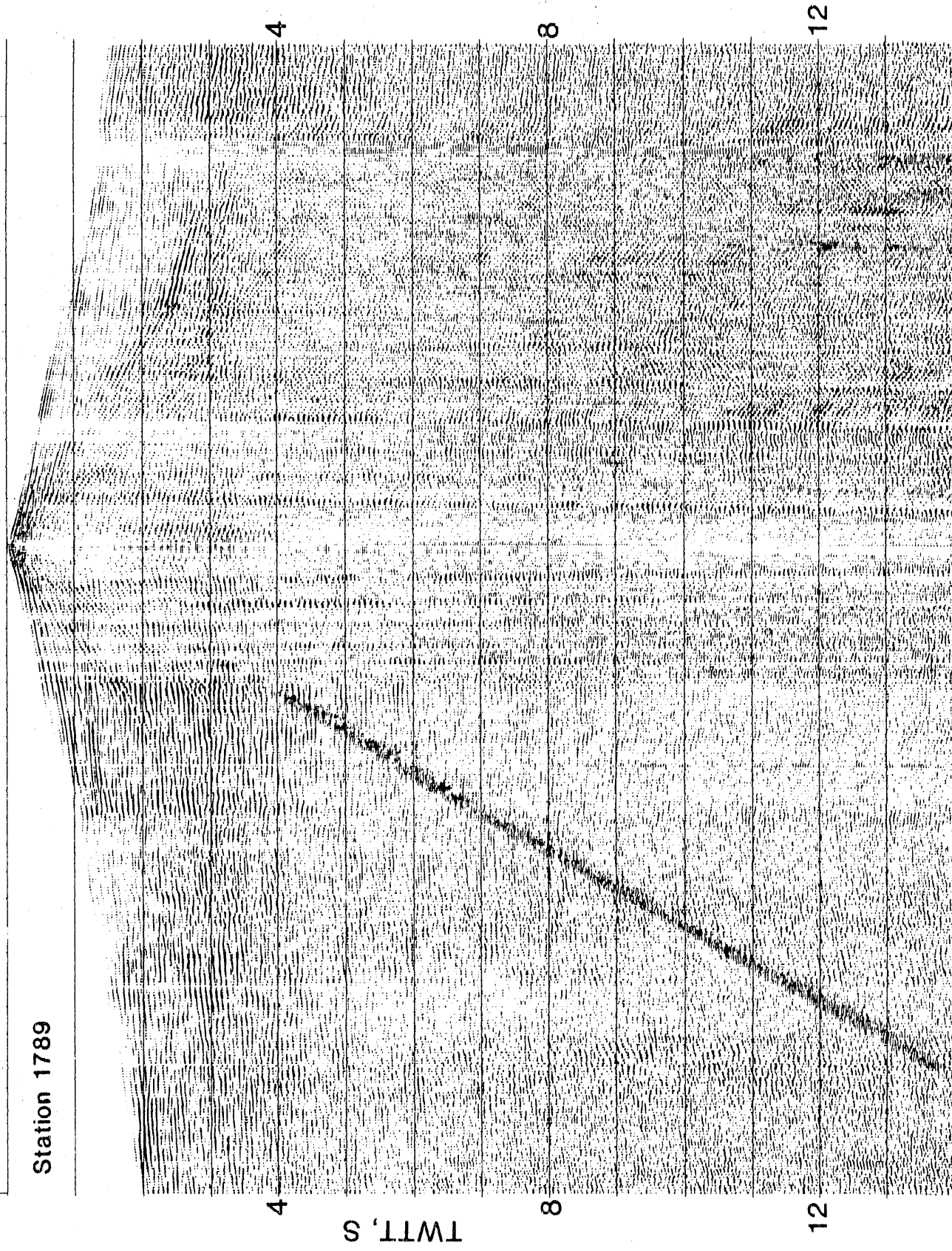
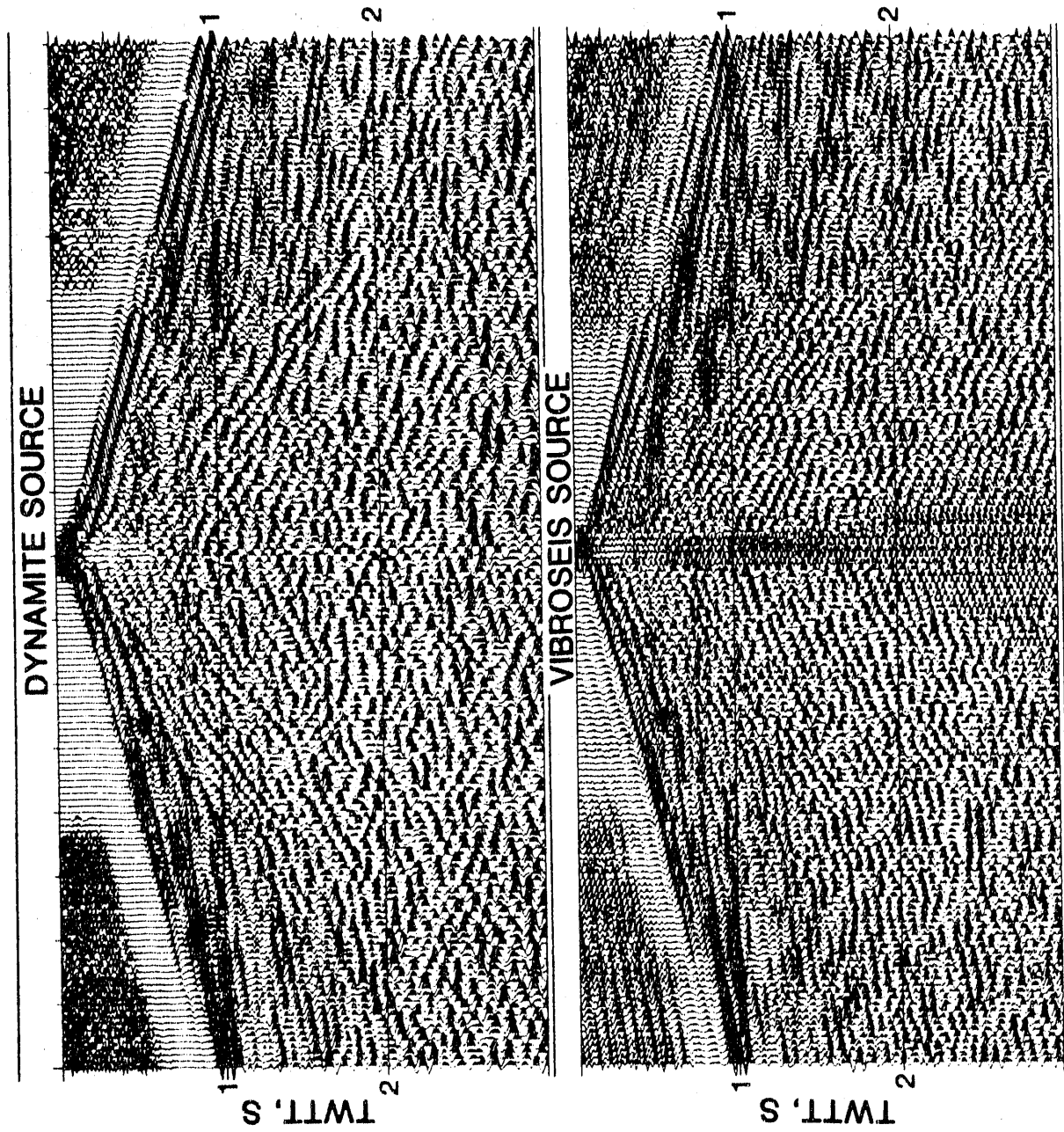


Figure 24f

Figure 25a



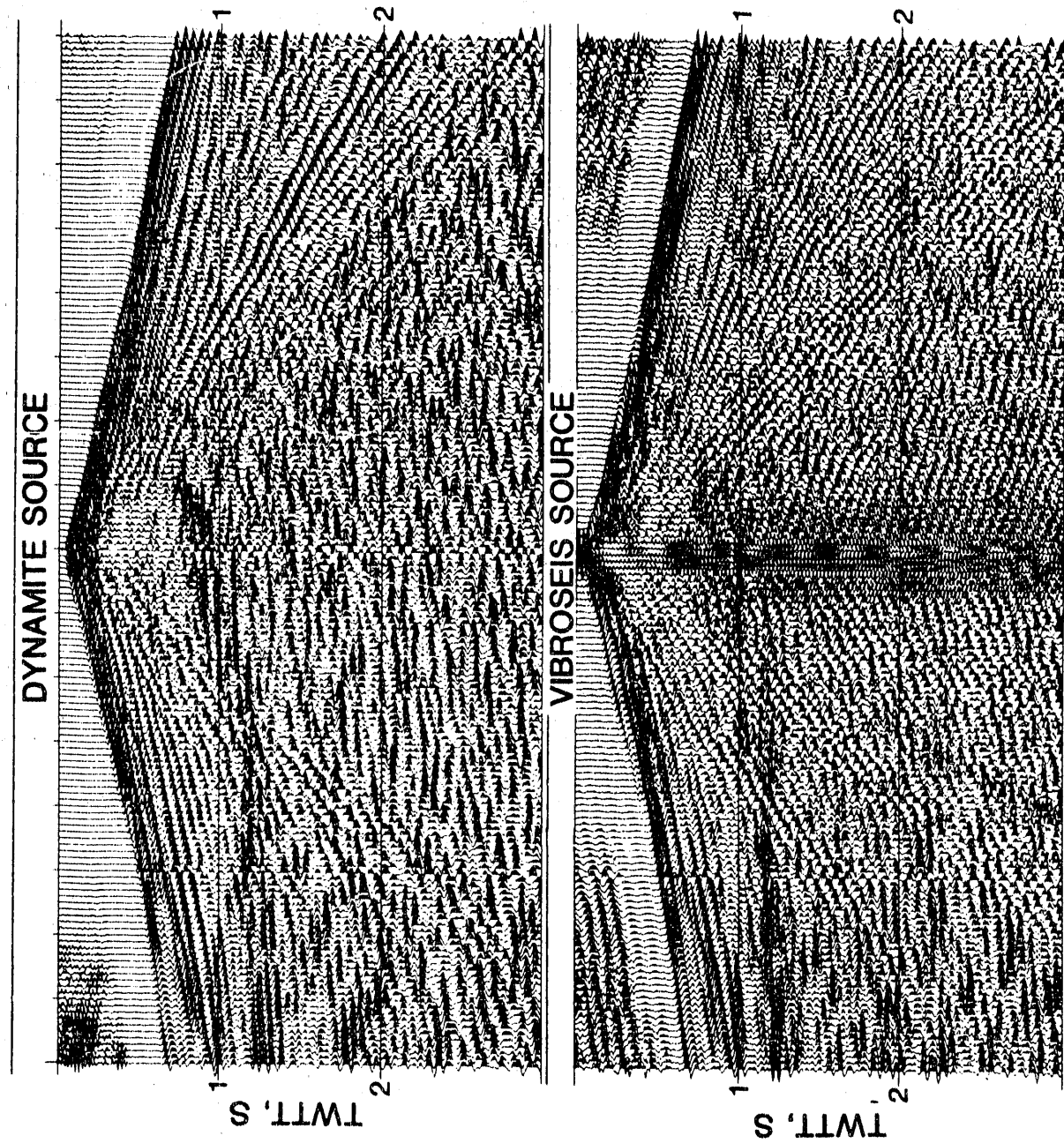


Figure 25b

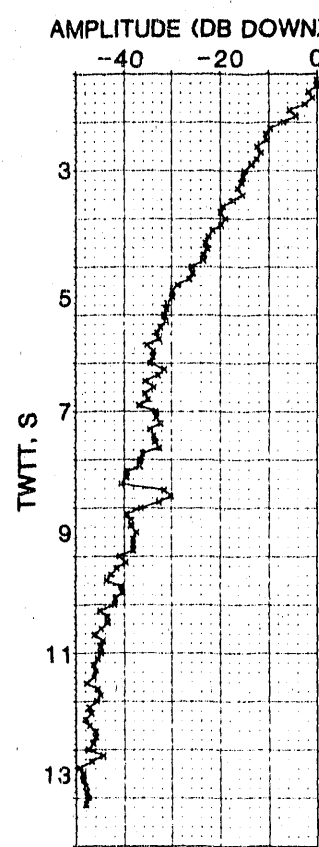
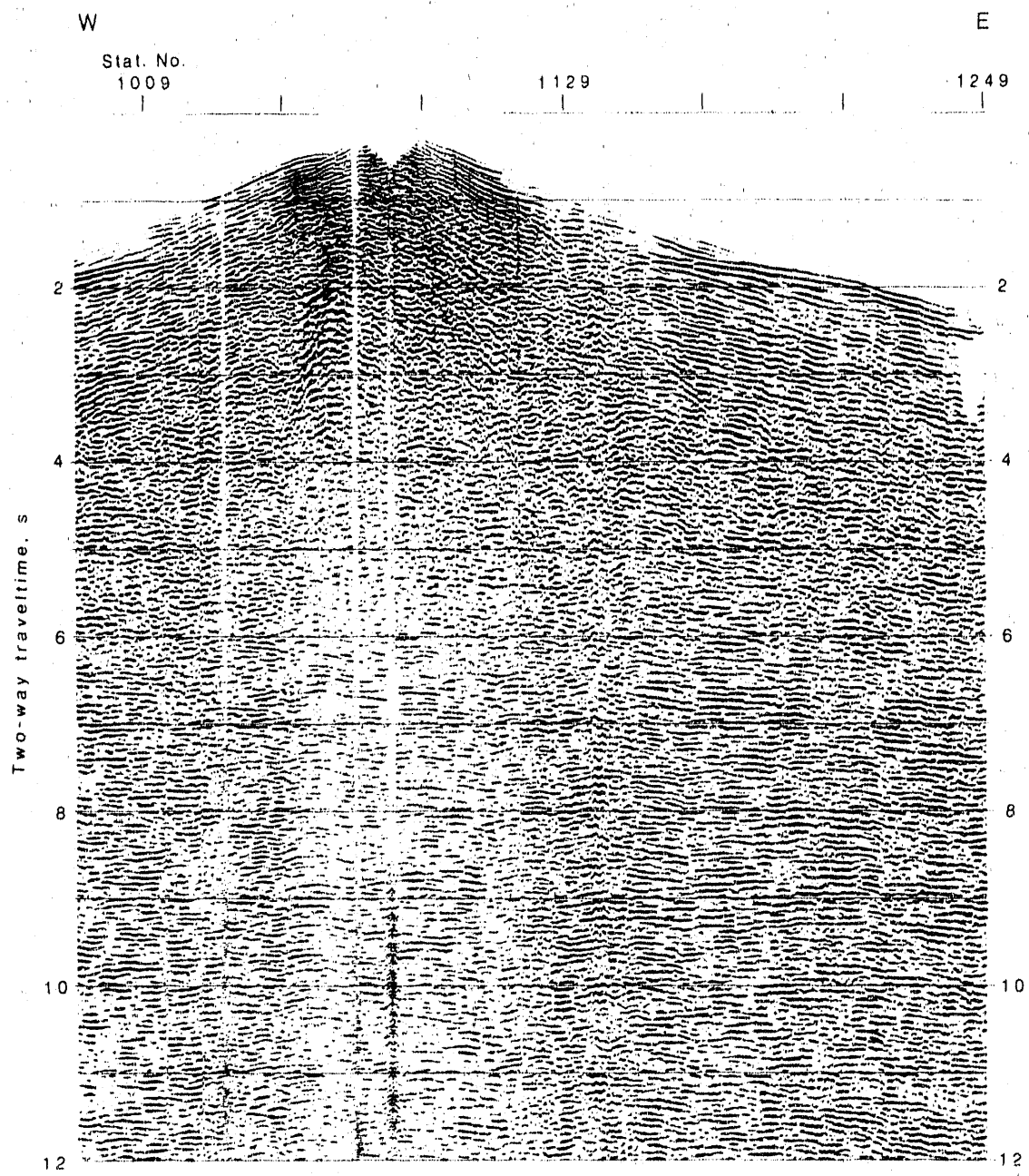


Figure 27



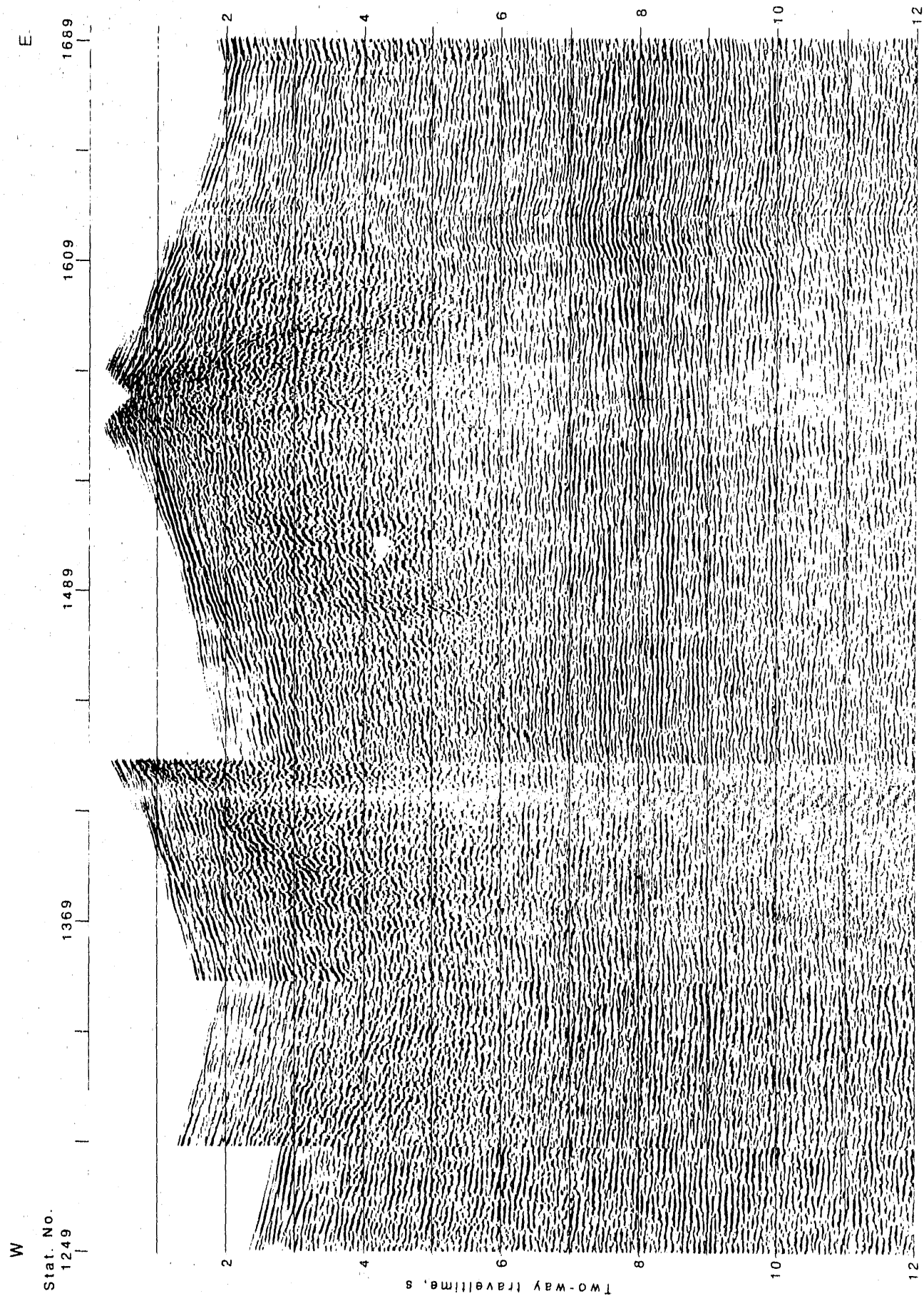
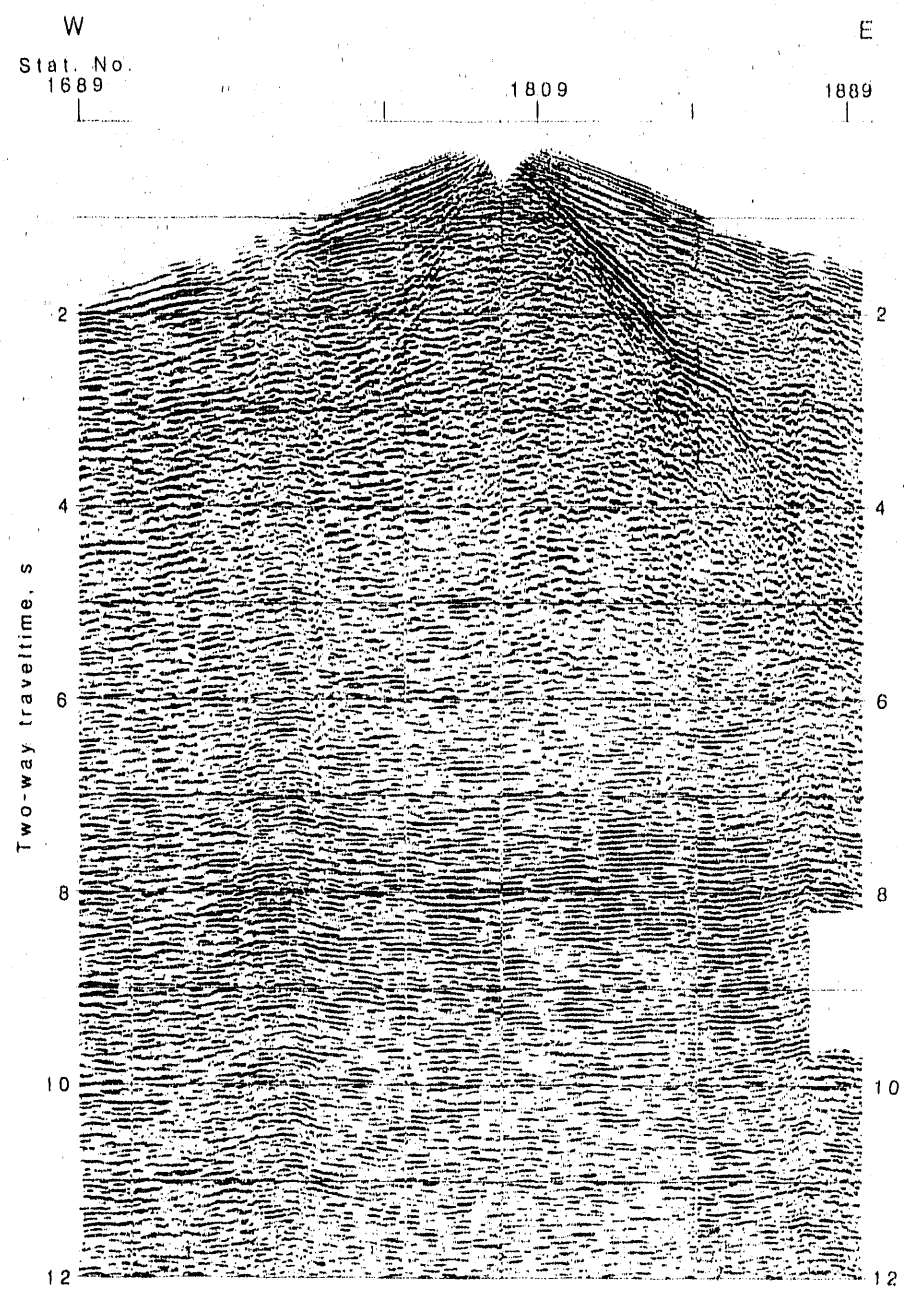


Figure 26b



138

Figure 26c

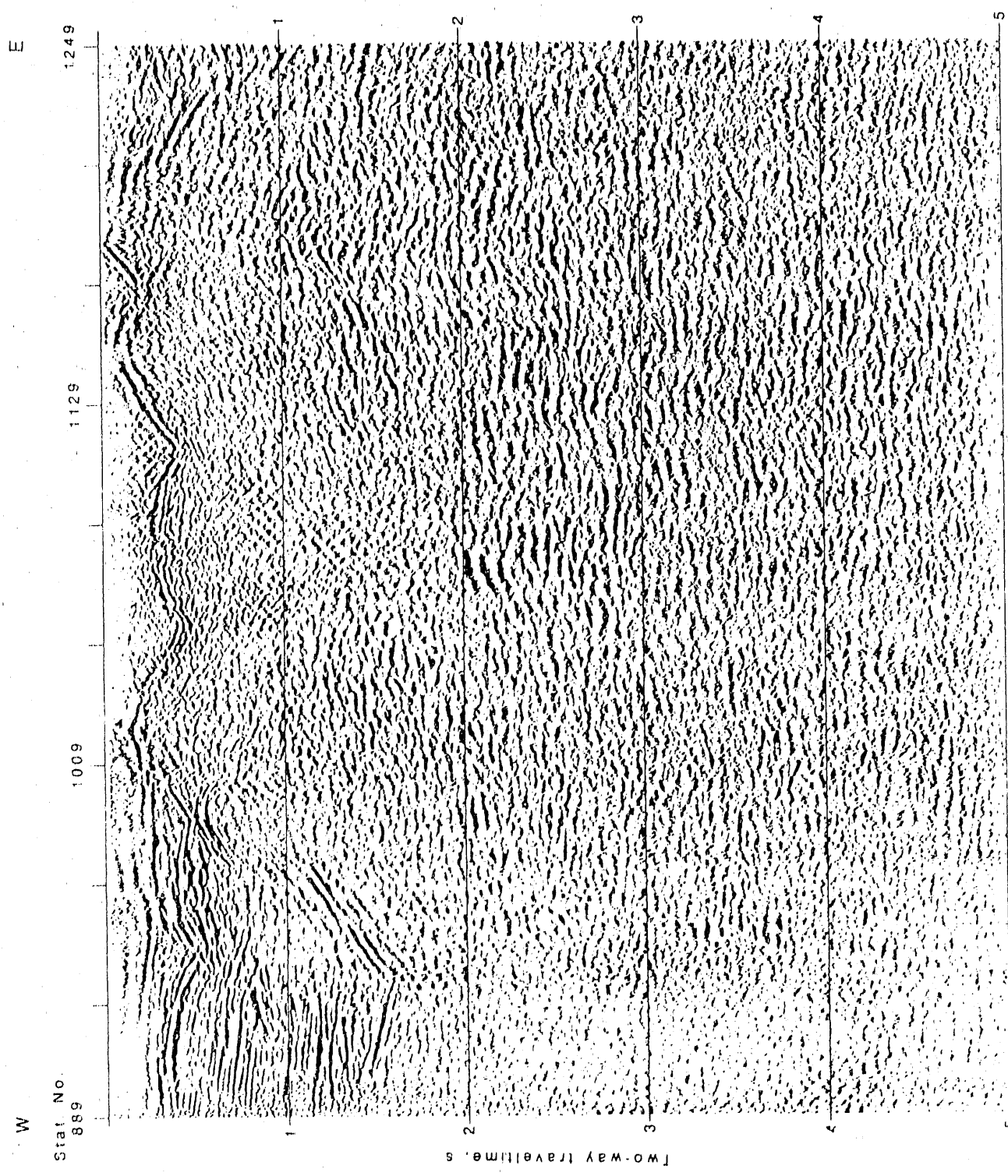
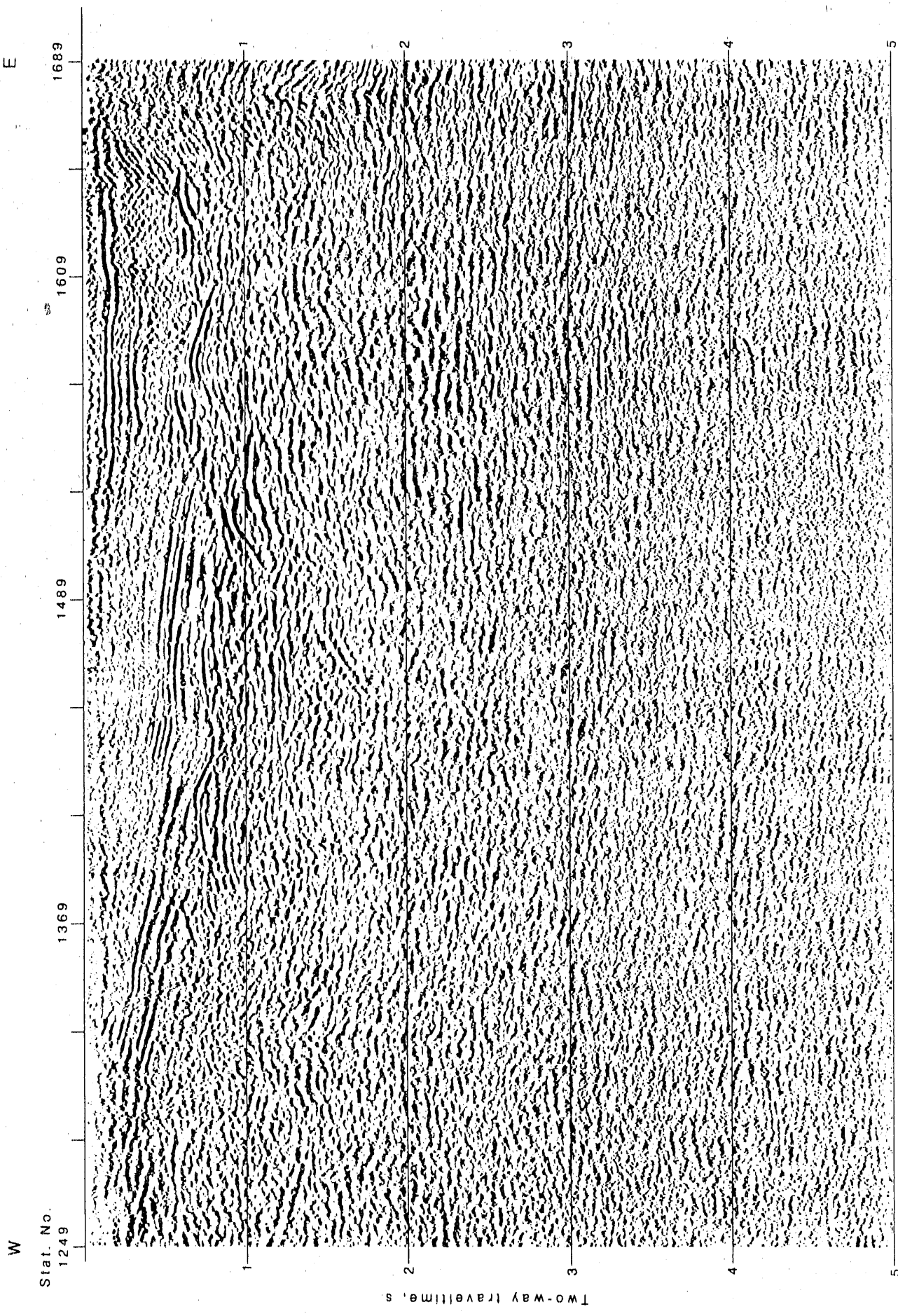
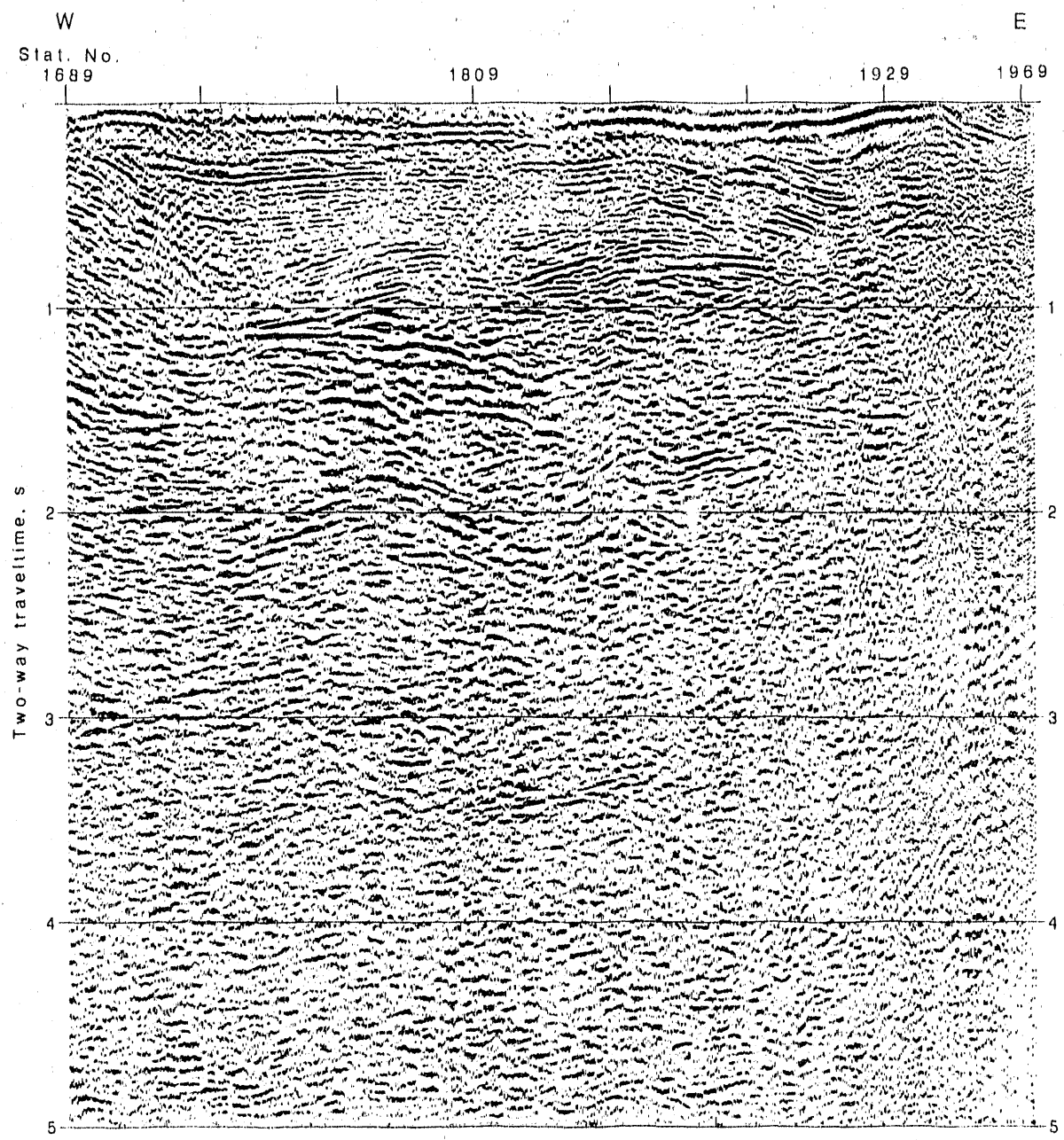


Figure 28a





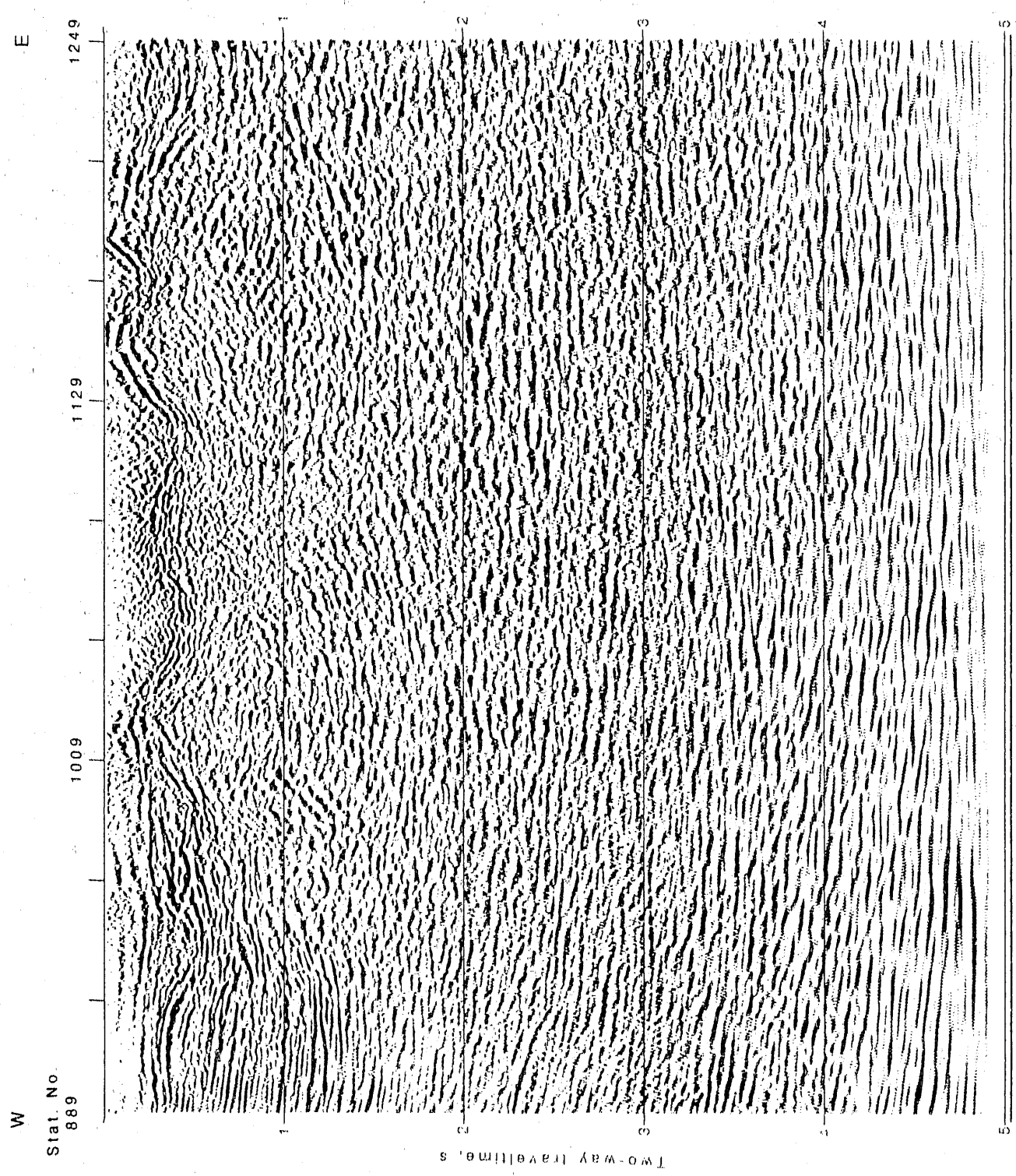


Figure 29a

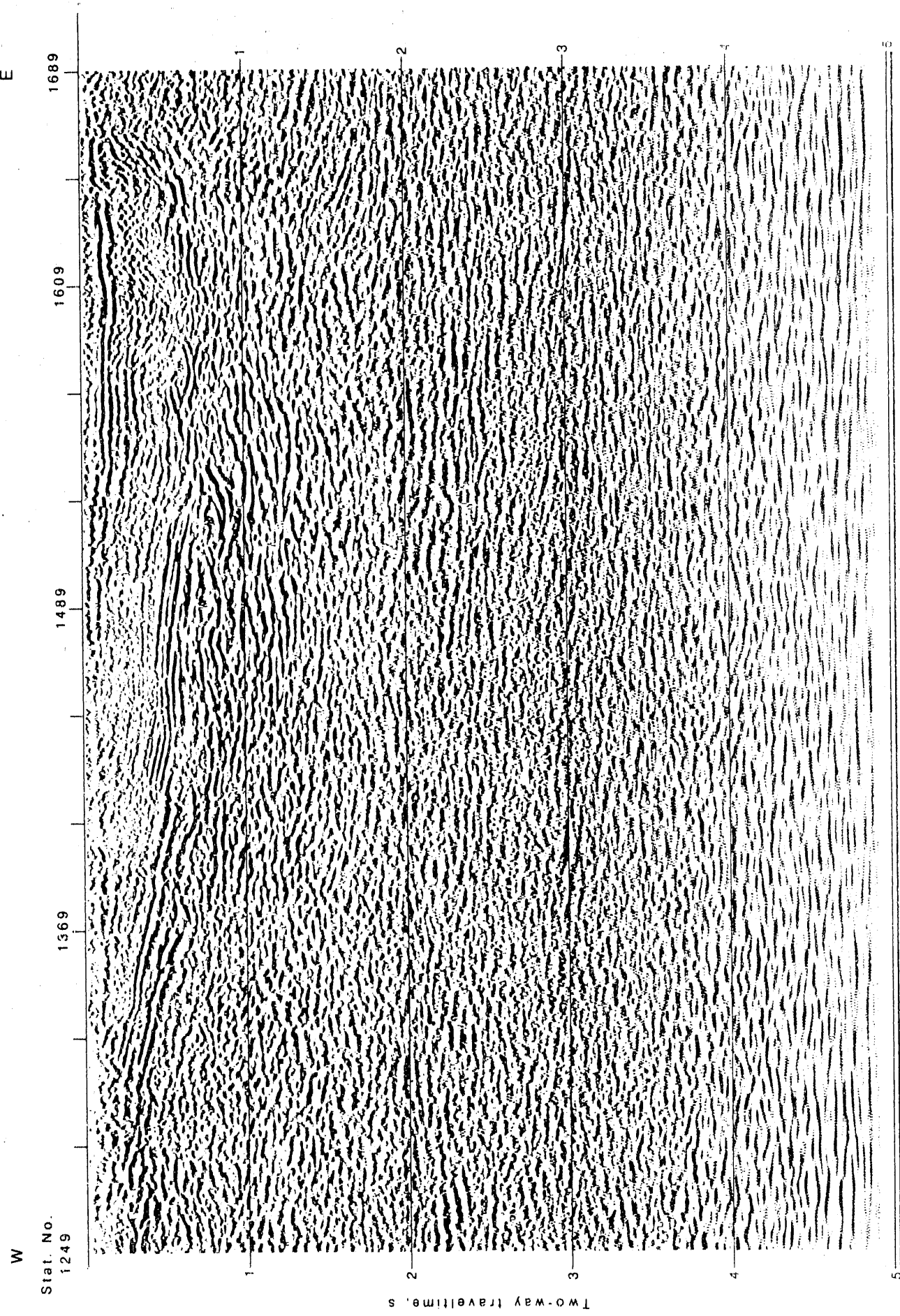


Figure 29b

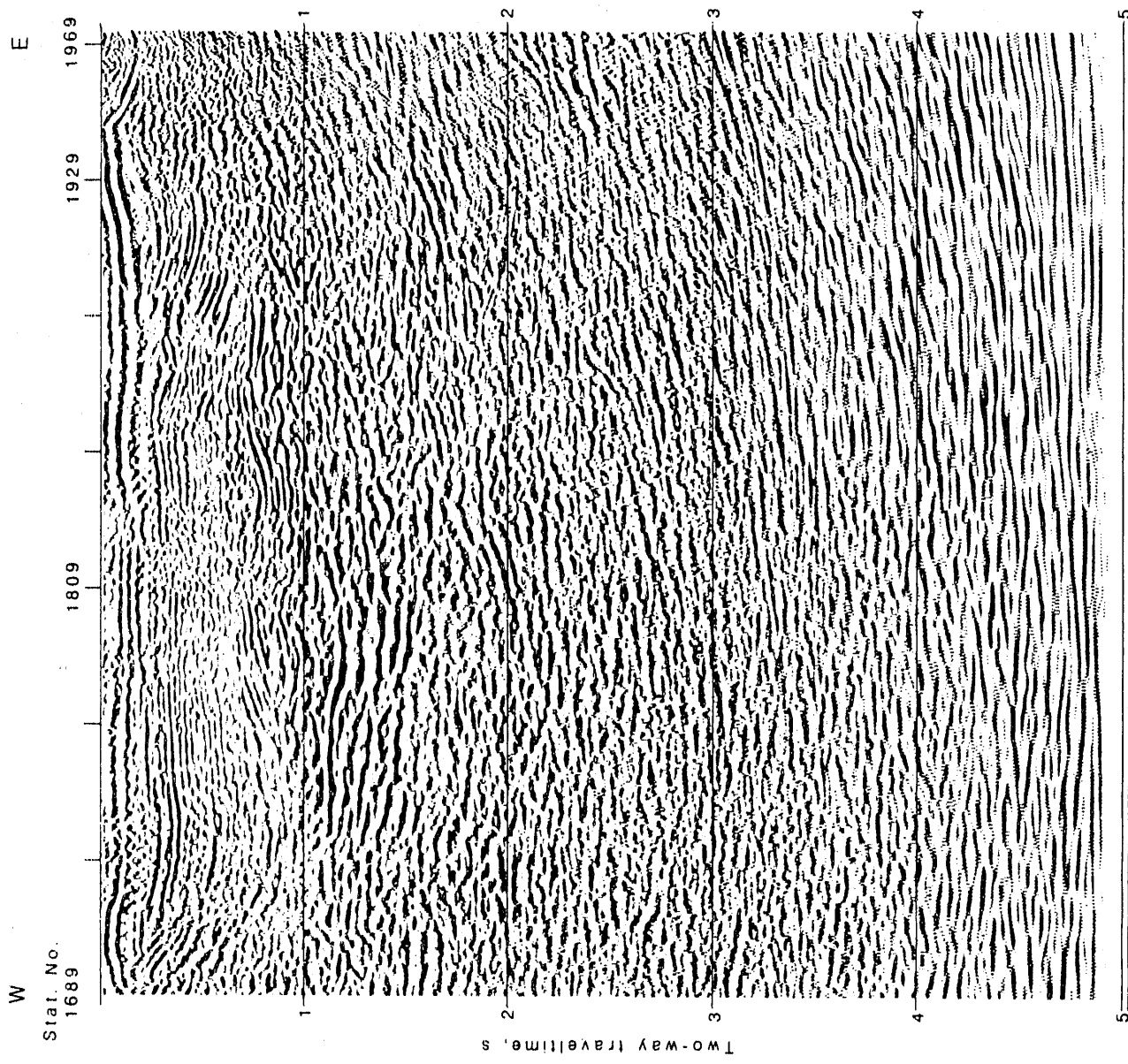


Figure 29c

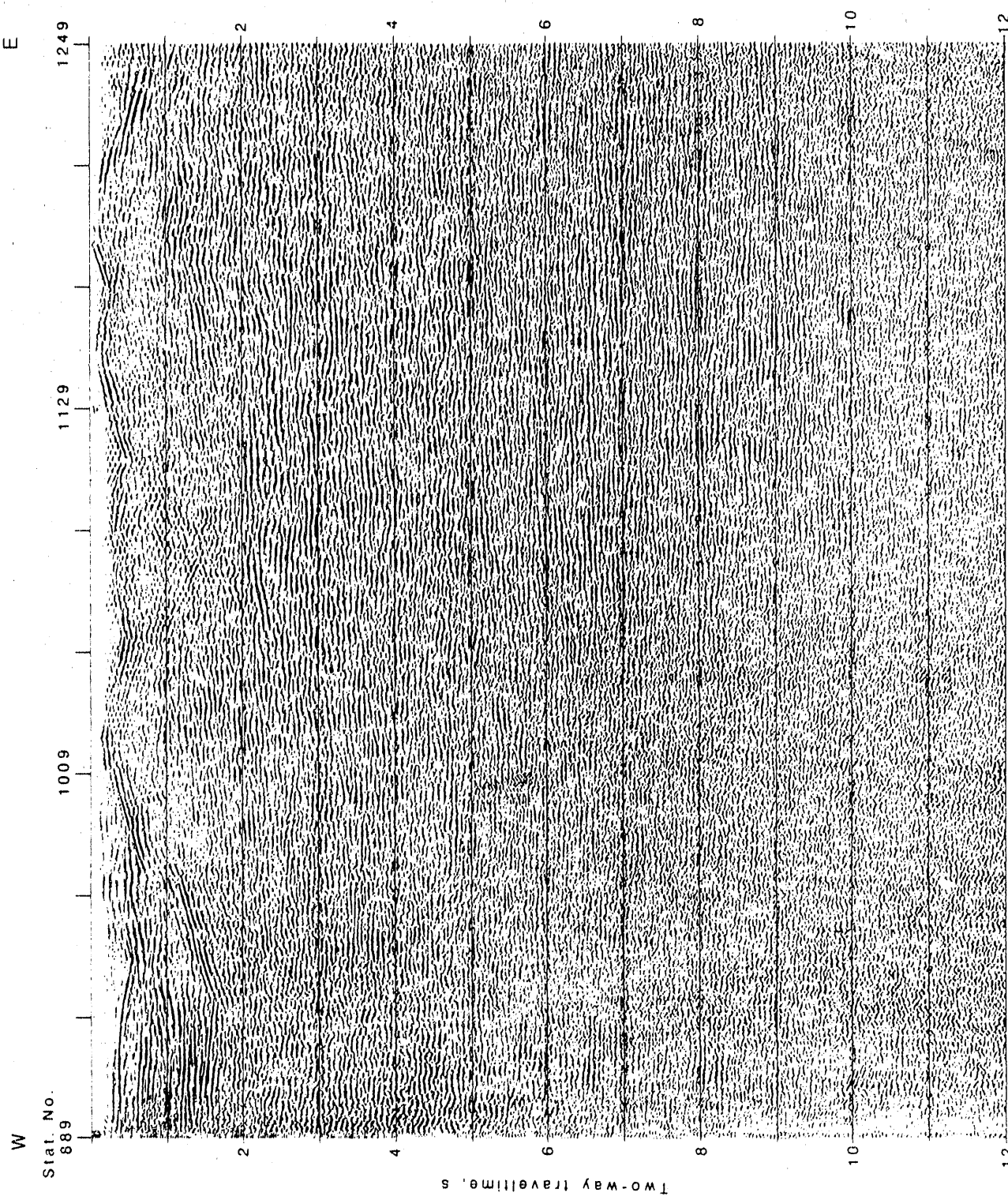


Figure 30a

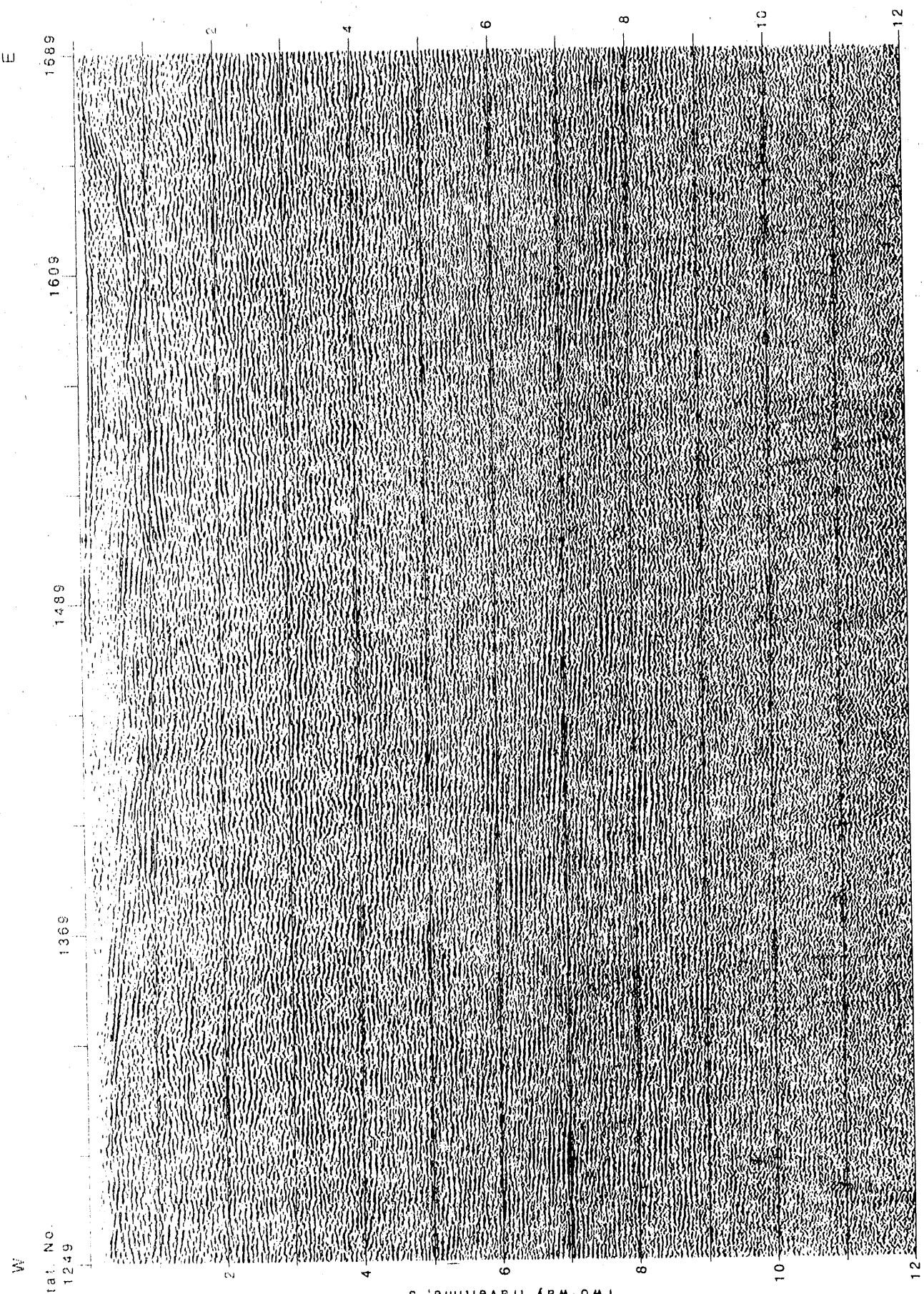


Figure 30b

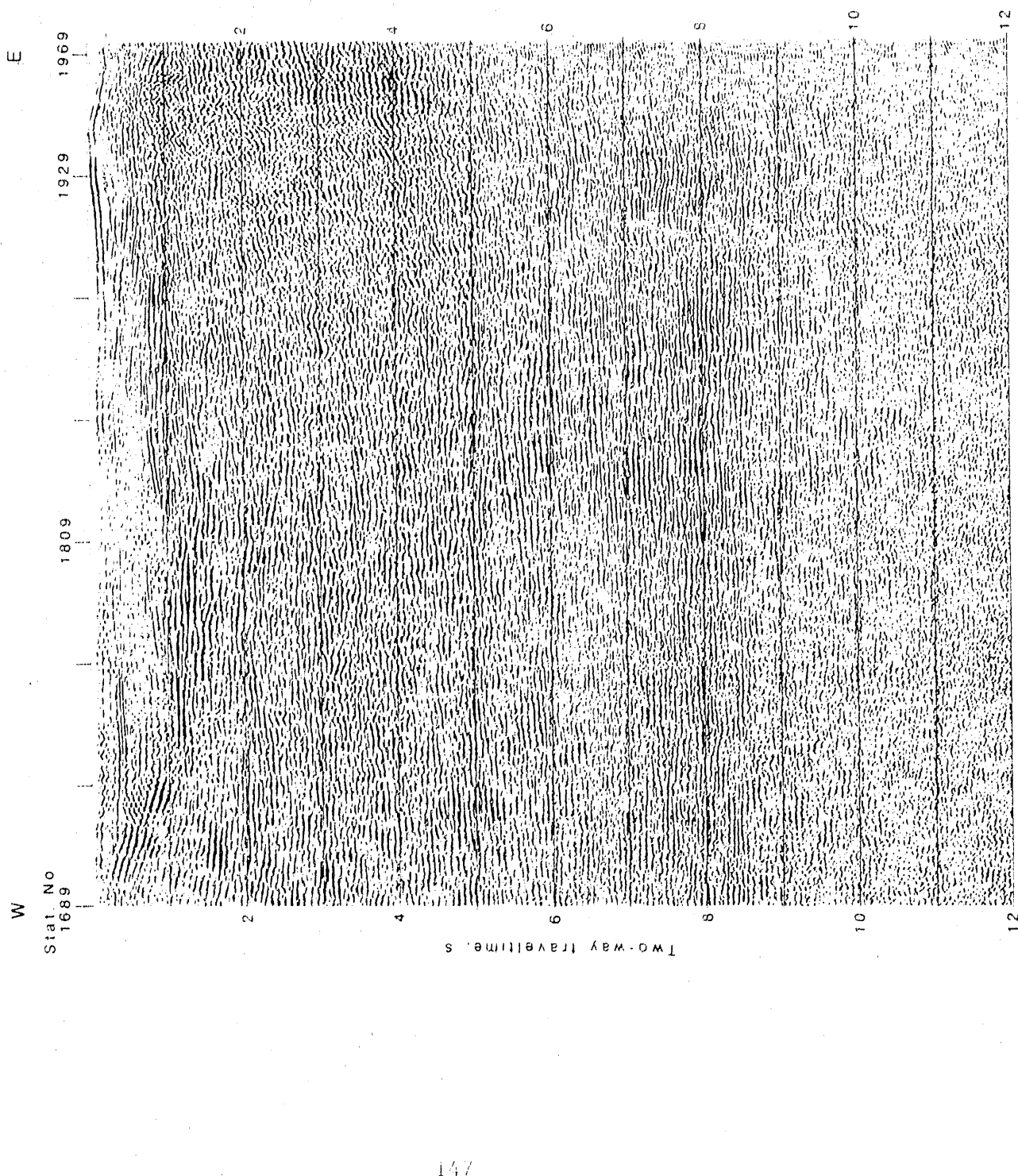


Figure 30c

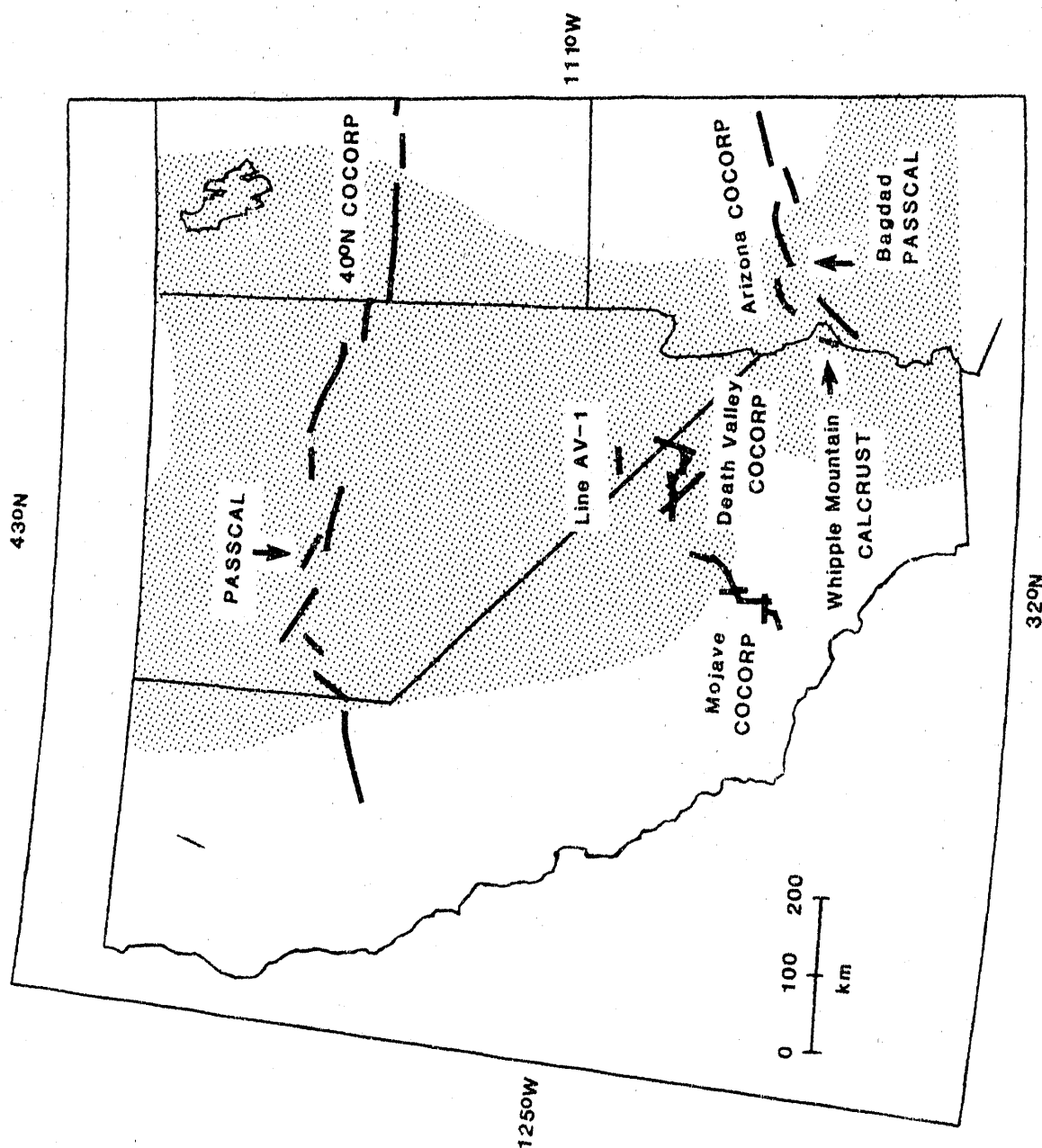


Figure 31

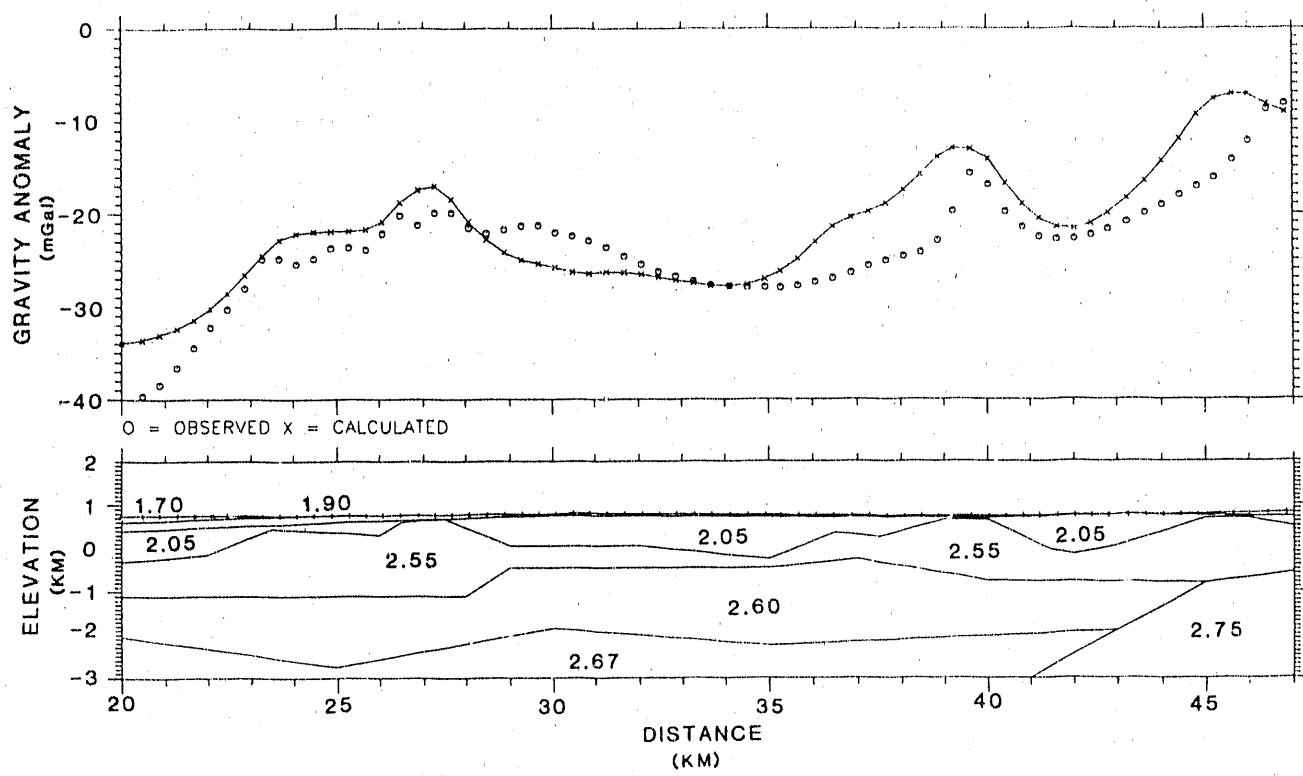


Figure 32

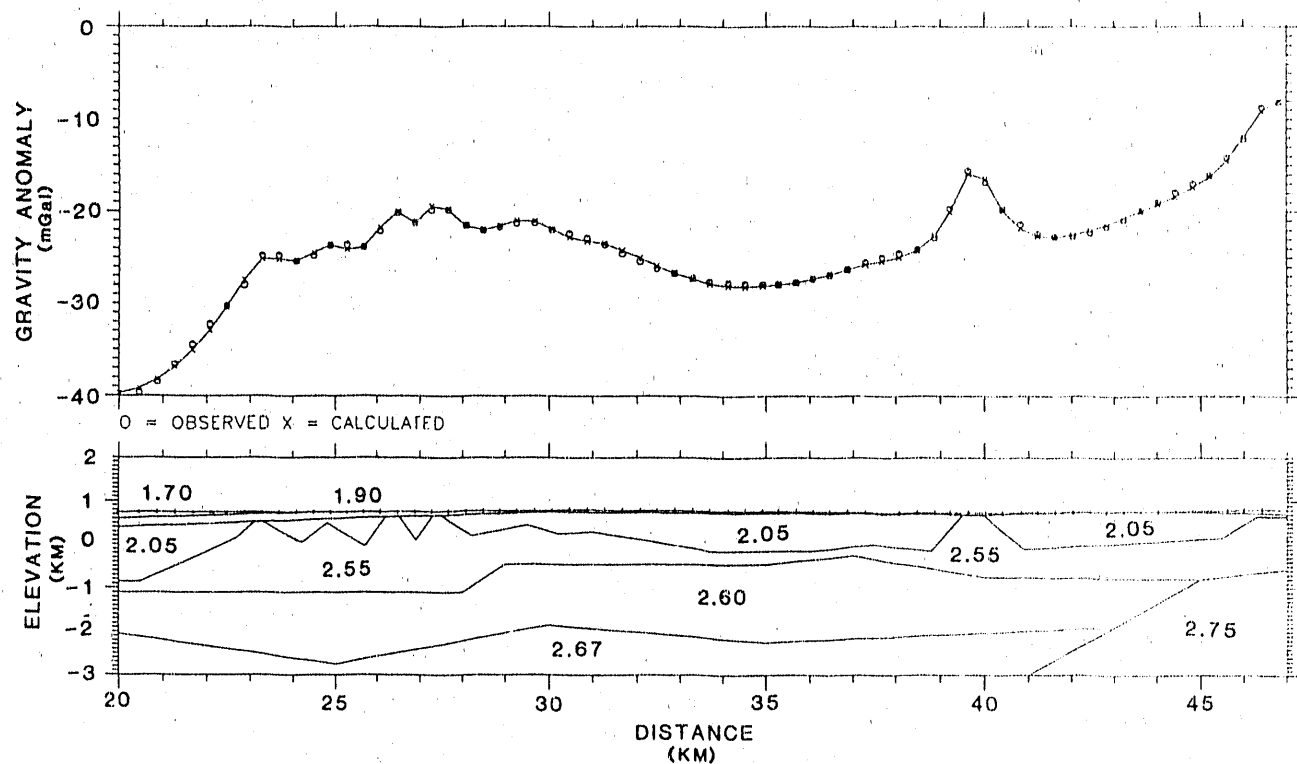


Figure 33

END

DATE FILMED

11/28/90

